NAVAL POSTGRADUATE SCHOOL

MONTEREY, CALIFORNIA

THESIS

MODELING OF HIGH-FREQUENCY ACOUSTIC PROPAGATION IN SHALLOW WATER

by

Juan C. Torres

June 2007

Thesis Advisor: Joseph A. Rice

Approved for public release; distribution is unlimited

THIS PAGE INTENTIONALLY LEFT BLANK

REPORT DOCUMENTATION PAGE			Form Approved OMB No. 0704-0188
Public reporting burden for this collection of information is estimated to average 1 hour per response, including the time for reviewing instruction, searching existing data sources, gathering and maintaining the data needed, and completing and reviewing the collection of information. Send comments regarding this burden estimate or any other aspect of this collection of information, including suggestions for reducing this burden, to Washington headquarters Services, Directorate for Information Operations and Reports, 1215 Jefferson Davis Highway, Suite 1204, Arlington, VA 22202-4302, and to the Office of Management and Budget, Paperwork Reduction Project (0704-0188) Washington DC 20503.			
1. AGENCY USE ONLY *(Leave blank)*	**2. REPORT DATE** June 2007	**3. REPORT TYPE AND DATES COVERED** Master's Thesis	
4. TITLE AND SUBTITLE Modeling of High-Frequency Acoustic Propagation in Shallow Water		**5. FUNDING NUMBERS**	
6. AUTHOR(S) Juan C. Torres			
7. PERFORMING ORGANIZATION NAME(S) AND ADDRESS(ES) Naval Postgraduate School Monterey, CA 93943-5000		**8. PERFORMING ORGANIZATION REPORT NUMBER**	
9. SPONSORING /MONITORING AGENCY NAME(S) AND ADDRESS(ES) N/A		**10. SPONSORING/MONITORING AGENCY REPORT NUMBER**	
11. SUPPLEMENTARY NOTES The views expressed in this thesis are those of the author and do not reflect the official policy or position of the Department of Defense or the U.S. Government.			
12a. DISTRIBUTION / AVAILABILITY STATEMENT Approved for public release; distribution is unlimited		**12b. DISTRIBUTION CODE** A	

13. ABSTRACT (maximum 200 words)

This research involves numerical modeling of acoustic signals through shallow water channels. The sound is computationally modeled in a vertical plane as a dense fan of beams radiating from the transmitter location. The cross section of each 2-dimensional beam is represented as a Gaussian distribution of acoustic energy. The Gaussian beam travels axially along rays governed by Snell's Law, dispersing in width as a function of travel distance. At arbitrary receiver locations in the planar sound field, the intensity of the propagated beams is integrated over time to synthesize the multipath channel response. The influence of the ocean channel is analyzed parametrically, including sensitivity of the eigenray structure and impulse response to water properties, channel boundaries, and source/receiver geometry. Specific maritime environments examined in this study are St. Andrew Bay, Panama City, FL, and Chesapeake Bay, Little Creek, VA. This research supports the possible use of high frequency acoustics (40-70 kHz) for short-range (500 m) through-water communications. Emphasis is on communications between seabed stations.

14. SUBJECT TERMS Acoustics, sound, ocean, propagation, shallow water, acoustic communications, computational, Bellhop.			**15. NUMBER OF PAGES** 150
			16. PRICE CODE
17. SECURITY CLASSIFICATION OF REPORT Unclassified	**18. SECURITY CLASSIFICATION OF THIS PAGE** Unclassified	**19. SECURITY CLASSIFICATION OF ABSTRACT** Unclassified	**20. LIMITATION OF ABSTRACT** UL

NSN 7540-01-280-5500

Standard Form 298 (Rev. 2-89)
Prescribed by ANSI Std. 239-18

THIS PAGE INTENTIONALLY LEFT BLANK

Approved for public release; distribution is unlimited

MODELING OF HIGH-FREQUENCY ACOUSTIC PROPAGATION IN SHALLOW WATER

Juan C. Torres
Ensign, United States Navy
B.S. United States Naval Academy, 2006

Submitted in partial fulfillment of the
requirements for the degree of

MASTER OF SCIENCE IN APPLIED PHYSICS

from the

NAVAL POSTGRADUATE SCHOOL
June 2007

Author: Juan C. Torres

Approved by: Joseph A. Rice
Thesis Advisor

James Luscombe
Chairman, Department of Physics

THIS PAGE INTENTIONALLY LEFT BLANK

ABSTRACT

This research involves numerical modeling of acoustic signals through shallow water channels. The sound is computationally modeled in a vertical plane as a dense fan of beams radiating from the transmitter location. The cross section of each 2-dimensional beam is represented as a Gaussian distribution of acoustic energy. The Gaussian beam travels axially along rays governed by Snell's Law, dispersing in width as a function of travel distance. At arbitrary receiver locations in the planar sound field, the intensity of the propagated beams is integrated over time to synthesize the multipath channel response. The influence of the ocean channel is analyzed parametrically, including sensitivity of the eigenray structure and impulse response to water properties, channel boundaries, and source/receiver geometry. Specific maritime environments examined in this study are St. Andrew Bay, Panama City, FL, and Chesapeake Bay, Little Creek, VA. This research supports the possible use of high frequency acoustics (40-70 kHz) for short-range (500 m) through-water communications. Emphasis is on communications between seabed stations.

THIS PAGE INTENTIONALLY LEFT BLANK

TABLE OF CONTENTS

LIST OF FIGURES

THIS PAGE INTENTIONALLY LEFT BLANK

LIST OF TABLES

THIS PAGE INTENTIONALLY LEFT BLANK

ACKNOWLEDGMENTS

I would like to thank the following people for their continued support and encouragement throughout my thesis work and my time in Monterey:

First and foremost, I need to thank to my wonderful family. To my father, for instilling me with an endless love for science and knowledge; to my mother, for always supporting me and being by my side in the important moments of my life; and to my sister, for reminding me that enjoying life is as important as studies and work.

To my advisor, Joseph Rice, for his patience and crucial guidance through the world of underwater acoustics, and who spent countless hours ensuring this project came to a successful fruition.

To Dr. Michael Porter, for his assistance in helping me understand the subtleties and details of the Bellhop propagation model and who provided me with the bases for the development of this thesis.

To Dr. Paul Baxley, for providing me with the sound-speed profile data for St. Andrew Bay and for giving me guidance on the significance of my graphical data.

To LT Bjørn Kerstens, NE, for providing me insight and helping me in the editing process of the thesis.

To Dr. Joseph Blau and ENS Charles Allen, USN, for helping me obtain the necessary knowledge to properly use the MATLAB software in support of my thesis.

To my uncle Jesus G. Torres and Ingrid, for their never-ending generosity and support during my time in the Monterey Bay.

To everyone in the Dietzen family, for their continued friendship and for providing me with a home away from home where I could watch sports, sing, watch fireworks and play cards.

And finally, I would like to thank every professor and colleague at the Naval Postgraduate School for making this an unforgettable year.

THIS PAGE INTENTIONALLY LEFT BLANK

I. INTRODUCTION

A. ANALYSIS OBJECTIVES

This thesis implements a model for the transmission of acoustic energy in shallow maritime waters. High-frequency (40-70 kHz) sound is propagated numerically through shallow (5-40 m) water channels. Parametric analysis determines the influence of environmental conditions by varying a specific factor while holding all other factors constant. This parametric analysis includes changes in the sound-speed profile (SSP) gradient, changes in transmission frequency, changes in transmission range, changes in channel depth, changes in the bottom sediment material of the channel, and changes in the height of the transmitter and the receiver in the channel.

Finally, the lessons learned from the parametric analyses are used to characterize two maritime environments where experimentation is being conducted in 2007. The testing sites are St. Andrew Bay, in Panama City, FL, and Chesapeake Bay, in Little Creek, VA. The purpose of characterizing these environments is to predict the performance of experimental communication systems before they are deployed.

B. UNDERWATER COMMUNICATIONS AND NETWORKS

Seaweb is an experimental undersea network technology consisting of medium range (500-5000 m) links between network nodes. The Seaweb wide-area network (WAN) concept includes local-area networks (LANs) having a sophisticated central node that collects and integrates undersea data from a set of simpler peripheral nodes. This local-area network with centralized topology is called Seastar and is motivated by the desire for an additional tier of local-area communications compatible with and complementary to Seaweb wide-area acoustic communications. Seastar uses a higher-frequency portion of the acoustic spectrum matched to the short range (50-500m) links. The high frequencies allow for a larger spectral bandwidth and thus a higher rate of information transfer in the LAN. The Seastar LAN and its place in the Seaweb WAN are

illustrated in Figure 1, with the red nodes representing peripheral nodes and the green nodes representing central nodes.

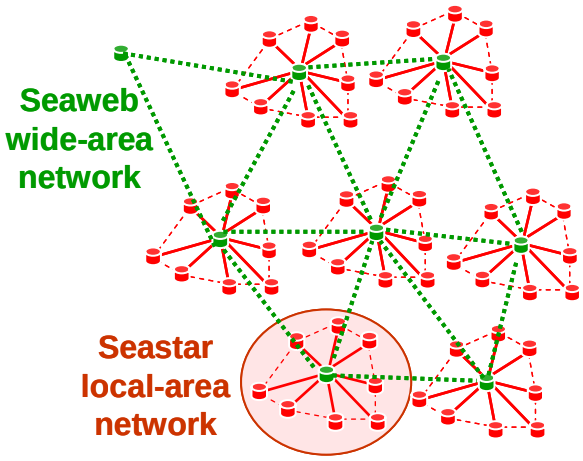

Figure 1. Seastar local-area network (LAN) concept.

The Seastar central node integrates data received from the peripheral nodes, and in turn transmits fused information to other central nodes or to a gateway node for transmission to command centers. Communications amongst central nodes and gateway nodes occur via Seaweb networking in a lower band of the acoustic spectrum.

The importance of Seastar is that it allows an order-of-magnitude increase in node density in the Seaweb infrastructure, and the use of a higher-frequency band means that central nodes can maintain both Seaweb and Seastar communications simultaneously without mutual interference. Seastar allows for high-bandwidth, low-power communications, advancing environmental sensing, intelligence preparation of the battlespace, maritime special ops, and littoral surveillance.

II. PHYSICAL BASIS FOR THE NUMERICAL MODEL

A. THEORETICAL BACKGROUND

The wave equation is a partial differential equation describing the motion of a wave in a medium. The acoustic wave equation is a linear approximation retaining only first-order terms of the wave equation. The propagation of sound in an elastic medium (such as seawater) is described mathematically by solving the acoustic wave equation while applying the appropriate boundary and medium conditions. The acoustic wave equation relates acoustic pressure p to spatial coordinates x, y, z and time t, and may be written in the standard form of the wave equation as

$$\nabla^2 p - \frac{1}{c^2}\frac{\partial^2 p}{\partial t^2} = 0 \tag{2.1}$$

where ∇ is the gradient operator, $\nabla = \frac{\partial}{\partial x} + \frac{\partial}{\partial y} + \frac{\partial}{\partial z}$, and c is the speed of sound in the medium and may vary with the spatial coordinates.[1]

1. Wave Theory

Wave theory describes sound propagation in terms of characteristic functions called normal modes, each of which is a solution to Equation (2.1). These normal modes are combined additively to satisfy the given boundary and medium conditions. Although this approach provides a formally complete solution for all frequencies, it has the disadvantages of not presenting an intuitive picture of the distribution of radiated energy, not easily handling real boundary conditions, and requiring significant computation since it tries to model the entire wave.[2]

---

[1] Robert Urick, *Principles of Underwater Sound 3rd Edition* (Los Altos: Peninsula Publishing, 1983), 120-122.

[2] *Ibid*, 122.

2. Ray Theory

Ray theory is an alternative theoretical approach to solving the wave equation. The main tenets of ray theory are the existence of a wavefront along which the phase of the solution is constant, and the existence of rays that describe the spatial location of acoustical energy radiating from the source in a manner analogous to optical ray theory. Ray tracing programs are commonly used in underwater acoustics for modeling the propagation of high-frequency acoustic waves as a function of time.[3]

Ray tracing traditionally involves integrating a set of differential equations called the ray equations, which describe the ray's trajectory. These equations are governed by given initial conditions in order to trace the path of a ray as it propagates away from the source. The amplitude of a ray is determined by the cross-section of the ray tube bounded by adjacent rays.

The main drawback associated with ray tracing is the existence of shadow zones, which are zones through which no rays pass, resulting in a pressure field of zero everywhere within them. In actuality, there is always some diffraction of sound into the areas given as shadow zones in ray tracing, resulting in a discrepancy between the exact solution and that predicted by ray tracing methods.[4]

Ray tracing is a useful tool for modeling the propagation of high-frequency sound. Ray tracing is intuitive and radiated sound is readily visualized and calculated.

B. MATHEMATICAL DERIVATION

Ray theory is mathematically derived from the acoustic wave equation. The derivation yields the time delay of the ray from source to receiver, the ratio of the pressure amplitude at the desired location to the pressure amplitude at a reference point, and the transmission loss. These functions are used to construct ray and impulse response diagrams.

---

[3] Urick, 122.

[4] *Ibid*.

The basis for ray theory is the acoustic wave equation, given in Equation (2.1). Separation of variables shows pressure depends on the three-dimensional position vector $\mathbf{x} = (x, y, z)$ and time *t,*

$$p = P(\mathbf{x}) \cdot T(t), \tag{2.2}$$

so that we are only separating the spatial and time dependences. Substituting this form into Equation (2.1) and taking the separation constant to be k^2 we obtain[5]

$$\nabla^2 P + k^2 P = 0, \qquad \frac{d^2 T}{dt^2} + k^2 c^2 T = 0. \tag{2.3}$$

The first equation in (2.3) is the time-independent version of the acoustic wave equation, called the Helmholtz equation. If we substitute $k = \omega / c$, then

$$\nabla^2 p + \frac{\omega^2}{c^2(\mathbf{x})} p = 0, \tag{2.4}$$

where $c(\mathbf{x})$ is the tri-dimensional sound speed and ω is the angular frequency of the source. Jensen et al. develop a solution of the Helmholtz equation of the form[6]

$$p(\mathbf{x}) = e^{i\omega\tau(\mathbf{x})} \sum_{j=0}^{\infty} \frac{A_j(\mathbf{x})}{(i\omega)^j}, \tag{2.5}$$

where $\tau(\mathbf{x})$ is the time it takes for the sound to reach location $\mathbf{x}$ and $A(\mathbf{x})$ is the amplitude of the signal at $\mathbf{x}$. Equation (2.5) is called the ray series. The first and second derivatives of the ray series, retaining only the first-order terms (a high-frequency approximation) gives the following infinite sequence of equations for the functions $\tau(\mathbf{x})$ and $A(\mathbf{x})$,

$$\mathrm{O}(\omega^2): \ |\nabla \tau|^2 = \frac{1}{c^2(\mathbf{x})} \tag{2.6}$$

$$\mathrm{O}(\omega): \ 2\nabla\tau \cdot \nabla A_0 + (\nabla^2 \tau) A_0 = 0 \tag{2.7}$$

---

[5] Kenneth F. Riley et al., *Mathematical Methods for Physics and Engineering* (Cambridge: Cambridge University Press, 1998), 566.

[6] Finn B. Jensen et al., *Computational Ocean Acoustics* (New York: Springer-Verlag, 2000), 143-151.

so that the solution to the Helmholtz equation is a product of a phase function, called the eikonal equation, and an amplitude function, called the transport equation.

To solve the eikonal equation, a family of rays perpendicular to the wavefronts of $\tau(\mathbf{x})$ are introduced. This family of rays defines a new coordinate system in ray coordinates in terms of the arc length, s. The ray trajectory is then defined by the differential equation

$$\frac{d\mathbf{x}}{ds} = c\nabla\tau \tag{2.8}$$

which can be squared to yield

$$\left|\frac{d\mathbf{x}}{ds}\right|^2 = c^2\left|\nabla\tau\right|^2. \tag{2.9}$$

Substituting Equation (2.6) into Equation (2.9) shows that the tangent vector $d\mathbf{x}/ds$ has unit length. Taking the Cartesian coordinates of Equation (2.8) and differentiating with respect to the arc length s gives the resultant vector equation for the ray trajectories

$$\frac{d}{ds}\left(\frac{1}{c}\frac{d\mathbf{x}}{ds}\right) = -\frac{1}{c^2}\nabla c \tag{2.10}$$

In cylindrical coordinates (r, z) the ray equations can be written in the first-order form

$$\begin{aligned} \frac{dr}{ds} &= c\xi(s), & \frac{d\xi}{ds} &= -\frac{1}{c^2}\frac{dc}{dr}, \\ \frac{dz}{ds} &= c\varsigma(s), & \frac{d\varsigma}{ds} &= -\frac{1}{c^2}\frac{dc}{dz}, \end{aligned} \tag{2.11}$$

where integrating these equations gives the trajectory of the ray [$r(s)$, $z(s)$]. For these equations, ξ and ζ are auxiliary variables arbitrarily introduced so the equations may be written in first-order form.

The initial conditions for solving the ray equations are that the ray starts at the source position (r_s, z_s) with a specified vertical launch angle θ, as shown in Figure 2.

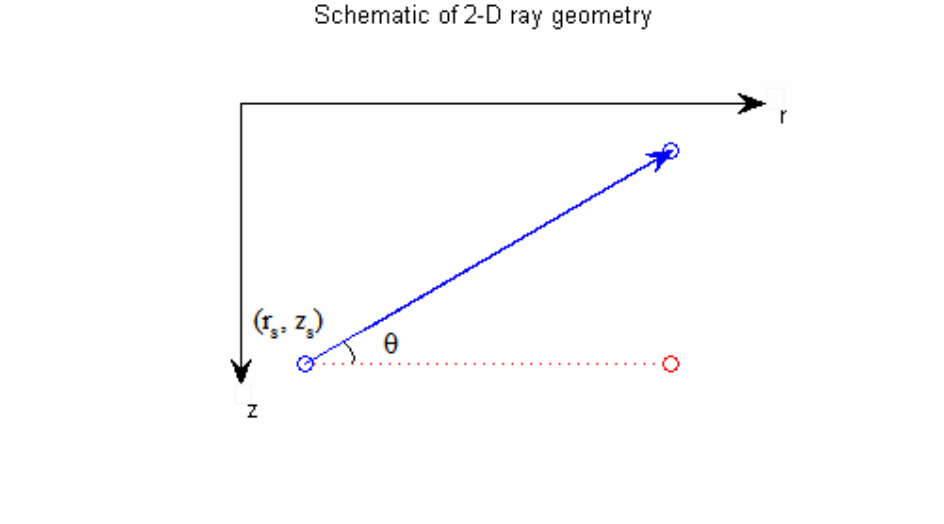

Figure 2. Schematic of 2-D ray geometry.

Thus we have

$$r = r_s, \qquad \xi = \frac{\cos\theta}{c(0)}, \tag{2.12}$$

$$z = z_s, \qquad \varsigma = \frac{\sin\theta}{c(0)}. \tag{2.13}$$

To obtain the pressure field the phase and amplitude of each ray are required. The phase is obtained by solving the eikonal equation in the ray coordinate system. Expanding Equation (2.6),

$$\nabla\tau \cdot \nabla\tau = \frac{1}{c^2}, \tag{2.14}$$

so that substituting the value of $\nabla\tau$ from Equation (2.8),

$$\nabla\tau \cdot \frac{1}{c}\frac{d\mathbf{x}}{ds} = \frac{1}{c^2}, \tag{2.15}$$

then

$$\frac{d\tau}{ds} = \frac{1}{c}. \tag{2.16}$$

Integrating this equation with respect to s yields

$$\int_0^s d\tau = \int_0^s \frac{1}{c(s)} ds$$

$$\tau(s) - \tau(0) = \int_0^s \frac{1}{c(s)} ds$$

$$\tau(s) = \tau(0) + \int_0^s \frac{1}{c(s)} ds \,. \tag{2.17}$$

The integral term in this equation is the travel time along a ray (time delay), so that the phase of the wave is delayed in accordance with its travel time.

The amplitude is obtained by solving the transport equation. Since the rays are perpendicular to the wavefronts, Equation (2.7) can be rewritten as

$$\frac{2}{c}\frac{d\mathbf{x}}{ds} \cdot \nabla A_0 + (\nabla^2 \tau) A_0 = 0 \tag{2.18}$$

which gives

$$\frac{2}{c}\frac{dA_0}{ds} + (\nabla^2 \tau) A_0 = 0 \,. \tag{2.19}$$

This equation thus states that the amplitude along a ray changes in relation to the spreading of a ray tube, which is the space bounded by two adjacent rays. the solution to the transport equation can be simplified by using the three-dimensional Jacobian determinant . Since the Jacobian satisfies the following condition,

$$\nabla^2 \tau = \frac{1}{J}\frac{d}{ds}\left(\frac{J}{c}\right) \tag{2.20}$$

Equation 2.19 then becomes

$$2\frac{dA_0}{ds} + \left[\frac{c}{J}\frac{d}{ds}\left(\frac{J}{c}\right)\right] A_0 = 0 \,. \tag{2.21}$$

Integrating this equation from 0 to s gives the solution for the transport equation

$$A_0(s) = A_0(0)\left|\frac{c(s)J(0)}{c(0)J(s)}\right|^{1/2}. \tag{2.22}$$

The sound pressure for a point source in a homogenous medium is defined as

$$p_0(s) = A_0(s)e^{i\omega\tau} = \frac{e^{i\omega s/c_0}}{4\pi s}. \tag{2.23}$$

So it follows that $A_0(s)$ and $\tau_0(s)$ are given by

$$A_0(s) = \frac{1}{4\pi s} \tag{2.24}$$

and

$$\tau_0(s) = \frac{s}{c_0}. \tag{2.25}$$

Substituting the limit of the quantity $A_0(0)\cdot J(0)$ into Equation (2.22) yields

$$A_0(s) = \frac{1}{4\pi}\left|\frac{c(s)\cos\theta}{c(0)J(s)}\right|^{1/2}, \tag{2.26}$$

so the sound pressure as a function of arc length s is

$$p(s) = \frac{1}{4\pi}\left|\frac{c(s)\cos\theta}{c(0)J(s)}\right|^{1/2} e^{i\omega\int_0^s \frac{1}{c(s)}ds}. \tag{2.27}$$

Thus, the pressure field is obtained by dividing the energy of the point source among each of the ray tubes. Since a point source in a shallow water channel follows spherical spreading, the sound pressure amplitude of a ray tube diminishes with range s by the factor $1/s^2$. The ratio of the pressure at a point a distance s from the source, $p(s)$, to the intensity measured at 1 m from the source, p_0, defines the transmission loss at that point. For convenience, the transmission loss along each ray tube is usually given in decibels (dB):

$$TL(s) = -20\log\frac{p(s)}{p_0} \tag{2.28}$$

The total pressure at the receiver will depend on the way in which the rays constructively and destructively interfere with each other.

III. BELLHOP

A. MODEL DESCRIPTION

Bellhop is a Gaussian beam tracing acoustic propagation model developed in 1987 by Porter and Bucker[7] at the Space and Naval Warfare Systems Center in San Diego. Bellhop was chosen for this analysis since it has proven to be an accurate modeling tool for high-frequency (>1 kHz) transmissions.

Bellhop is a range-independent program, which means that it assumes that the sound-speed profile (SSP), the surface and bottom properties, and the bathymetry of the ocean floor do not vary with range. Propagation is computed for a 2-dimensional vertical slice of the medium, under the assumption that this result applies for all bearings. These assumptions allow a reduction in the computational times. Bellhop includes an option that allows the program to import a bathymetry file, but this function was not used as part of the following set of analysis.

Bellhop uses Gaussian beam tracing to produce the ray-trace and impulse-response plots. Gaussian beam tracing uses standard ray tracing to describe a central ray, about which a beam is formed whose intensity decays on a normal from the ray following a Gaussian distribution. Beam tracing is computationally more efficient while being mathematically equivalent to standard ray tracing and it allows for a transition of the beams into shadow zones, thus mitigating an aforementioned drawback of simple ray tracing.

Bellhop is able to trace a user-defined fan of rays emitted from a sound source whose coordinates and frequency are specified by the user. It also calculates the amplitude and arrival time of an impulse signal arriving at the receiver via each ray path. Bellhop can also compute the intensity of the sound field at the receiver by finding only the rays that reach the receiver. These rays are called eigenrays.

---

[7] Michael B. Porter and Homer P. Bucker, "Gaussian beam tracing for computing ocean acoustic fields," *The Journal of the Acoustical Society of America* 82 (1987): 1349-1359.

B. INPUT ENVIRONMENT FILE

The main input file to Bellhop is called the environment file. The environment file is a simple text file given in a structured format specifying the details of the environment, the source and receiver characteristics, and the type of analysis to be performed. The environment information includes the sound-speed profile, the depth of the channel, the channel bottom composition, and surface boundary conditions. The source and receiver characteristics include the transmission frequency, the source and receiver locations, the angle limits for the fan of beams and the number of beams used. The type of analysis specified dictates the output of the algorithm in the form of a ray file, an eigenray file, an amplitude-delay file, or any of three different types of transmission loss files (coherent, incoherent and semi-coherent).

C. OUTPUT PRODUCTS

1. Ray-Trace Plots

Information in the output ray file can produce a plot showing the paths traveled by all the rays specified in the environment file. The plot has depth on the vertical axis and range on the horizontal axis. The rays in the plots presented in Appendix B are in three colors. A red ray is a direct path between the source and the receiver, generally signifying that this is the strongest path. A blue ray has only one reflection between the source and receiver, which signifies an intermediate strength path. A black ray has multiple surface and bottom reflections between source and receiver, meaning this is the weakest type of path. Ray-trace plots show all rays regardless of whether they pass through the receiver or not. This is useful for visualizing the radiated energy distribution in the channel.

2. Eigenray Plots

Bellhop can selectively plot the paths traveled by only those rays that reach the receiver. Since Bellhop uses geometric beams in its calculations, the eigenrays include those ray tubes where the receiver is between the adjacent rays. This plot has the same

axes and color scheme as the ray-trace plot. This plot displays the multipath propagation from source to receiver.

3. Impulse Response Plots

Bellhop can also create an amplitude-delay file, which is a text file stating transmission frequency, channel depth, source and receiver geometry and number of eigenrays. Also included is information about each eigenray such as amplitude, time delay, phase shift at the receiver, and the number of surface and bottom bounces experienced by the eigenray. An algorithm using the information in this file to plot the impulse response $h(\tau)$ is developed and listed in Appendix A. The impulse response $h(\tau)$ is defined as the output of the receiver to a very brief signal from the source, called an impulse.[8] The plot has the dimensionless amplitude at the receiver in the vertical axis and the time delay in seconds in the horizontal axis. The impulse response plot shows the time dispersion of an initial impulse at the source into multiple impulses at the receiver. This time dispersion is caused by the different pathlengths and travel times associated with each ray. An important implication of this multipath time dispersion of signal energy is the possibility of intersymbol interference for acoustic communications.

The implementation of Bellhop used here neglects the possibility of dispersion in the frequency domain, such as that occurring as a result of Doppler shift and Doppler spread associated with a moving source and/or receiver, and a non-stationary channel.

[8] Johnny R. Johnson, *Introduction to Digital Signal Processing* (Englewood Cliffs: Prentice Hall, 1989), 51.

THIS PAGE INTENTIONALLY LEFT BLANK

IV. SHALLOW WATER PARAMETRIC ANALYSIS

A. STANDARD CHANNEL DEFINITION

The standard channel is defined for this parametric analysis to be 10 m deep with a sand bottom boundary and a vacuum over the surface boundary, a source-to-receiver horizontal range of 500 m, and both source and receiver 1 m above the seabed. The standard transmission is assumed to be at 70 kHz with source power of 1 W. Three generic sound-speed profiles are analyzed. These three profiles (salinity-driven, temperature-driven and isospeed) represent typical conditions encountered in shallow water and are illustrated in Figure 3.

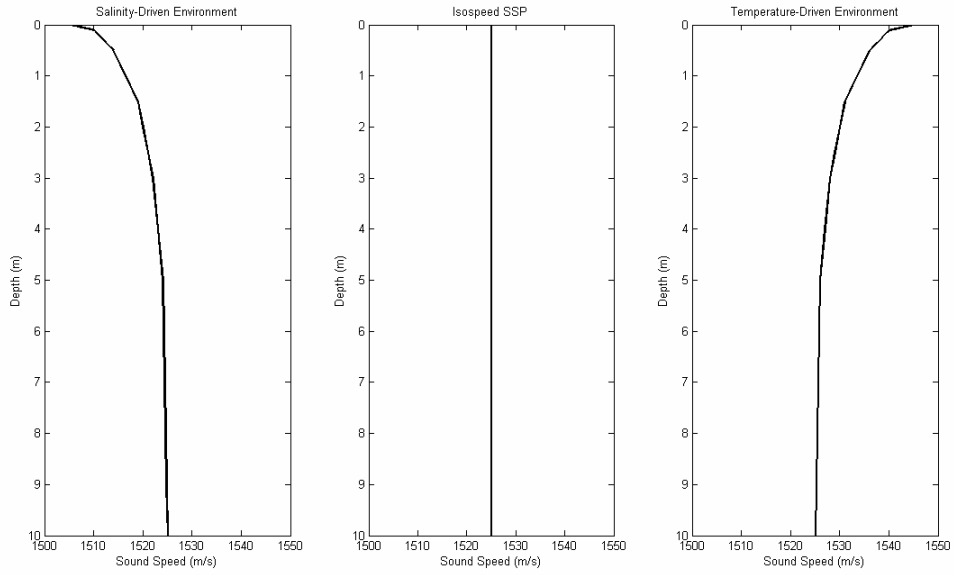

Figure 3. Sound-speed profiles (SSP) used in the parametric analyses

B. TRANSMITTER

The source level (SL) of a transmitter is defined as [9]

$$SL = \frac{I_{source@1m}}{I_{ref}}. \tag{4.1}$$

The source level of an omnidirectional projector is referenced to a standard range of 1 m from its acoustic center. At a radius of 1 m, the acoustic center is surrounded by a sphere of surface area

$$A_{sph} = 4\pi r^2 \Rightarrow A_{sph} = 12.6\,\text{m}^2. \tag{4.2}$$

If the power of the transmitter is given by P_{xmt}, the source intensity at 1 m is given by

$$I_1 = \frac{P_{xmt}}{12.6}\,\text{W/m}^2. \tag{4.3}$$

The standard reference pressure used in underwater acoustics is 1 μPa, which is approximately equivalent to $0.67 \cdot 10^{-18}$ W/m^2.[10] Using this conversion and Equation (4.3) the source level becomes

$$SL = \frac{P_{xmt}}{12.6} \cdot \frac{1}{0.67 \cdot 10^{-18}} \Rightarrow SL = 10\log(P_{xmt}) + 170.8\,\text{dB re 1 μPa @ 1 m}. \tag{4.4}$$

If we assume the source has a power of 1 W, then the source level is

$$SL = 10\log(1) + 170.8\,\text{dB re 1 μPa @ 1 m} \Rightarrow SL = 170.8\,\text{dB re 1 μPa @ 1 m}. \tag{4.5}$$

The amplitude-delay file produced by Bellhop contains the ratio of the pressure amplitude at the desired distance divided by the pressure amplitude at the source. The transmission loss is then calculated by using Equation 2.28. The amplitude of the sound signal at the receiver is obtained by

---

[9] Ashley D. Waite, *SONAR for Practising Engineers* (West Sussex: John Wiley & Sons Ltd., 2002), 4-5.

[10] Lawrence E. Kinsler et al., *Fundamentals of Acoustics 4th Edition* (New York: John Wiley & Sons, 2000), 131.

$$A(s) = SL - TL(s)\,, \tag{4.7}$$

where *A(s)* is given in dB. This amplitude is used as the vertical axes for all the summary figures and impulse response figures developed in this analysis, since this amplitude is a function of all the parameters being varied.

C. MARSH & SCHULKIN EQUATION

In 1962, Marsh and Schulkin[11] developed an equation for transmission loss in shallow water. The transmission loss in these media is dependent upon variables of the sea surface, water channel and sea botton. Since the channel is very sensitive to changes of these variables, the predicted transmission loss can only be approximated. The empirical basis for the Marsh & Schulkin equation is 100,000 sound level measurements they made in shallow water. The applicability of the equation is contingent upon determination of a factor *H*, which is defined as

$$H = \left(\frac{3.3}{8} D\right)^{1/2} \tag{4.8}$$

where *D* is the water depth in meters. Table 1 shows the value of *H* for the different channel depths used in this study.

D *(m)*	**H** *(km)*
5	1.44
10	2.03
20	2.87
40	4.06

Table 1. Marsh & Schulkin equation parameter H for different channel depths

There are three different transmission loss equations depending upon the relationship between *H* and the transmission range *r*. For this analysis only one equation

[11] H. W. Marsh et al., "Shallow Water Transmission." *The Journal of the Acoustical Society of America* 34 (1962): 863-864.

will be used since all of the transmission ranges used in this analysis are smaller than H. For this condition, the transmission loss in dB is given by

$$TL = 20 * \log\left(\frac{r}{.914}\right) + \alpha\left(\frac{r}{.914}\right) + 60\,\text{dB}, \tag{4.9}$$

where r is the transmission range in km, α is the absorption coefficient, 1/0.914 is the conversion factor between km and kyd, and 60 dB accounts for the factor of 1000 between m and km. Equation (4.9) is different from Equation (2.28) since the former computes transmission loss on the channel while the latter computes the transmission loss on a single ray tube. The Marsh & Schulkin equation for transmission loss is used as a baseline for comparison with the transmissions in this analysis.

D. SOUND-SPEED PROFILE (SSP)

Variations in sound velocity result in refraction of the sound rays. Sound velocity is influenced by temperature, salinity and water pressure. Temperature effects are mainly due to surface solar heating, nocturnal cooling and wind action. The salinity of seawater can vary due to precipitation, fresh-water runoff and mixing. Water pressure is a linear function of depth. The combination of these factors can lead to a wide array of sound-speed profiles. The purpose of this section is to analyze seven different profiles to identify advantageous and disadvantageous conditions for transmission. The salinity-driven and temperature-driven profiles are plotted in Figure 3, and the five linear sound-speed profiles are plotted in Figure 4.

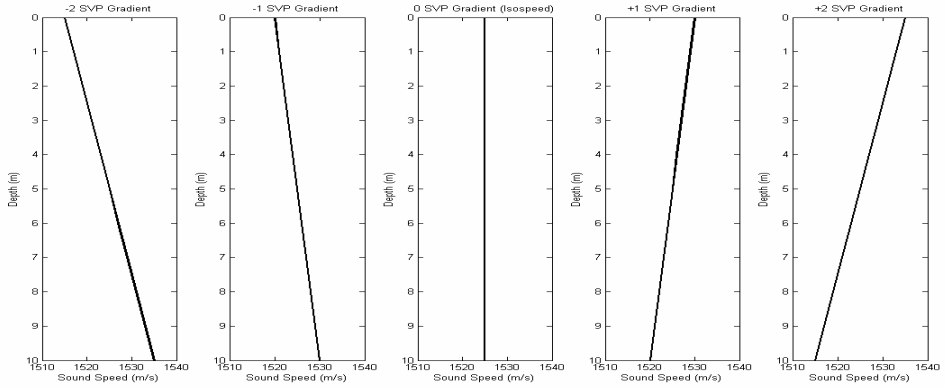

Figure 4. Linear sound-speed profiles (SSP)

Figure 5 shows the amplitudes obtained for seven different types of sound velocity profiles. The isospeed and temperature-driven profiles are observed to be similar in strength since they both have direct paths between the transmitter and receiver. The -2 SSP gradient profile is observed to strongly focus the sound energy towards the bottom of the channel. It is hypothesized that this focusing of energy and constructive interference contribute to this profile being the strongest; conversely, it is hypothesized that the +2 SSP gradient, a strongly linear upward refracting profile focuses the energy towards the top of the channel and therefore away from the receiver, so it displays the smallest amplitude. Small linear changes in the profile (+1 and -1 SSP gradients) and the salinity-driven profile are observed to disrupt the direct path of transmission but not the secondary paths, so they reduce the magnitude of the largest amplitude but not as drastically as the +2 SSP gradient profile.

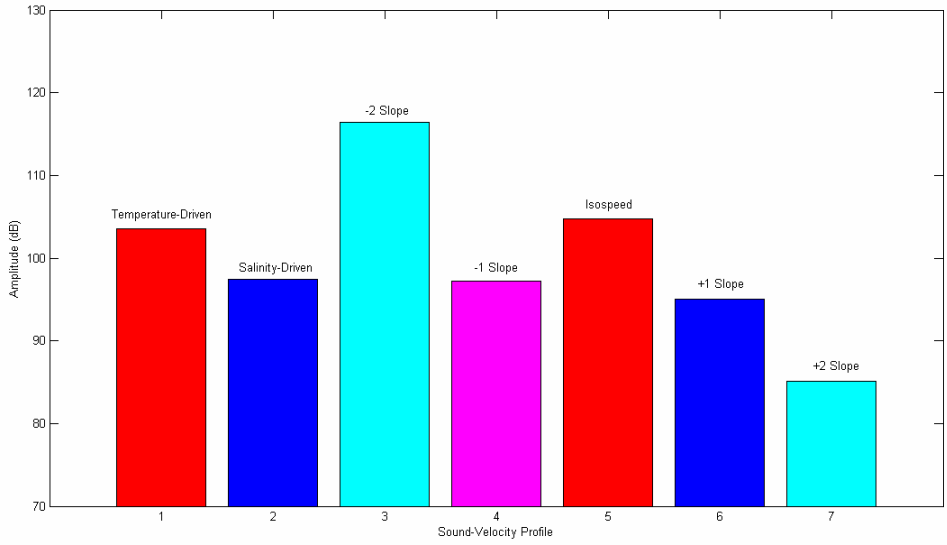

Figure 5. Impact of sound-speed profile (SSP)

E. TRANSMISSION FREQUENCY

When sound propagates in the ocean, part of the acoustic energy is absorbed and scattered by the medium. The combination of absorption and scattering effects is called attenuation and it is frequency-dependant. The quantity α is the logarithmic absorption coefficient, and it is expressed in units of dB/km. The following expression, developed by W. H. Thorp, relates frequency in kHz to the attenuation coefficient[12]

$$\alpha \cong 3.3x10^{-3} + \frac{0.11f^2}{1+f^2} + \frac{44f^2}{4100+f^2} + 3.0x10^{-4} f^2 . \qquad (4.10)$$

The attenuation coefficient α for frequencies in the 40-70 kHz band is calculated using Equation (4.10) and presented in Table 2 and Figure 6. These results show that as the frequency increases, the value of the attenuation coefficient increases as well, which leads to a greater transmission loss and thus smaller amplitude at the receiver. The theory thus predicts a reduction in amplitude at the receiver for each increase in frequency.

Frequency (kHz)	α (dB/km)
40	12.5
45	14.7
50	16.8
55	18.8
60	20.7
65	22.5
70	24.1

Table 2. Attenuation coefficients for the 40-70 kHz band

[12] Urick, 108.

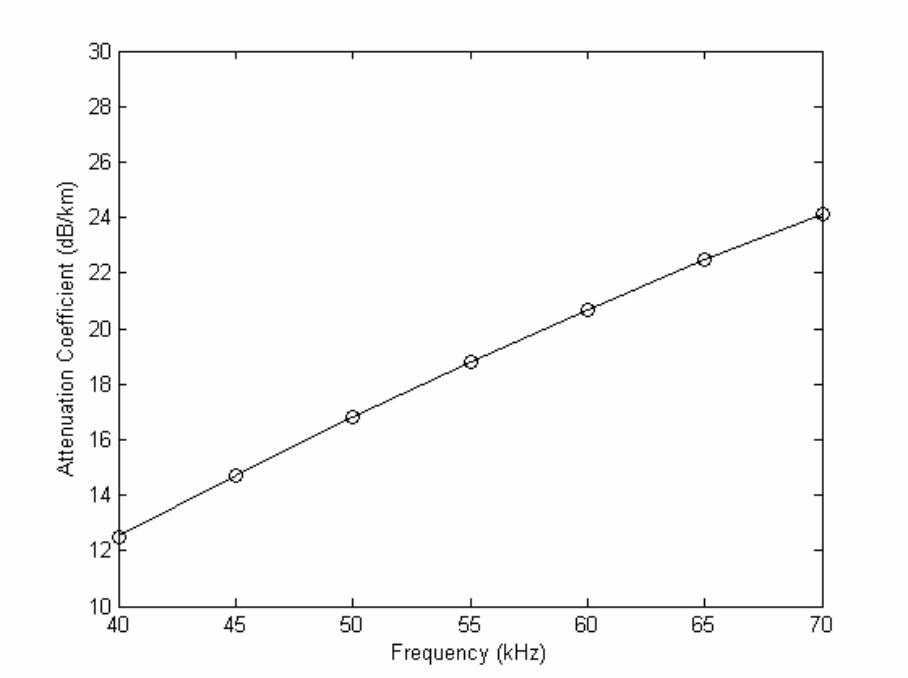

Figure 6. Attenuation coefficient vs. frequency

The results for the frequency parametric analysis are summarized in Figure 7. The figure shows that the isospeed environment and the temperature-driven environment behave as predicted by the theory, with diminishing amplitudes at the receiver for increasing frequencies. The figure also shows that the profiles behave similarly to the Marsh & Schulkin equation prediction.

In the salinity-driven case, the 40-45 kHz band and the 50-70 kHz band also behave as predicted. In the 45-50 kHz band, however, there is an increase in the amplitude at the receiver for increasing frequency. The reason for this anomaly is that the Bellhop algorithm apparently attributes the maximum impulse for the 40-50 kHz band and the 50-70 kHz band to different paths. Since the frequency is the only parameter being changed, the geometrical distribution of the rays should not change and the path or the maximum impulse should be the same for all frequencies.

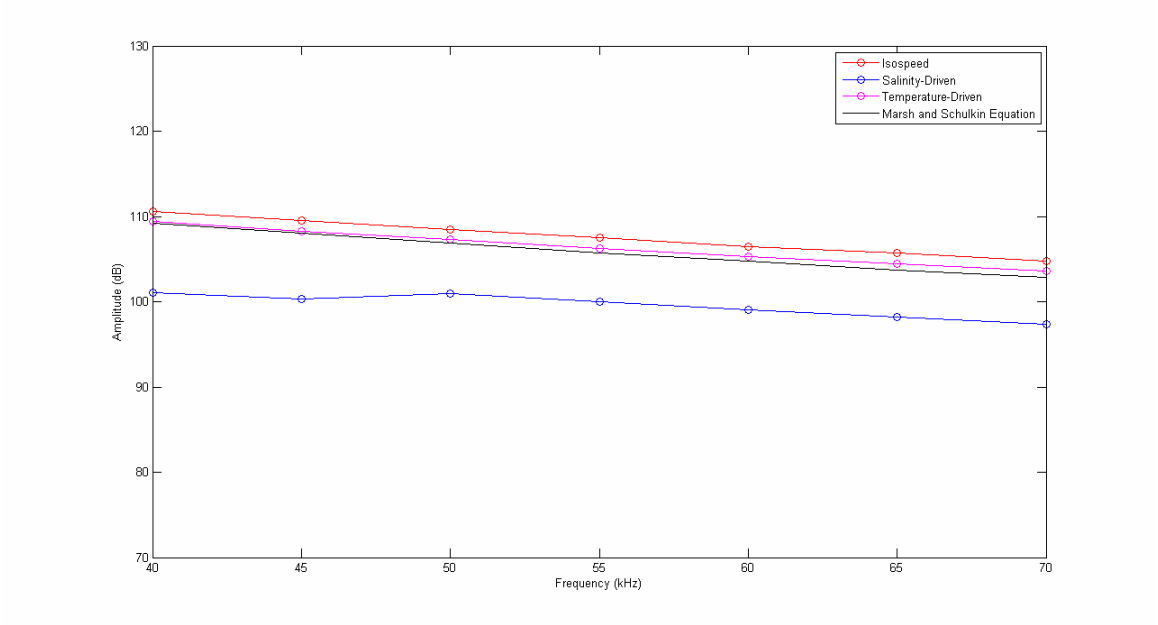

Figure 7. Impact of transmission frequency

F. TRANSMISSION RANGE

Sound produced by an omnidirectional point source in a homogenous, lossless and unbounded medium is radiated equally in all directions so as to be equally distributed over the surface of a sphere surrounding the source.[13] The intensity decreases as the square of the range, so the transmission loss is then

$$TL = 20\log(r) + \alpha \cdot (r/1000), \tag{4.11}$$

where r is in meters, α is the attenuation coefficient given in dB/km and the transmission loss has units of dB.

Sound produced by a point source propagating through a medium limited by plane-parallel surface and bottom boundaries is approximated as distributed over the surface of a cylinder having a radius equal to range and a height equal to the depth of the

[13] Urick, 100

channel.[14] The intensity of the sound is then inversely proportional to the surface of the cylinder, and the transmission loss increases proportionally to the transmission range.

$$TL = 10\log(r) + \alpha \cdot (r/1000), \tag{4.12}$$

where r is in meters, α is the attenuation coefficient given in dB/km, and the transmission loss has units of dB.

Figure 8 is a comparison of the amplitude at the receiver for a 1-W, 70-kHz source for three different transmission loss assumptions (cylindrical, spherical, and Marsh & Schulkin equation). The figure shows that cylindrical spreading causes the least amount of transmission loss, since the energy is reflected back into the channel from the boundaries. Spherical spreading causes more severe transmission loss since no energy is reflected back into the channel. The Marsh & Schulkin equation produces the greatest amount of transmission loss and most closely matches the Bellhop results. All three transmission loss equations display similar trends for increasing range.

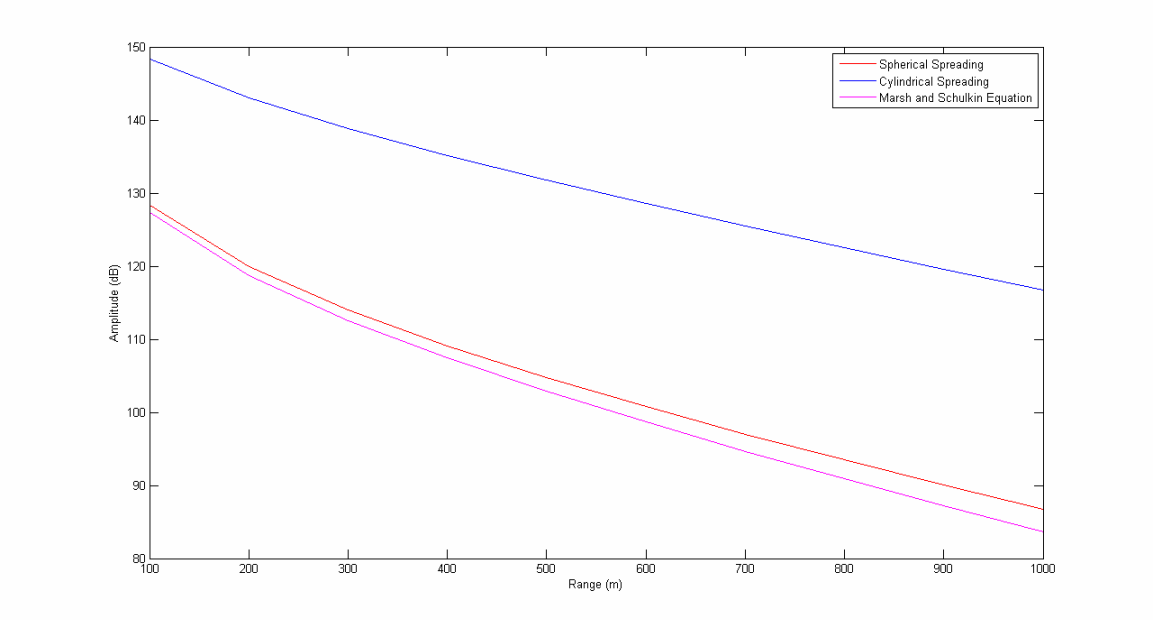

Figure 8. Amplitude vs. range for three different types of transmission loss

[14] *Ibid*, 102.

Figure 9 shows the amplitude at the receiver for the three different types of sound-speed profile at different transmission ranges. The figure shows that the temperature-driven profile gives the largest amplitude for distances less than 475 m. For distances greater than 475 m, the isospeed profile gives the largest amplitude. The figure also shows that the temperature-driven and salinity-driven environments follow similar trends, and that the isospeed profile closely resembles the prediction from the Marsh & Schulkin equation.

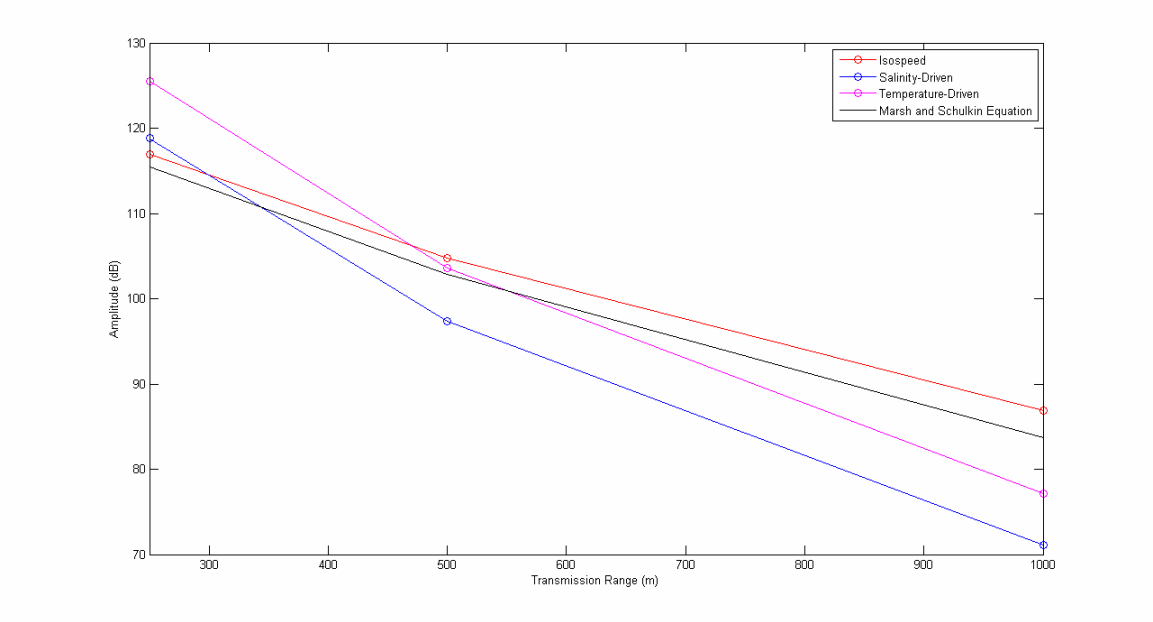

Figure 9. Impact of transmission range

G. CHANNEL DEPTH

Four different channel depths (5, 10, 20 and 40 m) are analyzed. Table 1 shows that these depths fall within the condition of the Marsh & Schulkin equation. To obtain the 5 m deep channel, the 10 m standard profiles are cut at the 5 m mark. To obtain the 20 m and 40 m deep channels, it is assumed that all the profiles are nearly isospeed at the bottom. Thus, isospeed extrapolation completes the profile. All tests have the transmitter and receiver 1 m from the bottom of the channel. Figure 10 shows the amplitude at the receiver for the three sound-speed profiles at different channel depths. The figure shows

that, since there is no variation in the Marsh & Schulkin equation parameters, the amplitude at the receiver is predicted to be constant. The isospeed profile closely resembles this prediction. The temperature-driven profile displays a poor transmission in the 5 m channel, but a transmission nearly identical to the isospeed profile in the 10 m channel, and closely approximating the Marsh & Schulkin results for the deeper channels. The salinity-driven profile has good transmission at 5 m depth, followed by the poorest transmission quality at 10 m depth and transmission similar to the temperature-driven profile in the deeper channels.

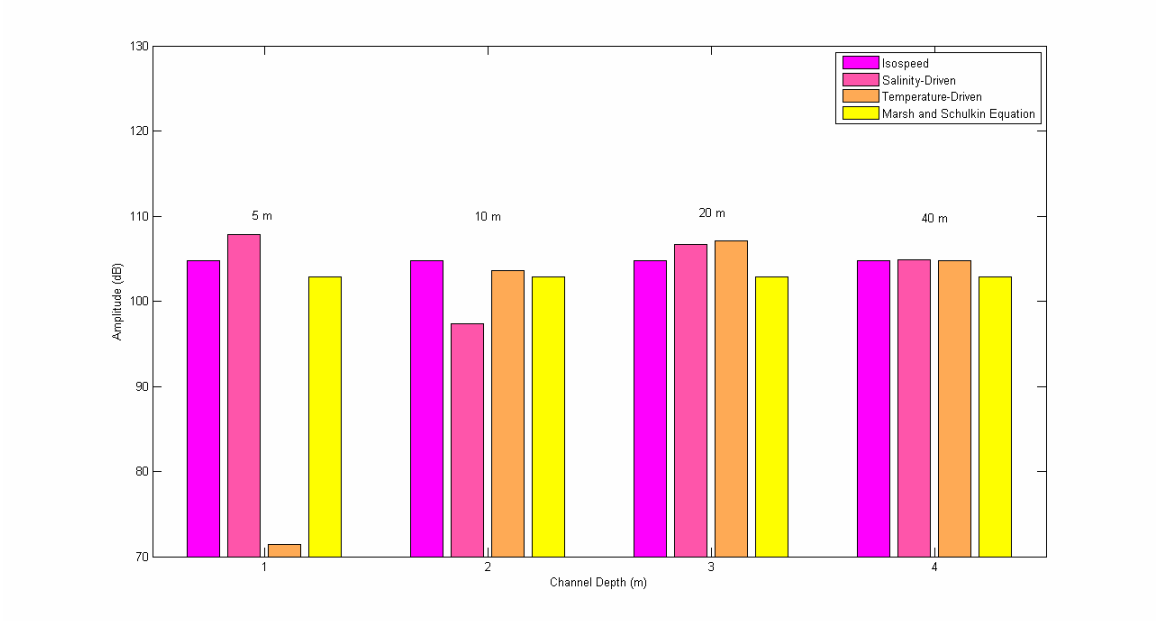

Figure 10. Impact of channel depth

H. BOTTOM SEDIMENT MATERIAL

The composition of the ocean bottom is an important parameter since sound energy interacts with the seafloor. Ocean bottom sediment materials are often modeled as fluids, so they only support compressional sound waves. This is an acceptable approximation since the shear speed of the sediment in usually considerably less than that of a solid. High-frequency sound energy does not deeply penetrate the seabed, so it is acceptable to assume that the entire seafloor is homogenous, neglecting the underlying

strata below the sediment.[15] Parametric analysis of transmission quality for different bottom sediment materials indicates which geoacoustic property is more important in determining the transmission absorption characteristics of the material. Table 3 shows the geoacoustic properties of the most common bottom sediment materials. ρ_b/ρ_w is the ratio of the material density to seawater density, c_p is the compressional wave speed, c_p/c_w is the ratio of material compressional wave speed to seawater compressional wave speed, and α_p is the compressional wave attenuation.

Bottom Type	***Porosity*** (%)	ρ_b/ρ_w	c_p (m/s)	c_p/c_w	α_p (dB/λ_p)
Sand	45	1.9	1650	1.10	0.8
Clay	70	1.5	1500	1.00	0.2
Silt	55	1.7	1575	1.05	1
Gravel	35	2.0	1800	1.20	0.6

Table 3. Geoacoustic properties of channel bottom sediment materials[16]

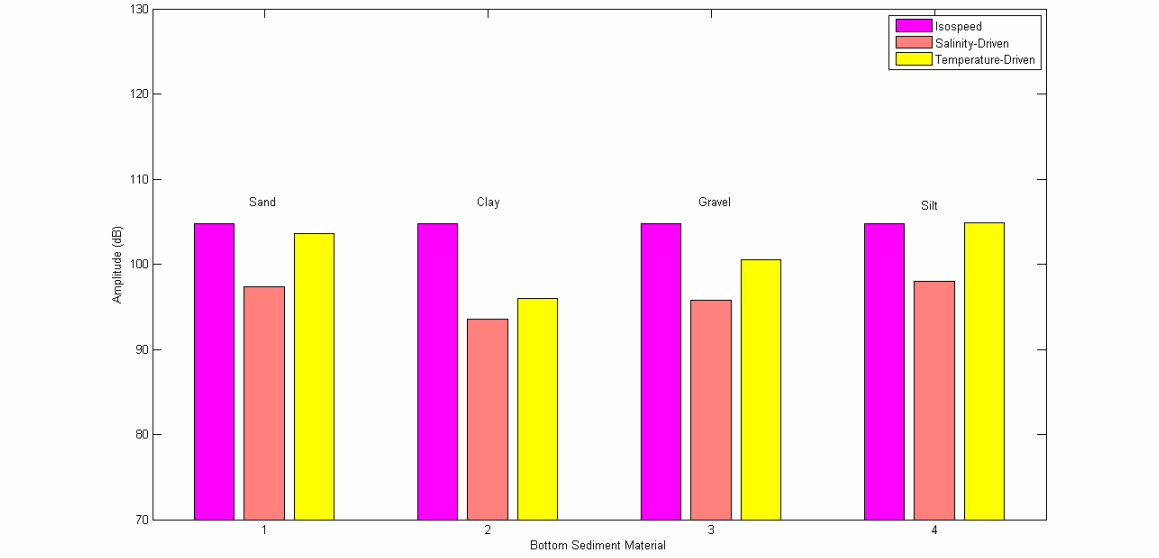

Figure 11. Impact of bottom sediment material

[15] Jensen, 38.

[16] *Ibid.*

Figure 11 is the summary of the tests done for different bottom sediment materials. The figure shows that the temperature-driven and salinity-driven environments exhibit similar trends regarding the order of the strength of the signals at the receiver. For both cases, the silt sediment gave the strongest signal, followed by sand, gravel and clay. The only geoacoustic parameter in which the silt has the greatest magnitude is the compressional wave attenuation, and the order in magnitudes for this parameter reflects the order of transmission strength, so the value of the compressional wave attenuation is hypothesized to be the dominating factor in attenuating the signal.

For an isospeed environment, the value of the maximum path strength does not change since the maximum amplitude is the result of a direct path between the source and the receiver, which is unaffected by the characteristics of the bottom sediment. As` expected, the secondary arrivals are observed to follow the same trend as the maximum arrivals in the salinity and temperature-driven cases.

I. TRANSMITTER AND RECEIVER GEOMETRY

Nine different combinations of receiver and transmitter height in the channel were tested for each sound-speed profile. The transmitter and receiver were placed at heights of 1, 2 and 4 m above the seabed. Figure 12 shows the amplitude at the receiver for transmissions in the standard channel with a salinity-driven environment. The figure shows that eight out of the nine combinations display very similar transmission qualities. The transmission with both transmitter and receiver at 4 m is hypothesized to have higher amplitude due to the presence of a strong single surface bounce path.

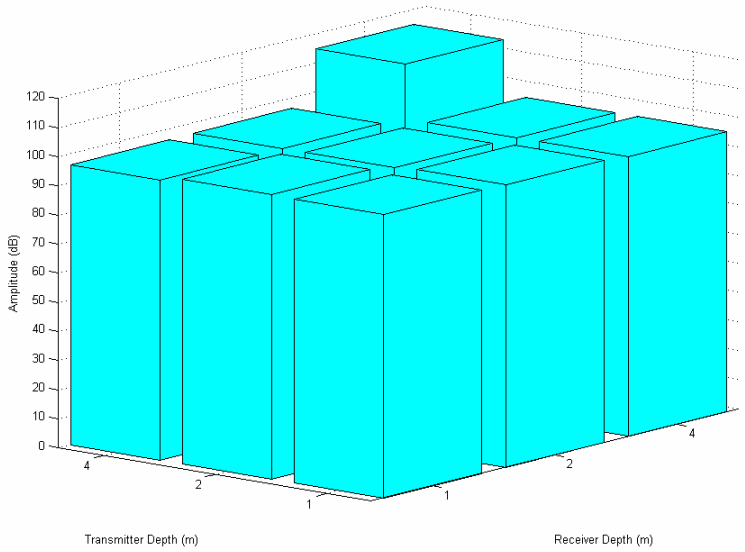

Figure 12. Amplitude for different transmitter and receiver geometries for a salinity-driven environment

Figure 13 shows the amplitude at the receiver for transmissions in the standard channel with a temperature-driven profile. As in the salinity-driven profile, most of the transmissions are observed to have similar amplitudes. In the temperature-driven profile, however, it is observed that transmissions with receiver and transmitter at the same height are stronger than those with dissimilar heights. The transmission with both transmitter and receiver at 4 m is hypothesized to have the highest amplitude due to a strong single bottom bounce path. This amplitude is slightly less than the maximum amplitude in the salinity-driven profile because of losses in the bottom boundary.

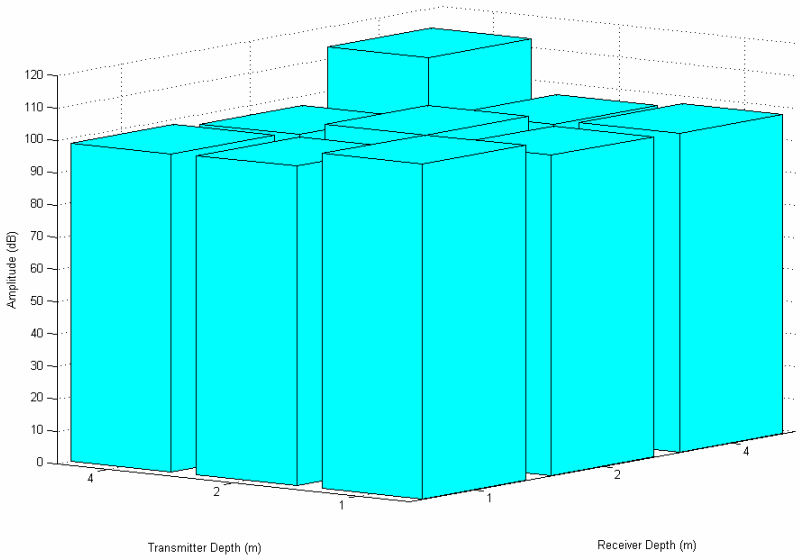

Figure 13. Amplitude for different transmitter and receiver geometries for a temperature-driven environment

Figure 14 shows the amplitude at the receiver for transmissions in the standard channel with an isospeed profile. The figure shows no change in the maximum amplitude with changes in transmitter and receiver geometry. This is because the maximum amplitude in this case is from an unrefracted direct path between source and receiver, and no changes in transmitter-receiver geometry affect that straight-line path.

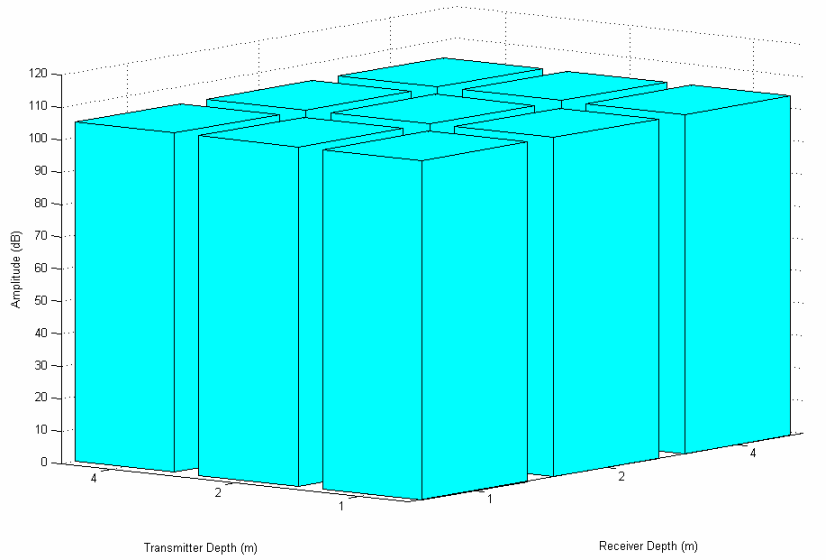

Figure 14. Amplitude for different transmitter and receiver geometries for an isospeed environment

V. MARITIME ENVIRONMENT CHARACTERIZATION

A. ST. ANDREW BAY, PANAMA CITY, FLORIDA

The first maritime environment considered is St. Andrew Bay, Florida, where transmission experiments are taking place in June 2007. Sound-speed profile data were obtained during testing here in July 2003. Conductivity-Temperature-Depth (CTD) measurements were performed through the channel to determine the sound-speed profile. Figure 15 shows the bathymetry at the site.

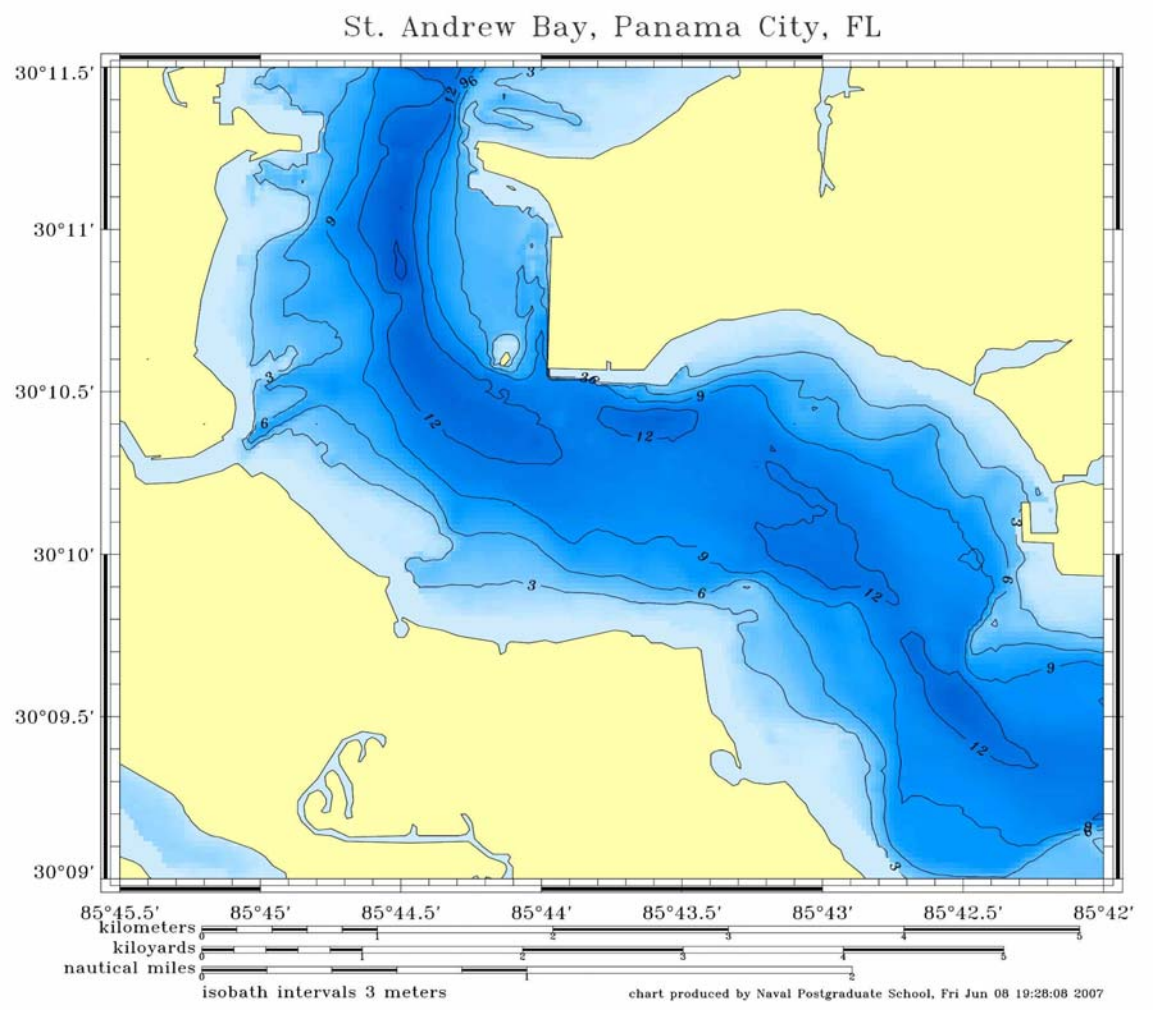

Figure 15. Bathymetric chart of St. Andrew Bay, Panama City, FL

The average channel depth for this location is 10 m, and the desired transmission range is 500 m. Planned transmissions in this channel are in the 9-14 kHz band, with the model assuming a 14-kHz transmission since the upper band displays the highest amount of transmission loss due to frequency-dependence. The 2003 test revealed that the bay is characterized by the presence of warmer, fresher, less conductive, and less dense water overlaying colder, more saline, more conductive, denser water due to fresh water from rivers and rain run-off with variations in the profile due to the interaction of these two layers. The sound-speed profiles were compiled over a span of 7 days. The average SSP for three different days are illustrated in Figure 16.

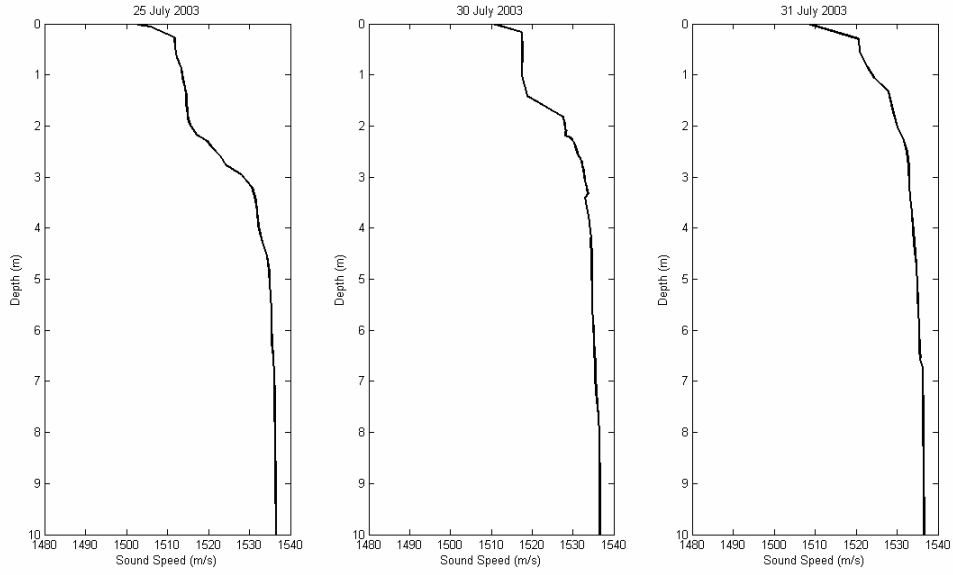

Figure 16. July 2003 average sound-speed profiles in the shallow-water channel in St. Andrew Bay, Panama City, FL

The figure shows that all profiles are salinity-driven, with sound speed increasing with depth, resulting in upward-refracting propagation. The test also found that the bottom material composition was a mud/silt combination.

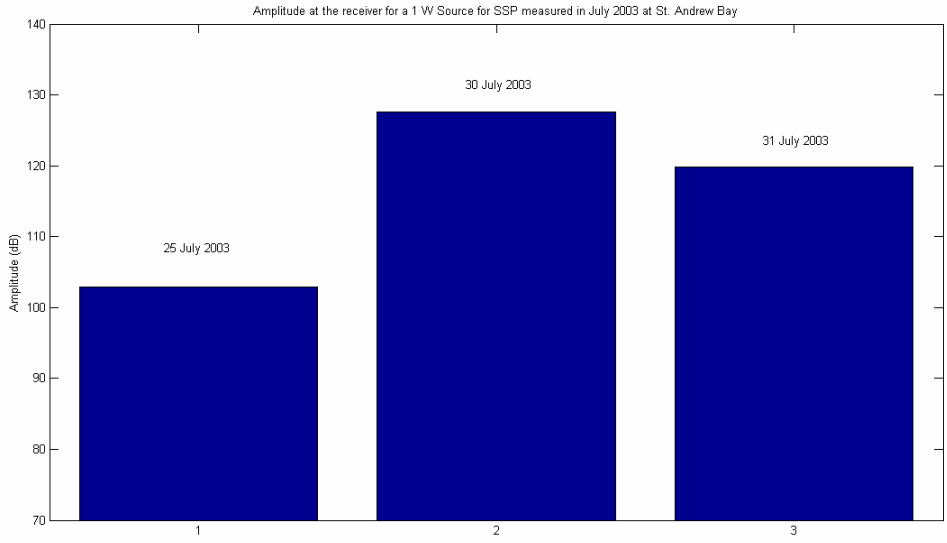

Figure 17. Amplitude at the receiver for different SSP measured in St. Andrew Bay, FL

Figure 17 shows the maximum amplitude for each of the profiles shown in Figure 16. Figure 17 shows that there can be drastic changes to the transmission characteristics of a shallow water channel for slight changes in the profile and for small lapses in time. The sound-speed profile for 25 July causes two families of multipaths to be formed, which creates two modes of arrivals with similar magnitudes in very short periods of time. These multiple arrivals have small magnitude, however, and do not constructively interfere with one another. The rest of the impulse response plot is similar to those of the other days. The impulse response plots for 30 July and 31 July have similar impulse distribution, and the higher amplitude for 30 July is hypothesized to be due to the convergence at the receiver of multiple rays experiencing a single surface reflection.

B. CHESAPEAKE BAY, LITTLE CREEK, VIRGINIA

The second maritime environment is Chesapeake Bay, Virginia, where transmission experiments are taking place in June 2007. Figure 18 shows the bathymetry at the site.

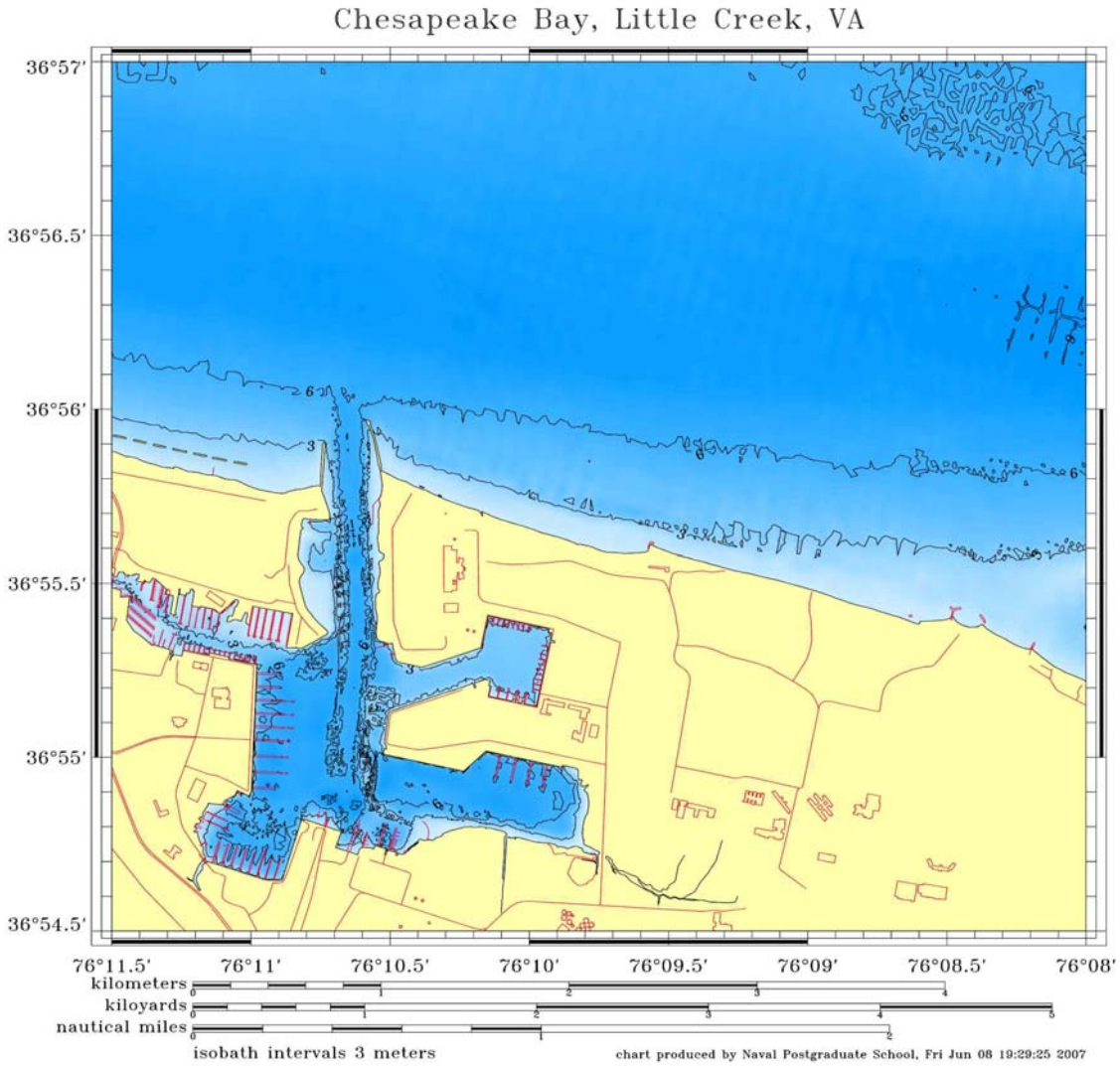

Figure 18. Bathymetric chart of Chesapeake Bay, Little Creek, VA

The typical channel depth for this location is 5 m, and the desired transmission range is 1000 m. As in St. Andrew Bay, planned transmissions in this channel are in the 9-14 kHz band, with the model assuming a 14-kHz transmission since the higher frequencies are prone to greater transmission loss. The sound-speed profiles for this analysis were the slowest, fastest, and average SSP measured during testing. These sound-speed profiles are illustrated in Figure 19.

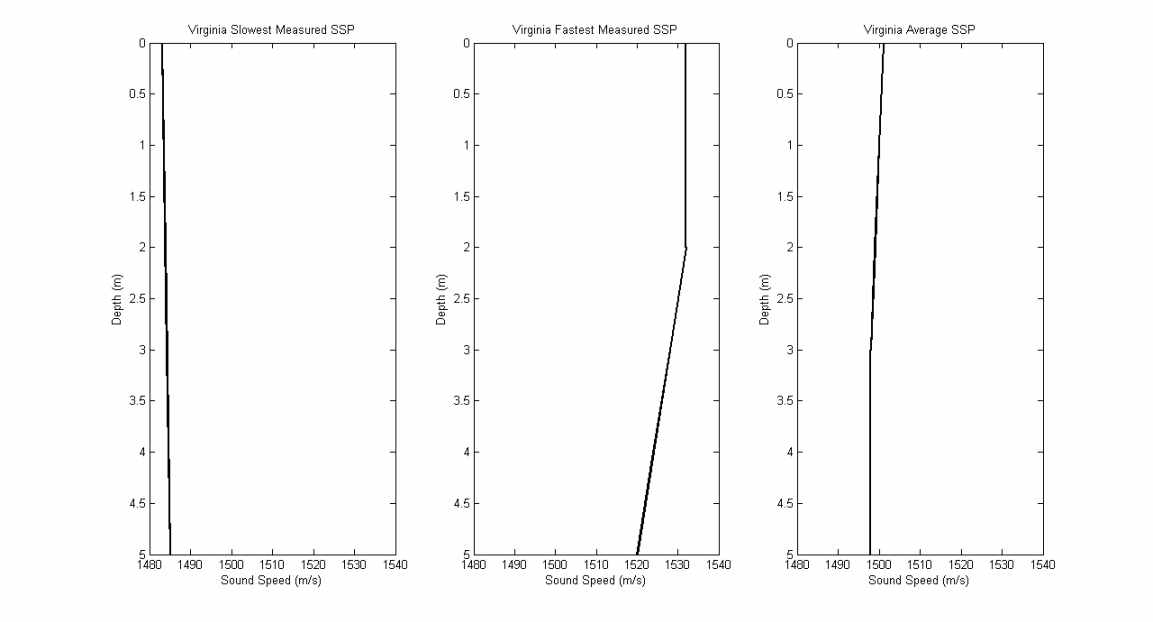

Figure 19. Measured sound-speed profiles in the shallow-water channel in Chesapeake Bay, Little Creek, VA

The figure shows that the slowest measured SSP is linear and very slightly upward refracting, while the fastest measured SSP is isospeed from the surface to a 2 m depth, then strongly downward refracting. The average SSP is slightly downward refracting from the top to a 3 m depth, then isospeed until the bottom.

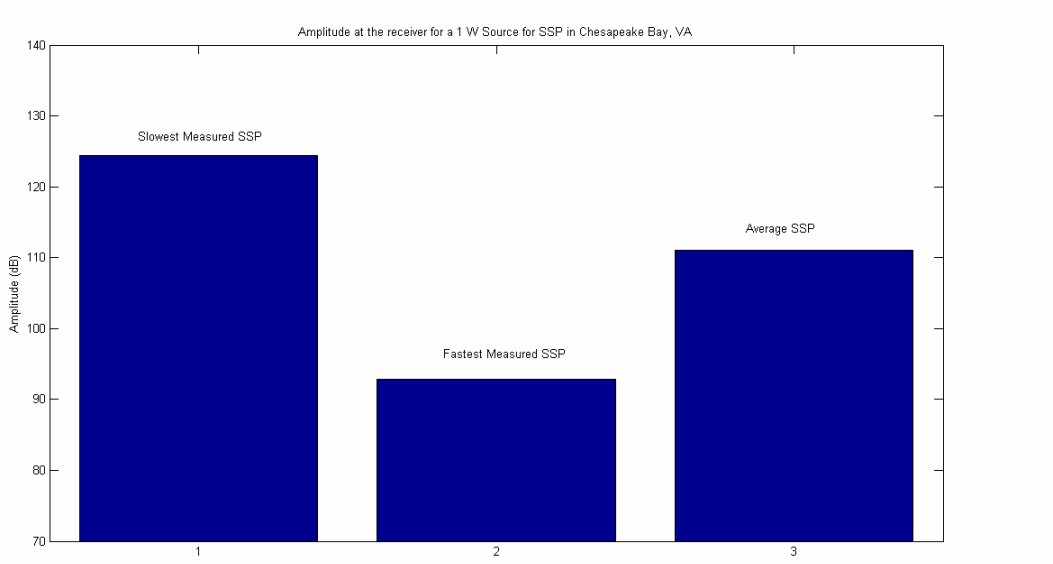

Figure 20. Amplitude at the receiver for the measured sound-speed profiles in Chesapeake Bay, Little Creek, VA

Figure 20 shows the maximum amplitude for each of the profiles shown in Figure 19. Figure 20 shows that the slowest measured SSP has the greatest amplitude at the receiver, and that the fastest measured SSP has the smallest amplitude at the receiver. Analysis shows that the fastest SSP concentrates most of the beams and energy in the isospeed part of the channel, with only a fraction reaching the bottom. This is hypothesized to be the cause of the small amplitude at the receiver. The slowest SSP is very slightly upward refracting and thus does not severely affect the energy distribution in the water channel. The average SSP develops a duct at 2.75 m that concentrates most of the sound energy at the bottom of the channel. The duct in the average SSP case supports a direct path from source to receiver which curiously gives a lower amplitude than the surface-reflected paths of the slowest-measured SSP case. These amplitudes were confirmed with Bellhop runs using very dense ray fans.

VI. CONCLUSIONS

A. FINDINGS

The Bellhop propagation model is a useful and intuitive tool for assessing the propagation characteristics of shallow water channels. Ray-trace plots display the distribution of sound energy in the water channel, while eigenray plots identify the paths that transport energy from the transmitter to a specific receiver location. The impulse response plots show the multipath time dispersion of the acoustic signal arising from the difference in pathlength traveled by each ray.

In the shallow waters of coastal regions, the velocity profile tends to be irregular and unpredictable, with little temporal or spatial stability. The shallow water profile is complicated by the effects of salinity changes caused by nearby sources of fresh water. Characterizing real sound velocity profiles results in more complicated ray-trace and impulse response plots due to the irregularities in the SSP. Careful examination of the channel conditions is imperative before system deployment to ensure successful communications. The propagation model implemented here is a useful tool for mission planning.

The Marsh & Schulkin equation closely matches the results obtained from the Bellhop algorithm.

Parametric analysis shows that transmission range is the factor giving the largest impact on signal strength. Channel depth, transmission frequency and bottom sediment material also affect the quality of transmission but their effect is less than that of range. Transmitter and receiver geometry can have a discernible effect on transmissions under specific conditions. A library of cases is included as Appendix B to illustrate how changes in each parameter affect the ray structure and impulse response of the transmission.

B. RECOMMENDATIONS FOR FUTURE WORK

There is a need to perform experiments to validate and tune the Bellhop model. This experiments need to occur in a controlled environment in which each parameter can be varied individually.

Additionally, the assumption here that the sea surface is a perfect reflector should be examined. An additional parametric study involving sea states greater than sea-state 0 should be undertaken to examine the impact of the sea surface on propagation.

Once this work is completed, the Bellhop model may be used to predict performance of acoustic communications in maritime water channels.

APPENDIX A. MATLAB CODES

A. COMPOSITE FIGURE SUBROUTINE

```
%Composite Figure Subroutine
%*********************************
%Open Sound-Speed Profile (SSP) from text file and plot it
fid=fopen('filename.txt');
xy=textscan(fid,'%f %f');
x=xy{2};
y=xy{1};
subplot(3,4,[1 5])
plot(x,y,'k','LineWidth',2)
set(gca,'YDir','reverse')
xlabel('Sound Speed (m/s)')
ylabel('Depth (m)')
title('Sound Speed Profile')
axis([1500.0 1550.0 0.0 10.0])
%*********************************
%Import Eigenray plot
subplot(3,4,[2 8])
hold on
plotray('filename')
%*********************************
```

```
%Import Impulse Response plot
subplot(3,4,[9 12])
hold on
filenameA
```

B. IMPULSE RESPONSE PLOT SUBROUTINE

```
%Impulse Response Plot Subroutine
%*********************************
%Open Amplitude-delay arrival file
fid=fopen('filename.arr');
%Ignore the first six lines of the amplitude-delay arrival file code (which display frequency, receiver depth, source depth, transmission range and number of arrivals)
for i=1:6
tline=fgetl(fid);
end
xy=textscan(fid,'%f %f %f %f %f %d %d');
x=xy{3};
z=xy{1};
y=170.8+20*log10(z);
stem(x,y,'b.')
xlabel('Time (s)')
ylabel('Amplitude in dB')
title('Channel Impulse Response for a SL of 1 W')
axis([0 1 90.0 140.0])
axis 'auto x'
```

APPENDIX B. COMPOSITE FIGURES

A. PARAMETRIC ANALYSIS

Bellhop Analysis, Case 10.500.1.1.70.Sand.Temp

Parameter	Magnitude
Channel Depth (m)	10
Transmission Range (m)	500
Transmitter Height (m)	1
Receiver Height (m)	1
Frequency (kHz)	70
Bottom Sediment Material	Sand
SSP Gradient	Temperature-Driven

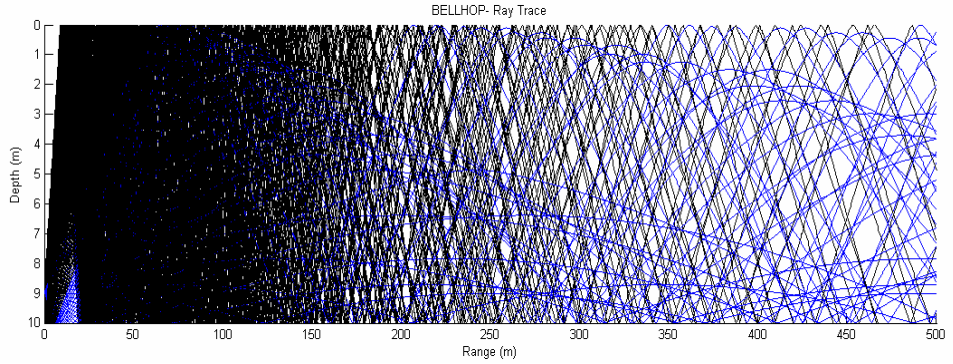

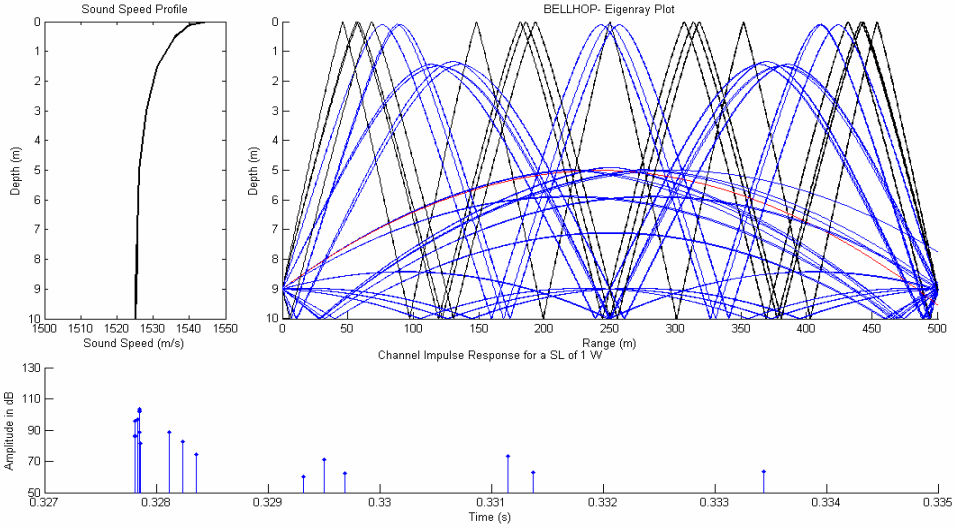

Bellhop Analysis, Case 10.500.1.1.70.Sand.Sal

Parameter	Magnitude
Channel Depth (m)	10
Transmission Range (m)	500
Transmitter Height (m)	1
Receiver Height (m)	1
Frequency (kHz)	70
Bottom Sediment Material	Sand
SSP Gradient	Salinity-Driven

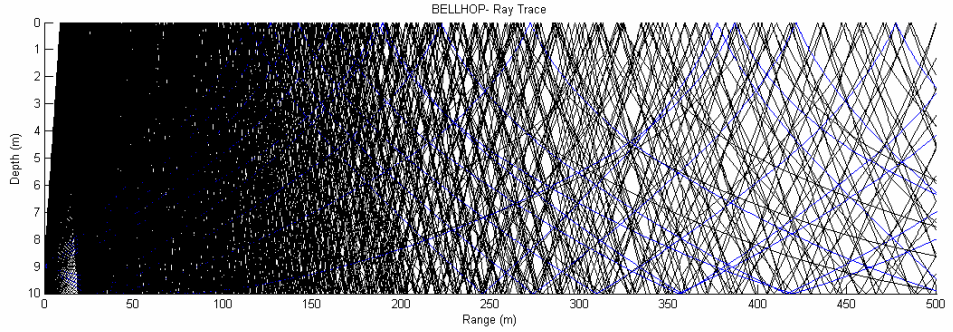

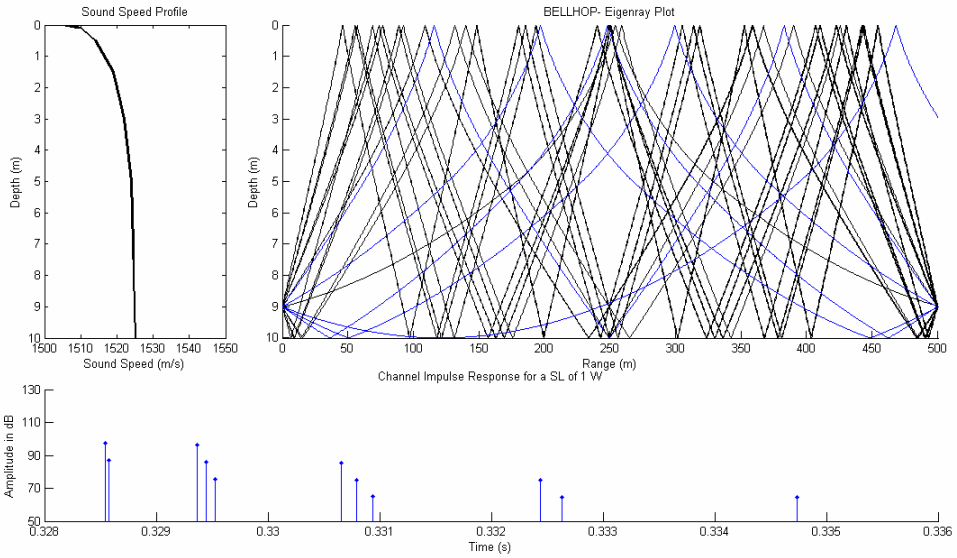

Bellhop Analysis, Case 10.500.1.1.70.Sand.-2

Parameter	Magnitude
Channel Depth (m)	10
Transmission Range (m)	500
Transmitter Height (m)	1
Receiver Height (m)	1
Frequency (kHz)	70
Bottom Sediment Material	Sand
SSP Gradient	-2

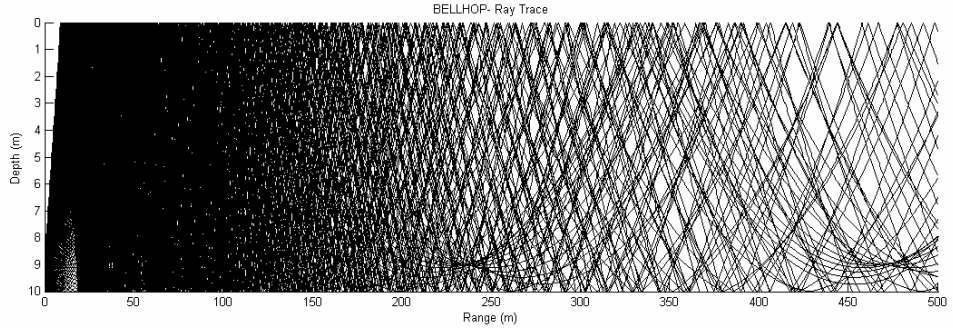

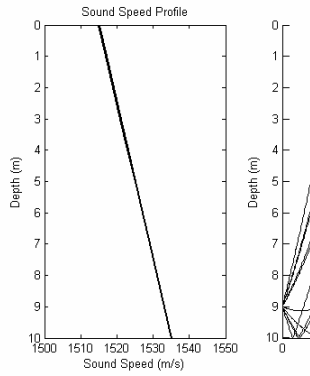

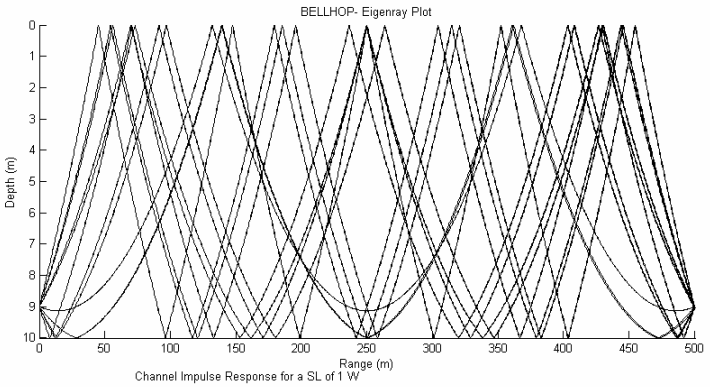

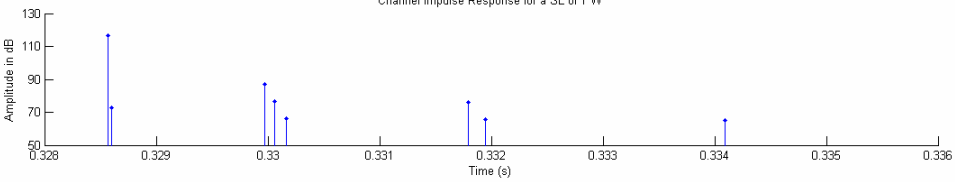

Bellhop Analysis, Case 10.500.1.1.70.Sand.-1

Parameter	Magnitude
Channel Depth (m)	10
Transmission Range (m)	500
Transmitter Height (m)	1
Receiver Height (m)	1
Frequency (kHz)	70
Bottom Sediment Material	Sand
SSP Gradient	-1

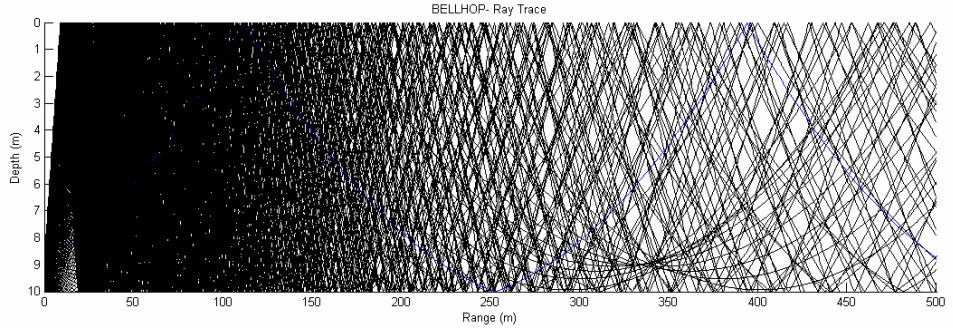

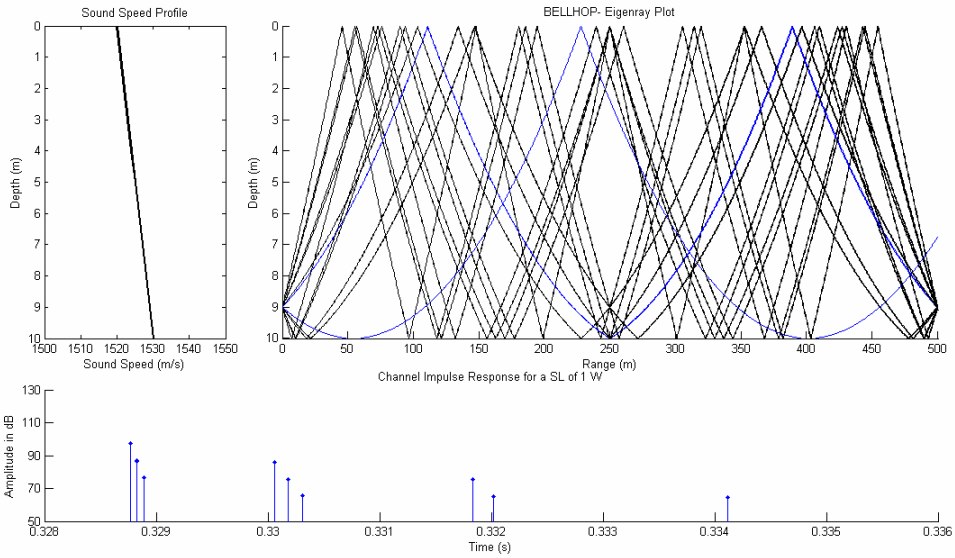

Bellhop Analysis, Case 10.500.1.1.70.Sand.0

Parameter	Magnitude
Channel Depth (m)	10
Transmission Range (m)	500
Transmitter Height (m)	1
Receiver Height (m)	1
Frequency (kHz)	70
Bottom Sediment Material	Sand
SSP Gradient	0 (Isospeed)

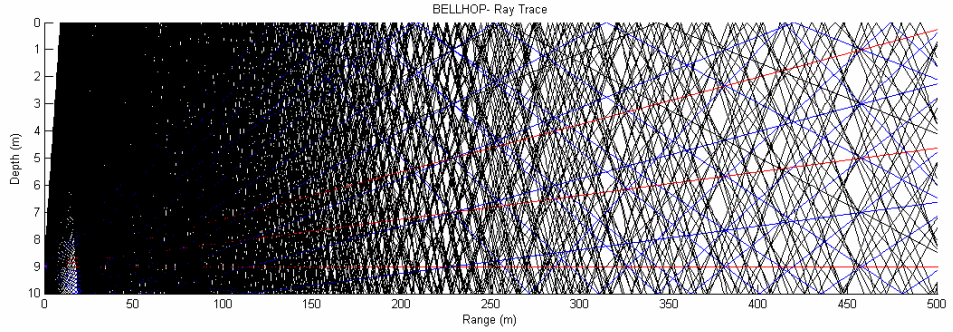

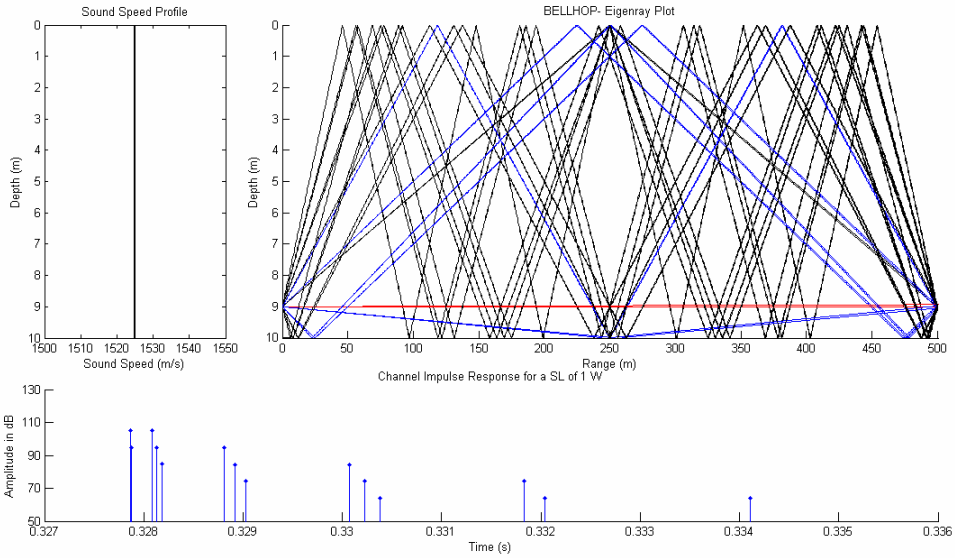

Bellhop Analysis, Case 10.500.1.1.70.Sand.+1

Parameter	Magnitude
Channel Depth (m)	10
Transmission Range (m)	500
Transmitter Height (m)	1
Receiver Height (m)	1
Frequency (kHz)	70
Bottom Sediment Material	Sand
SSP Gradient	+1

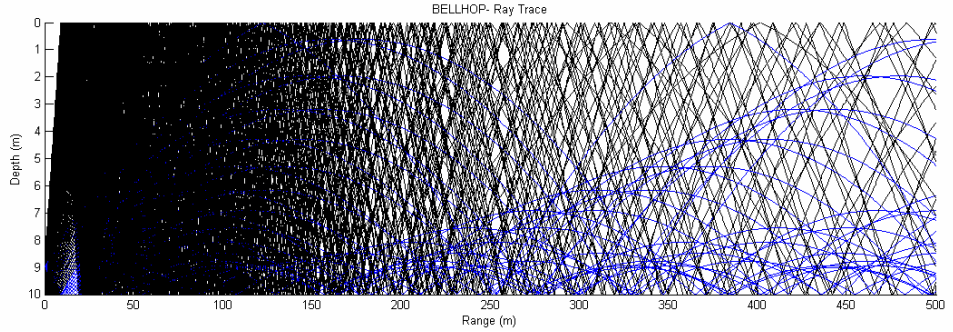

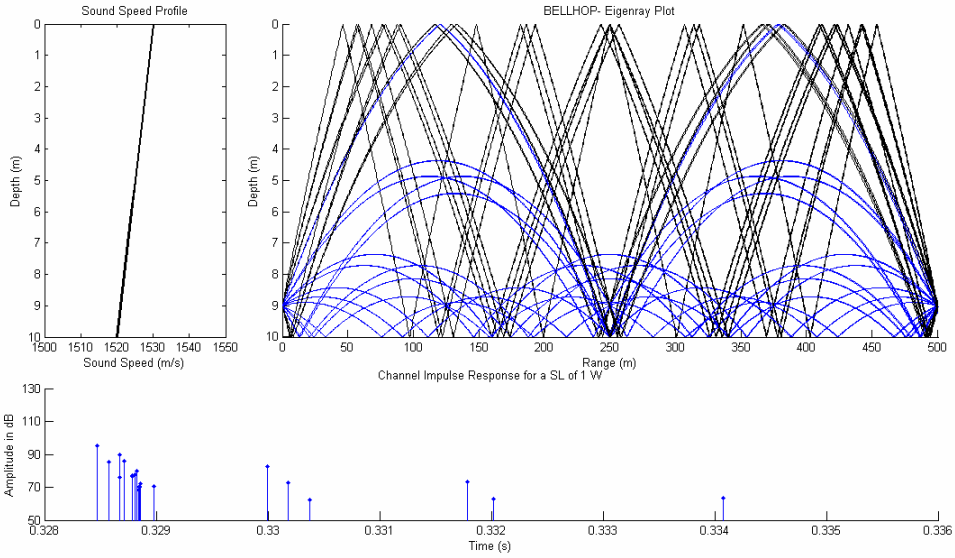

Bellhop Analysis, Case 10.500.1.1.70.Sand.+2

Parameter	Magnitude
Channel Depth (m)	10
Transmission Range (m)	500
Transmitter Height (m)	1
Receiver Height (m)	1
Frequency (kHz)	70
Bottom Sediment Material	Sand
SSP Gradient	+2

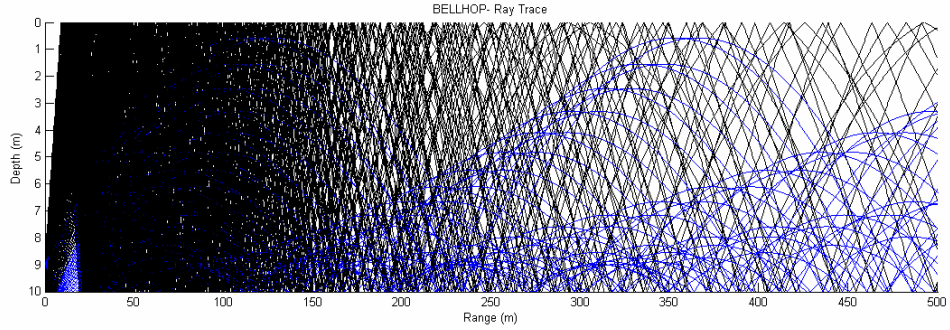

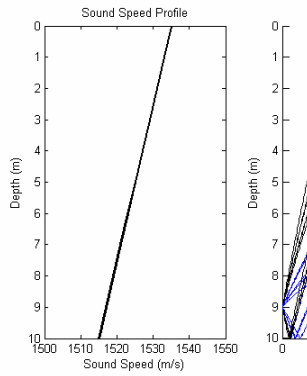

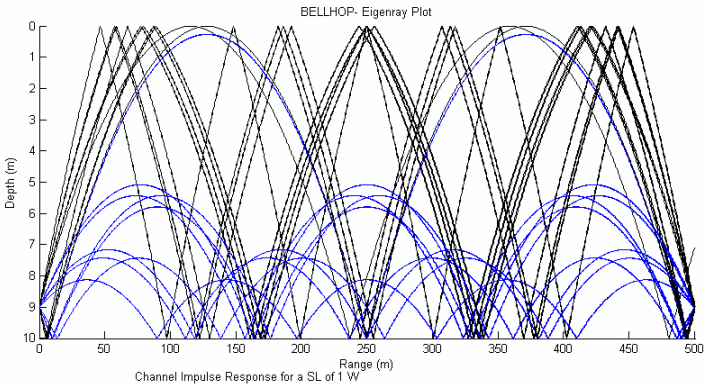

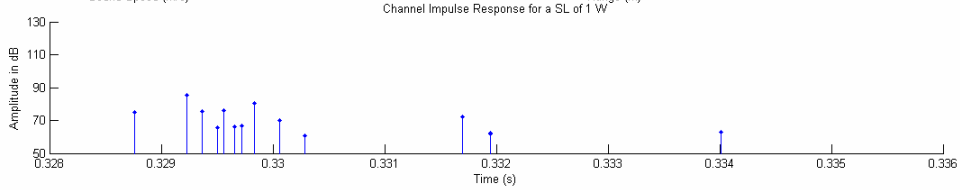

Bellhop Analysis, Case 10.500.1.1.70.Clay.Temp

Parameter	Magnitude
Channel Depth (m)	10
Transmission Range (m)	500
Transmitter Height (m)	1
Receiver Height (m)	1
Frequency (kHz)	70
Bottom Sediment Material	Clay
SSP Gradient	Temperature-Driven

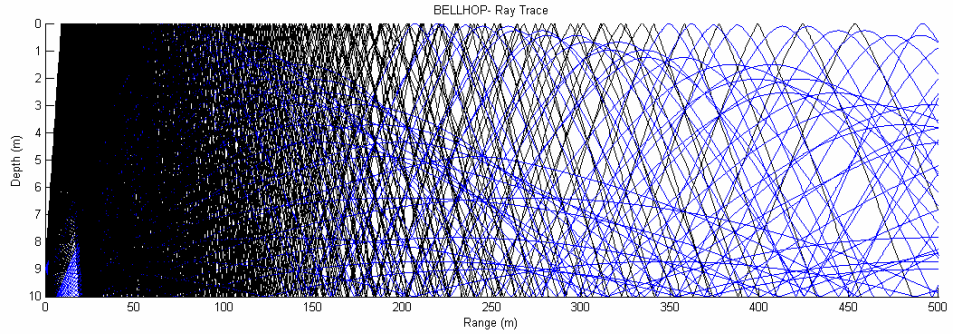

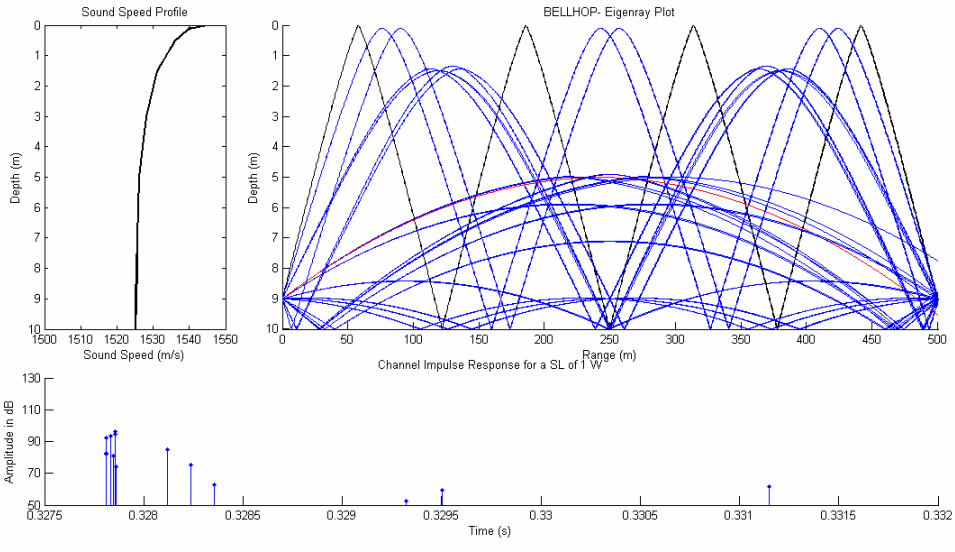

Bellhop Analysis, Case 10.500.1.1.70.Clay.Sal

Parameter	Magnitude
Channel Depth (m)	10
Transmission Range (m)	500
Transmitter Height (m)	1
Receiver Height (m)	1
Frequency (kHz)	70
Bottom Sediment Material	Clay
SSP Gradient	Salinity-Driven

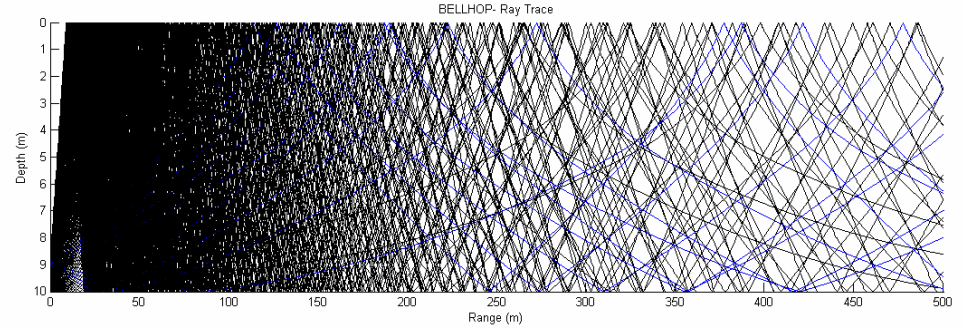

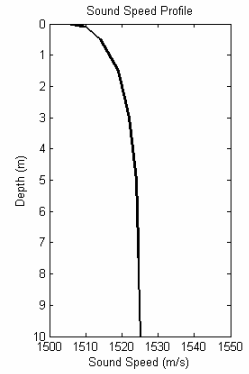

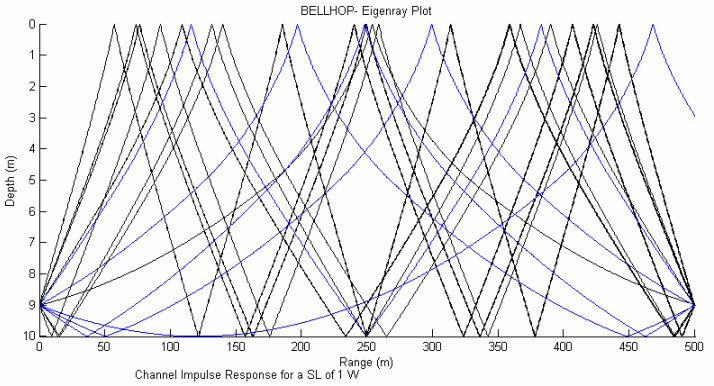

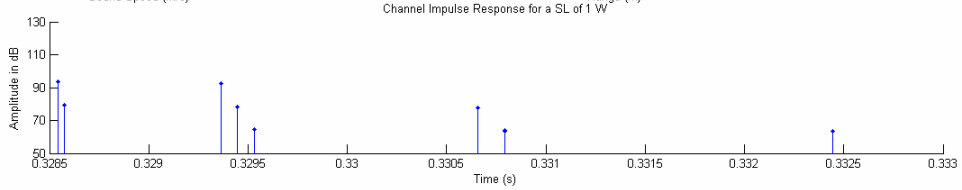

Bellhop Analysis, Case 10.500.1.1.70.Clay.0

Parameter	Magnitude
Channel Depth (m)	10
Transmission Range (m)	500
Transmitter Height (m)	1
Receiver Height (m)	1
Frequency (kHz)	70
Bottom Sediment Material	Clay
SSP Gradient	Isospeed

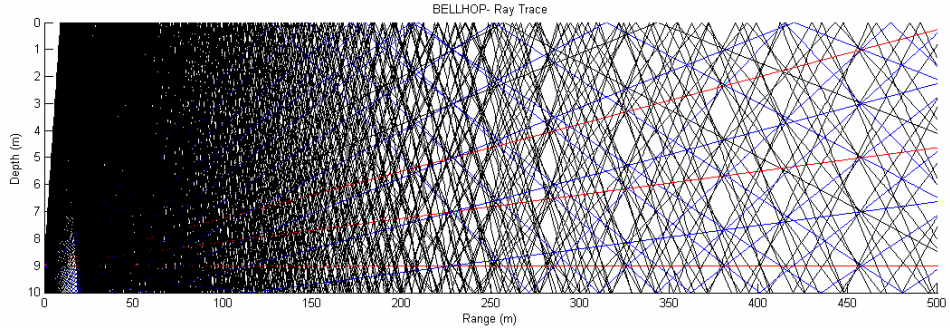

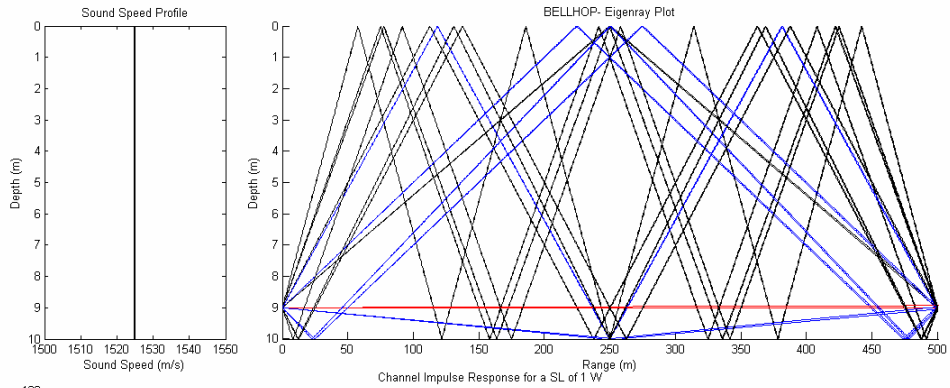

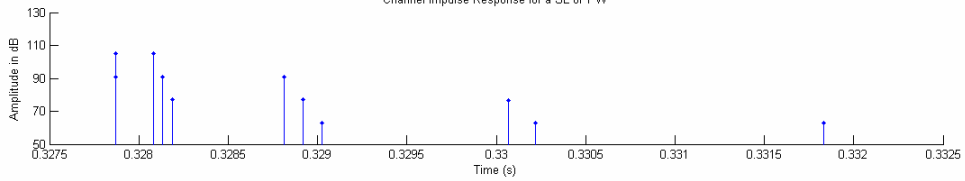

Bellhop Analysis, Case 10.500.1.1.70.Silt.Temp

Parameter	Magnitude
Channel Depth (m)	10
Transmission Range (m)	500
Transmitter Height (m)	1
Receiver Height (m)	1
Frequency (kHz)	70
Bottom Sediment Material	Silt
SSP Gradient	Temperature-Driven

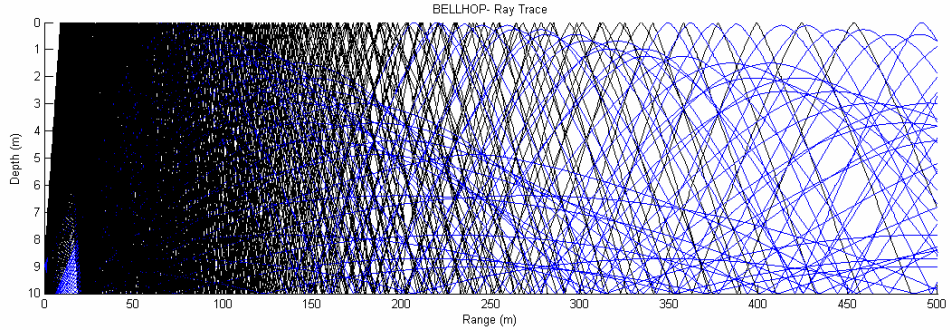

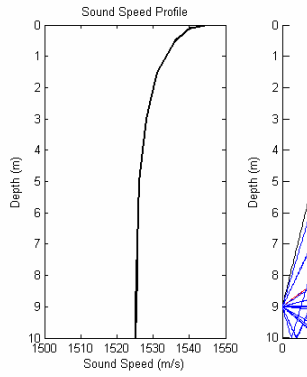

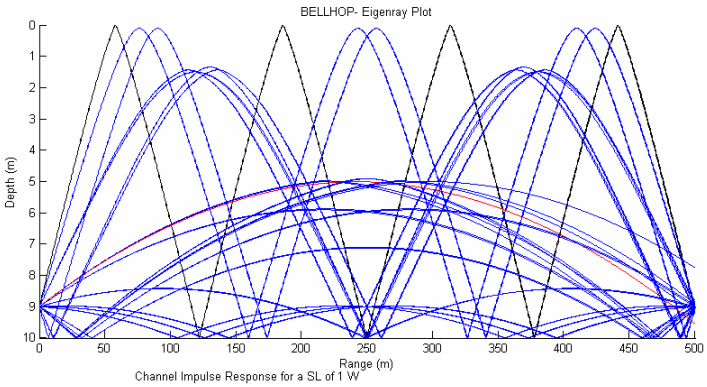

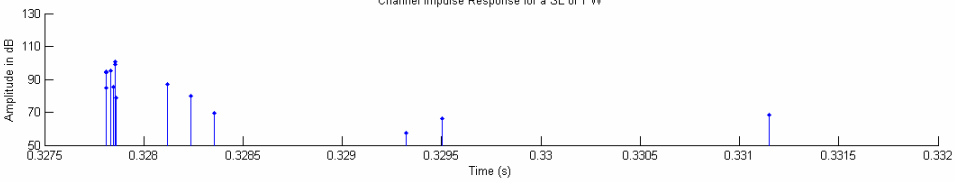

Bellhop Analysis, Case 10.500.1.1.70.Silt.Sal

Parameter	Magnitude
Channel Depth (m)	10
Transmission Range (m)	500
Transmitter Height (m)	1
Receiver Height (m)	1
Frequency (kHz)	70
Bottom Sediment Material	Silt
SSP Gradient	Salinity-Driven

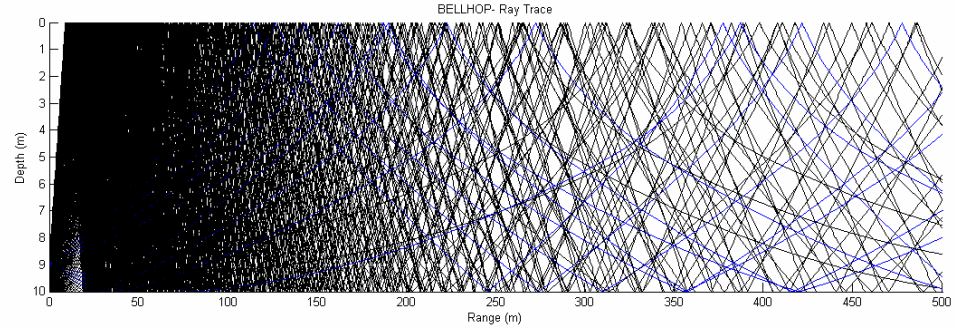

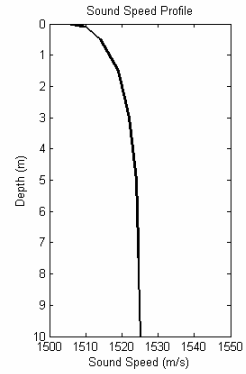

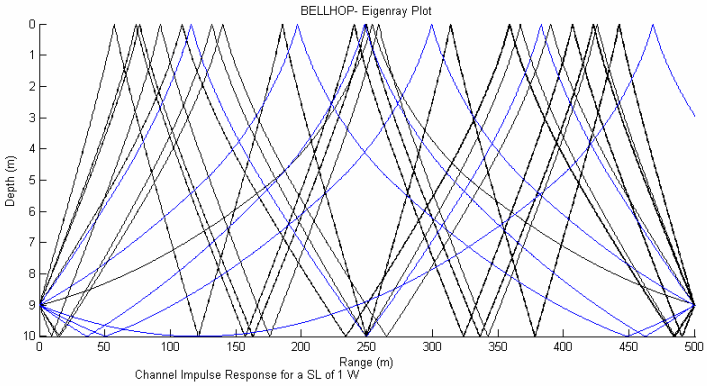

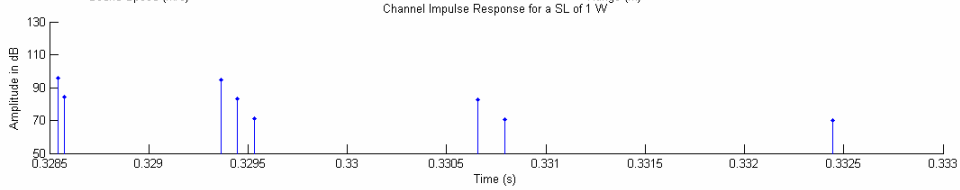

Bellhop Analysis, Case 10.500.1.1.70.Silt.0

Parameter	Magnitude
Channel Depth (m)	10
Transmission Range (m)	500
Transmitter Height (m)	1
Receiver Height (m)	1
Frequency (kHz)	70
Bottom Sediment Material	Silt
SSP Gradient	Isospeed

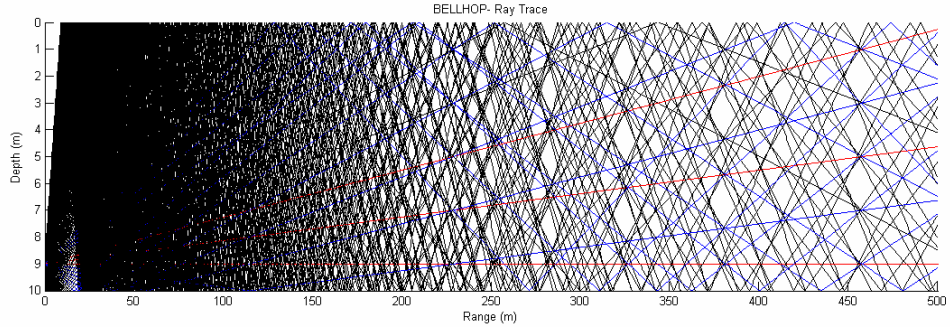

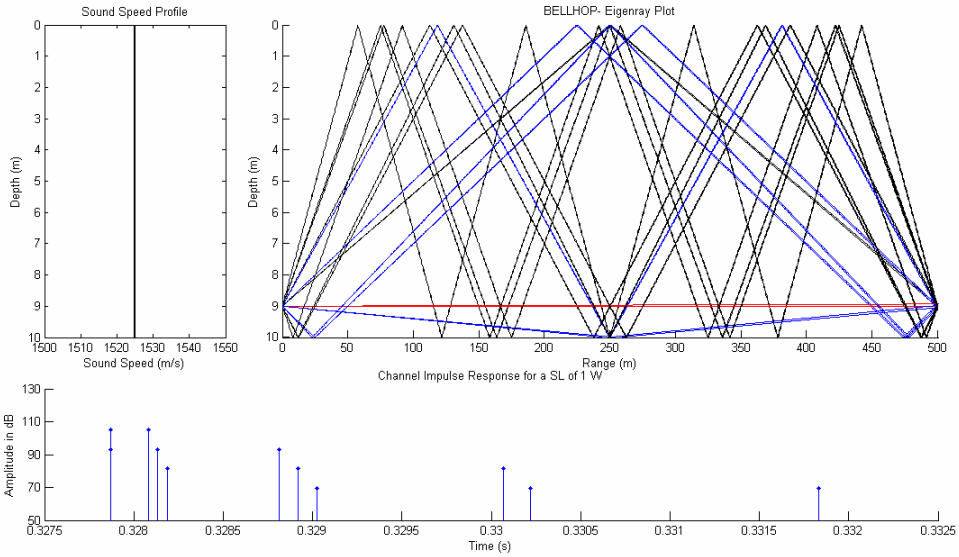

Bellhop Analysis, Case 10.500.1.1.70.Gravel.Temp

Parameter	Magnitude
Channel Depth (m)	10
Transmission Range (m)	500
Transmitter Height (m)	1
Receiver Height (m)	1
Frequency (kHz)	70
Bottom Sediment Material	Gravel
SSP Gradient	Temperature-Driven

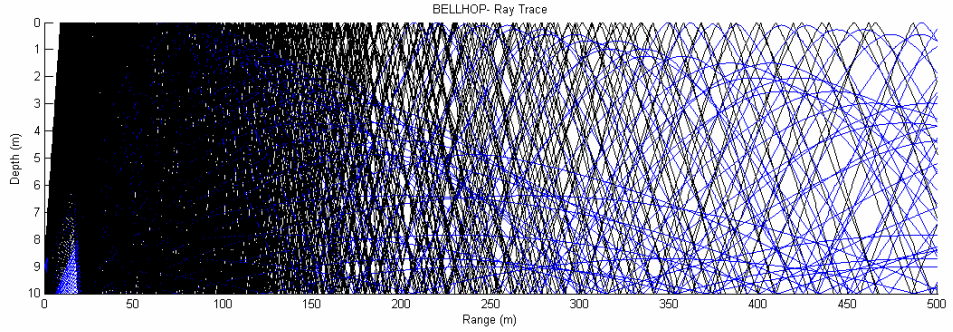

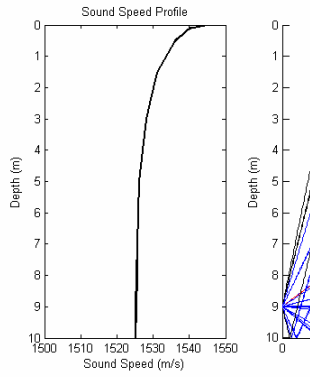

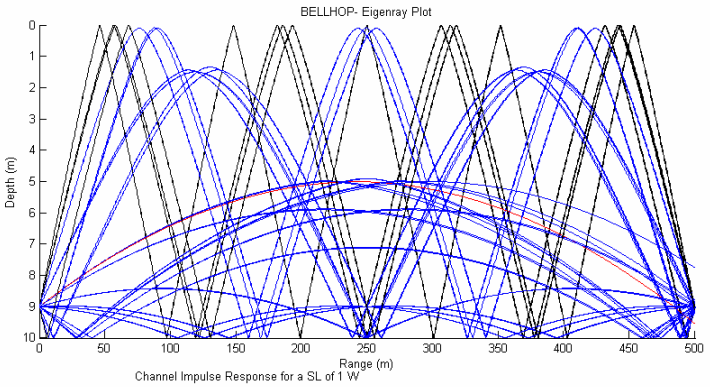

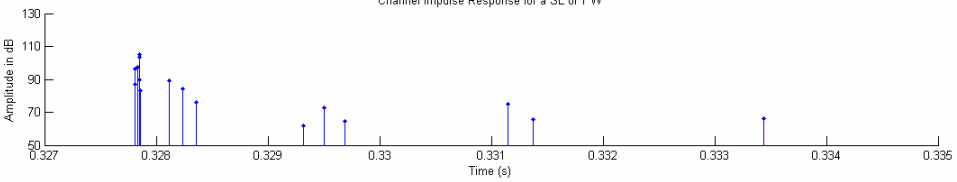

Bellhop Analysis, Case 10.500.1.1.70.Gravel.Sal

Parameter	Magnitude
Channel Depth (m)	10
Transmission Range (m)	500
Transmitter Height (m)	1
Receiver Height (m)	1
Frequency (kHz)	70
Bottom Sediment Material	Gravel
SSP Gradient	Salinity-Driven

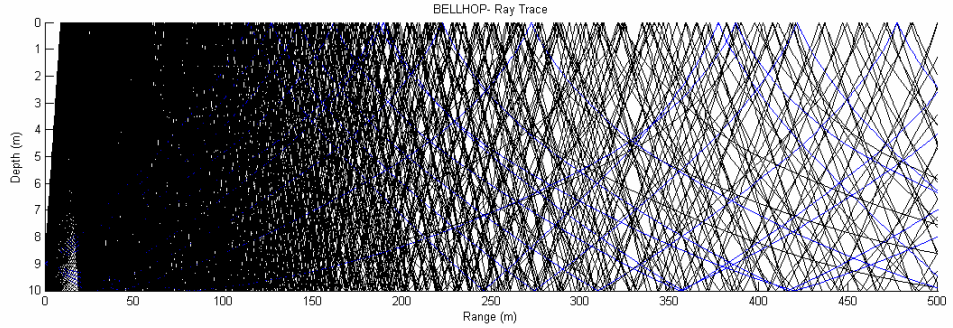

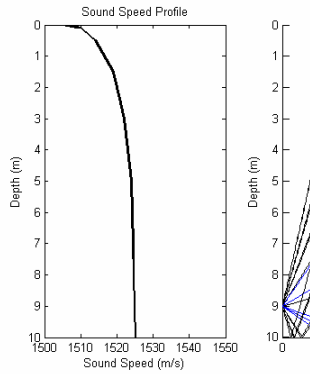

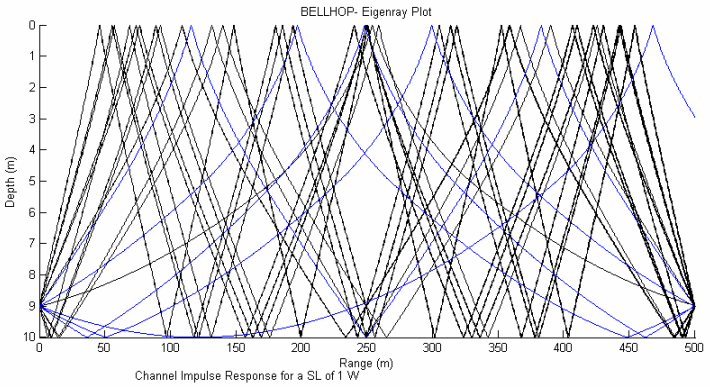

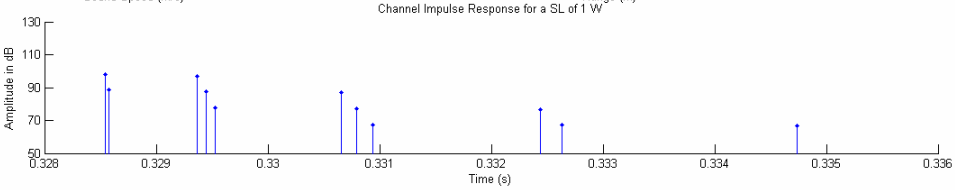

Bellhop Analysis, Case 10.500.1.1.70.Gravel.0

Parameter	Magnitude
Channel Depth (m)	10
Transmission Range (m)	500
Transmitter Height (m)	1
Receiver Height (m)	1
Frequency (kHz)	70
Bottom Sediment Material	Gravel
SSP Gradient	Isospeed

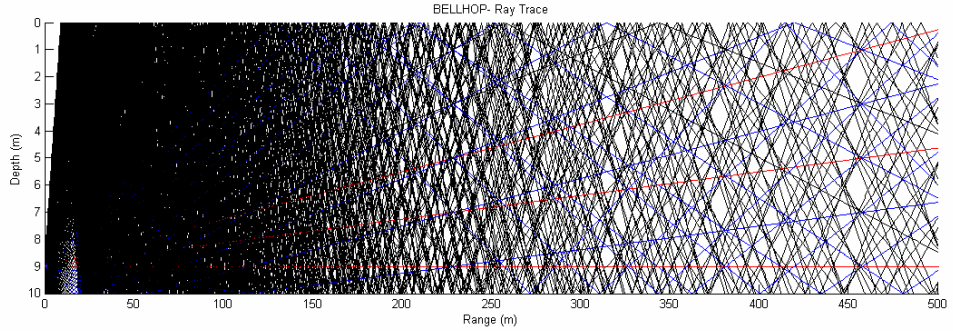

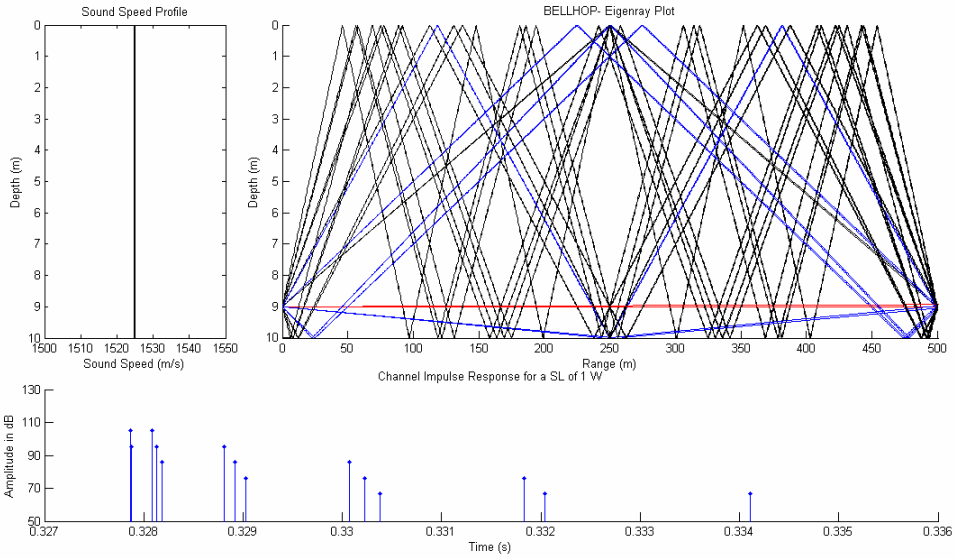

Bellhop Analysis, Case 10.500.1.1.65.Sand.Temp

Parameter	Magnitude
Channel Depth (m)	10
Transmission Range (m)	500
Transmitter Height (m)	1
Receiver Height (m)	1
Frequency (kHz)	65
Bottom Sediment Material	Sand
SSP Gradient	Temperature-Driven

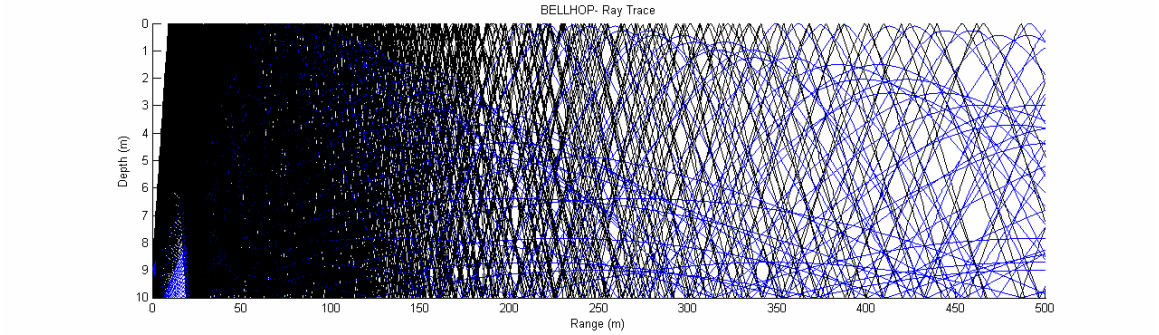

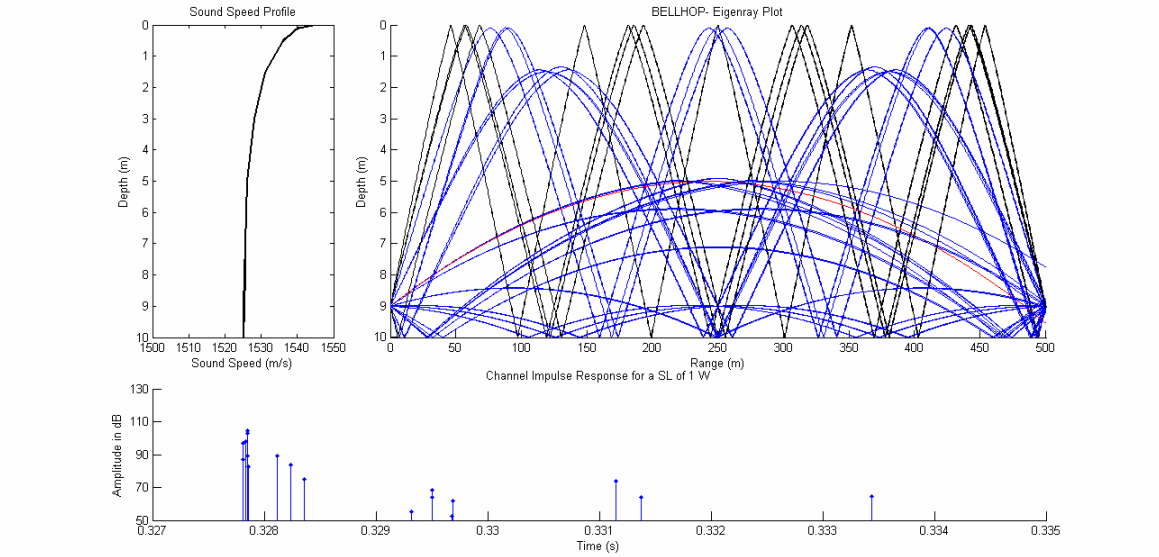

Bellhop Analysis, Case 10.500.1.1.65.Sand.Sal

Parameter	Magnitude
Channel Depth (m)	10
Transmission Range (m)	500
Transmitter Height (m)	1
Receiver Height (m)	1
Frequency (kHz)	65
Bottom Sediment Material	Sand
SSP Gradient	Salinity-Driven

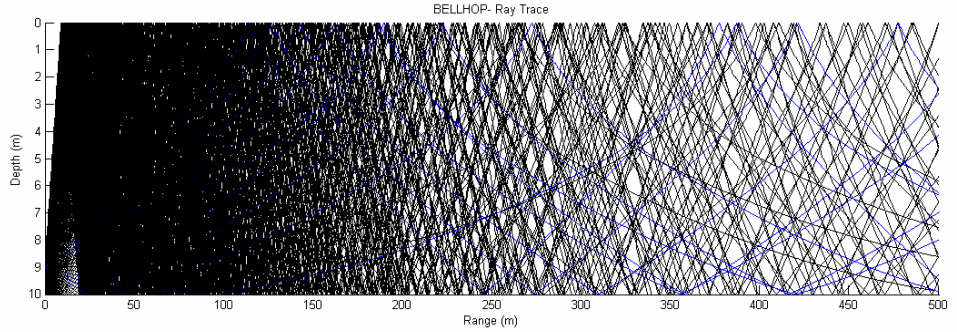

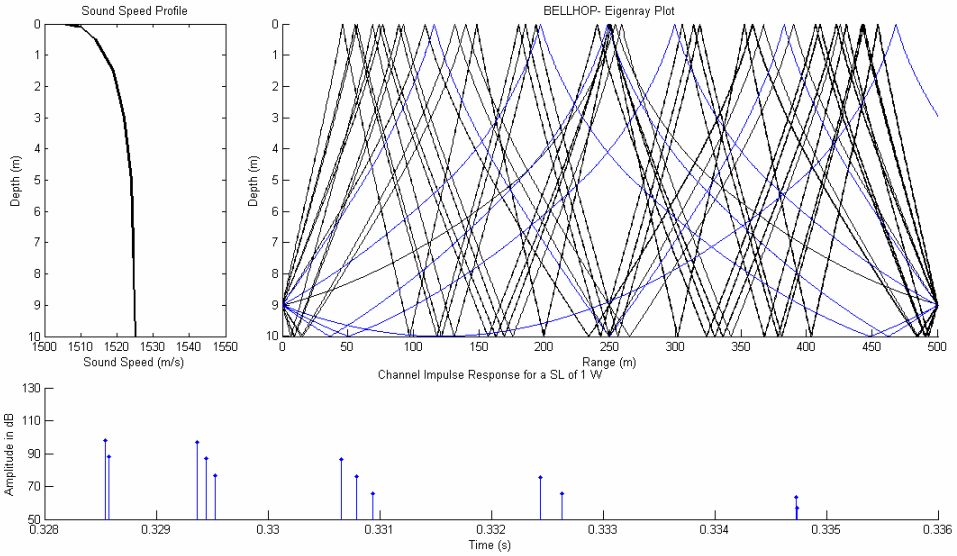

Bellhop Analysis, Case 10.500.1.1.65.Sand.0

Parameter	Magnitude
Channel Depth (m)	10
Transmission Range (m)	500
Transmitter Height (m)	1
Receiver Height (m)	1
Frequency (kHz)	65
Bottom Sediment Material	Sand
SSP Gradient	Isospeed

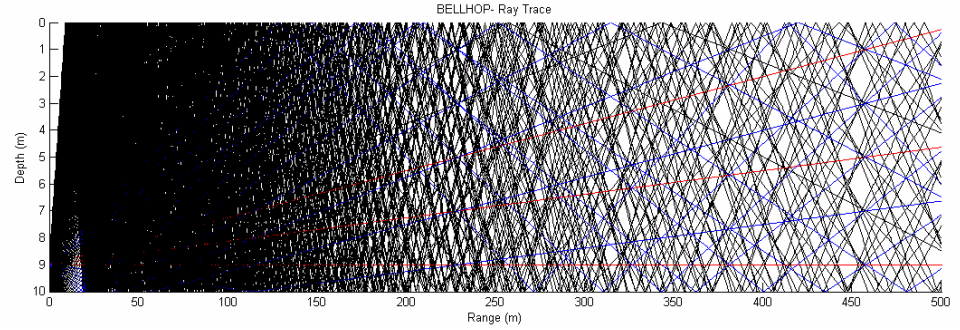

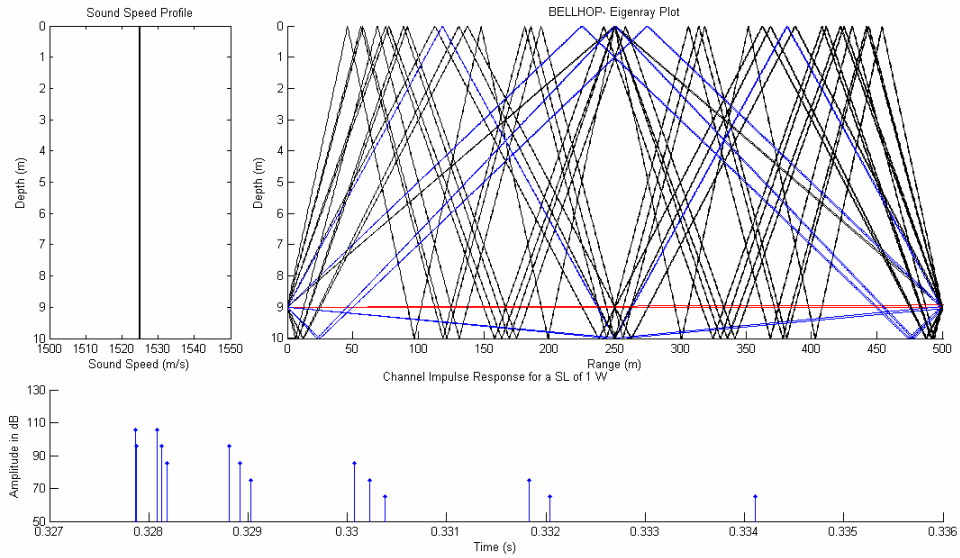

Bellhop Analysis, Case 10.500.1.1.60.Sand.Temp

Parameter	Magnitude
Channel Depth (m)	10
Transmission Range (m)	500
Transmitter Height (m)	1
Receiver Height (m)	1
Frequency (kHz)	60
Bottom Sediment Material	Sand
SSP Gradient	Temperature-Driven

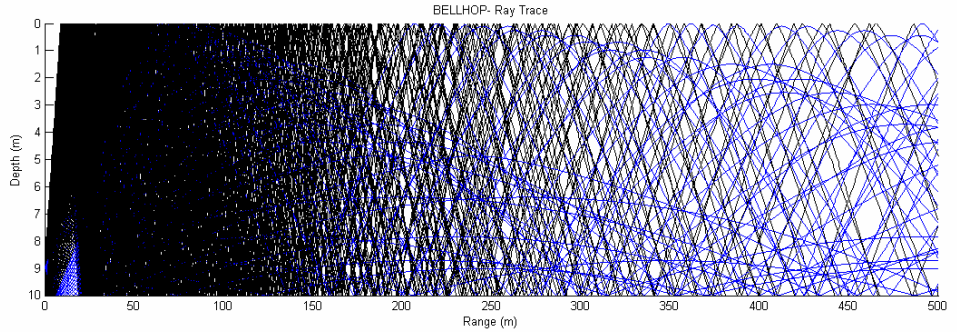

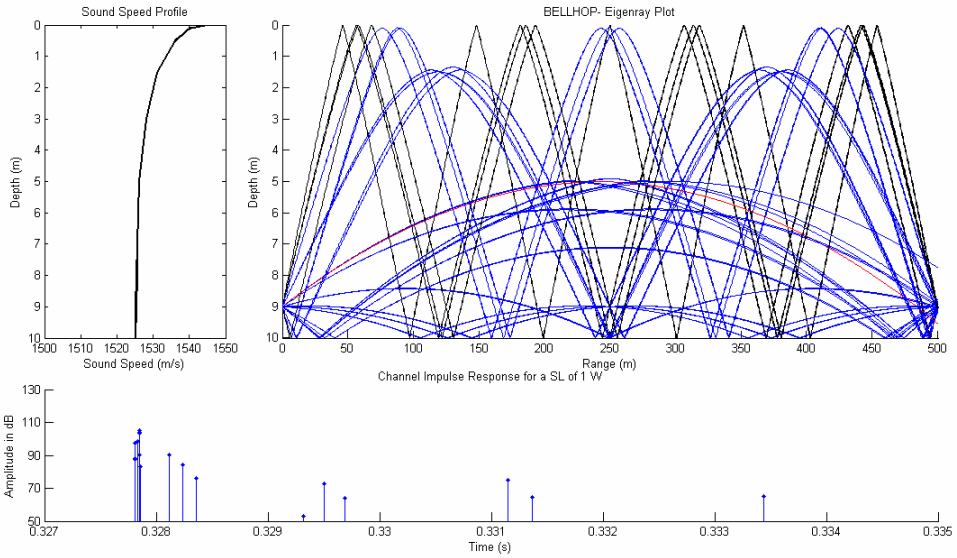

Bellhop Analysis, Case 10.500.1.1.60.Sand.Sal

Parameter	Magnitude
Channel Depth (m)	10
Transmission Range (m)	500
Transmitter Height (m)	1
Receiver Height (m)	1
Frequency (kHz)	60
Bottom Sediment Material	Sand
SSP Gradient	Salinity-Driven

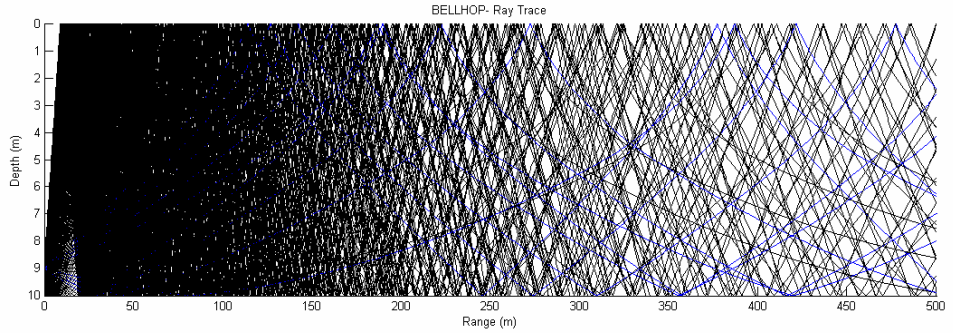

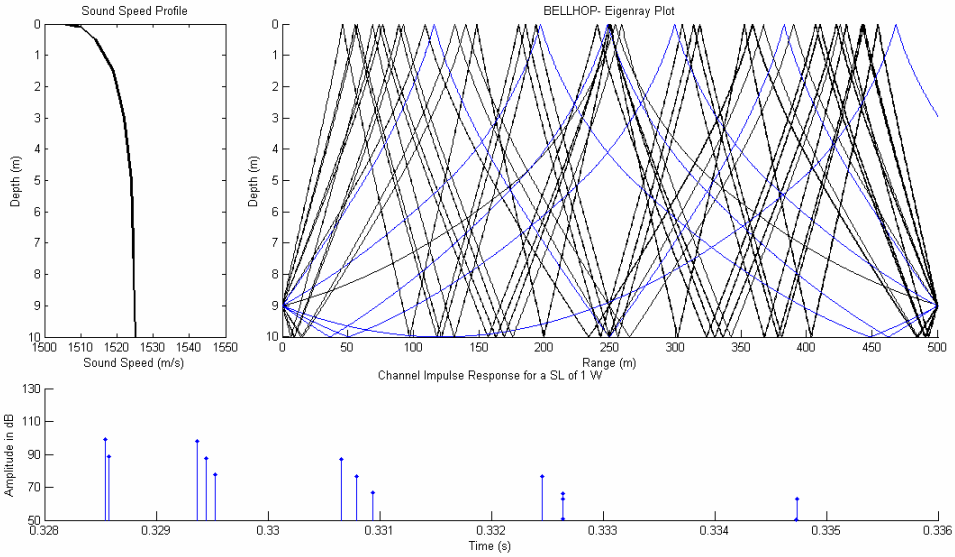

Bellhop Analysis, Case 10.500.1.1.60.Sand.0

Parameter	Magnitude
Channel Depth (m)	10
Transmission Range (m)	500
Transmitter Height (m)	1
Receiver Height (m)	1
Frequency (kHz)	60
Bottom Sediment Material	Sand
SSP Gradient	Isospeed

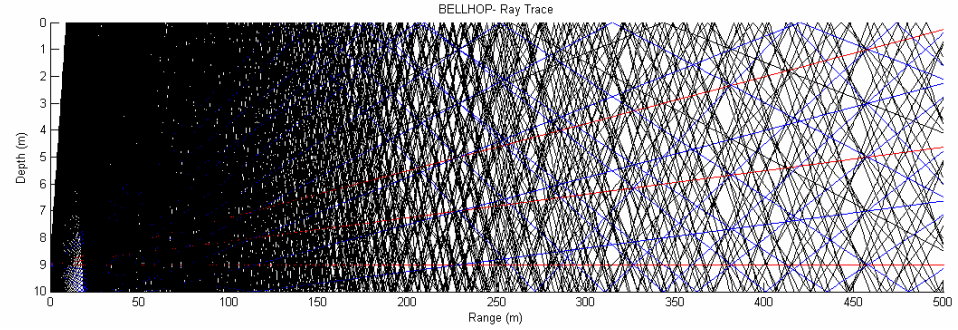

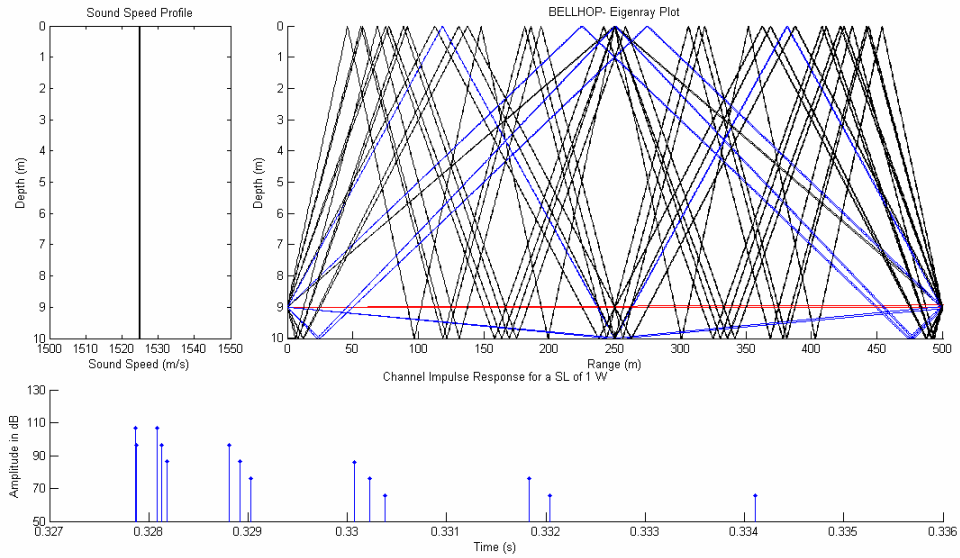

Bellhop Analysis, Case 10.500.1.1.55.Sand.Temp

Parameter	Magnitude
Channel Depth (m)	10
Transmission Range (m)	500
Transmitter Height (m)	1
Receiver Height (m)	1
Frequency (kHz)	55
Bottom Sediment Material	Sand
SSP Gradient	Temperature-Driven

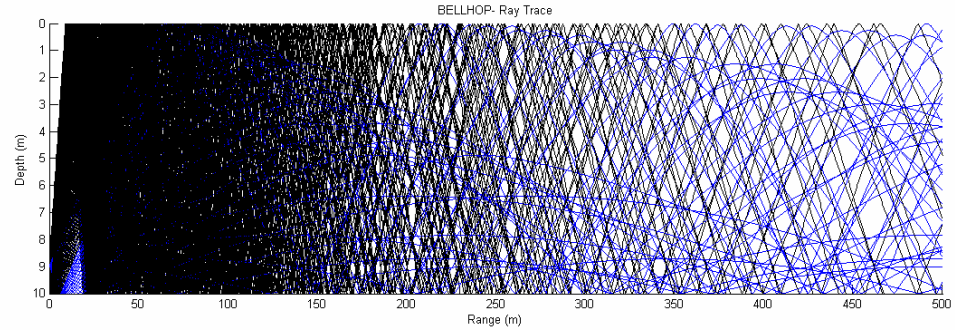

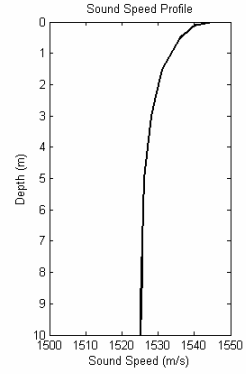

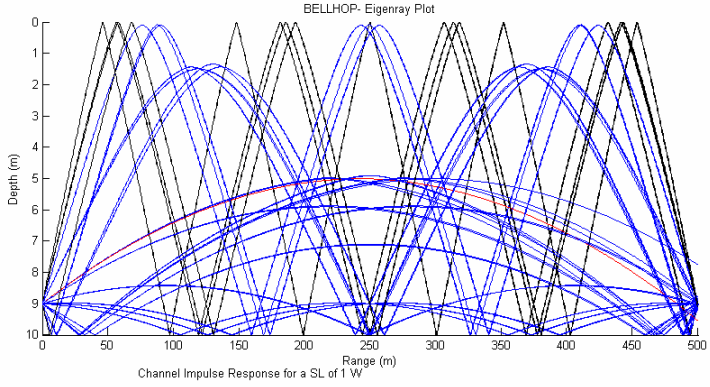

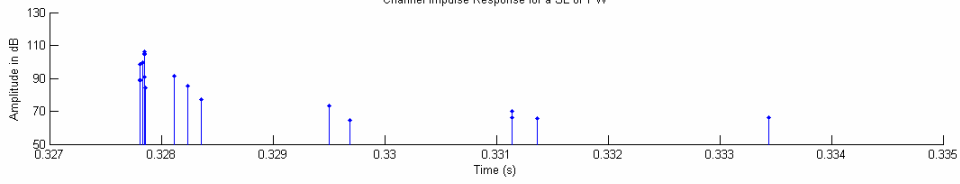

Bellhop Analysis, Case 10.500.1.1.55.Sand.Sal

Parameter	Magnitude
Channel Depth (m)	10
Transmission Range (m)	500
Transmitter Height (m)	1
Receiver Height (m)	1
Frequency (kHz)	55
Bottom Sediment Material	Sand
SSP Gradient	Salinity-Driven

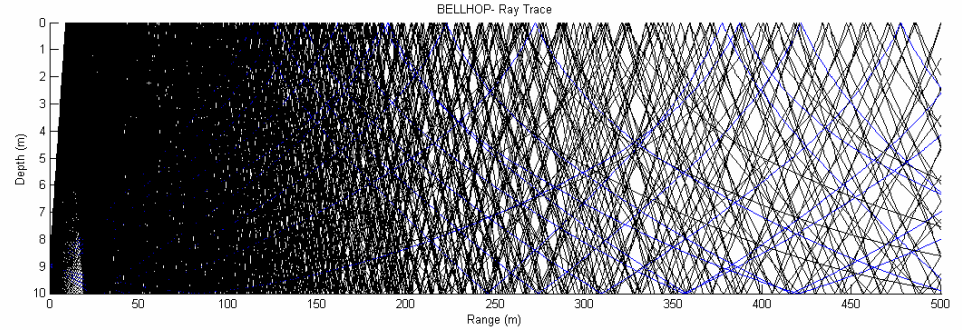

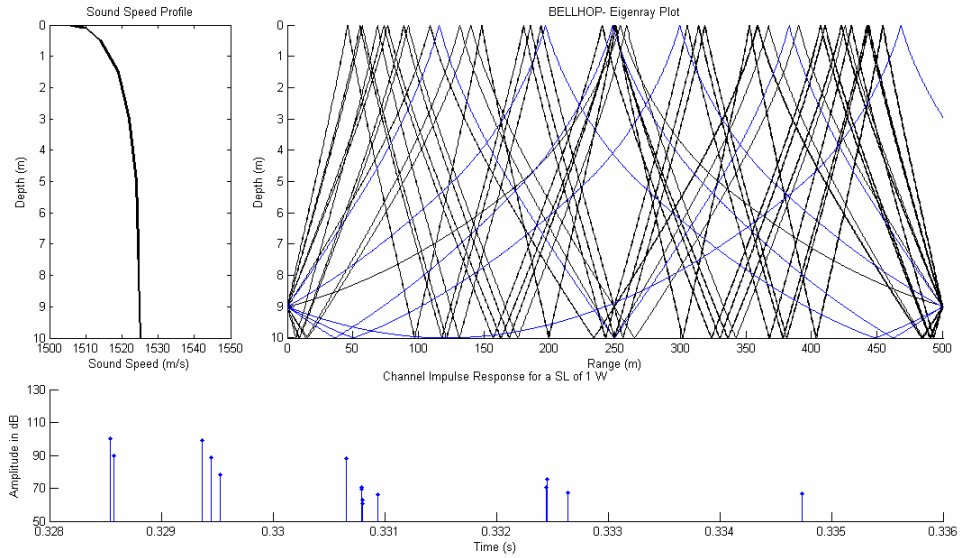

Bellhop Analysis, Case 10.500.1.1.55.Sand.0

Parameter	Magnitude
Channel Depth (m)	10
Transmission Range (m)	500
Transmitter Height (m)	1
Receiver Height (m)	1
Frequency (kHz)	55
Bottom Sediment Material	Sand
SSP Gradient	Isospeed

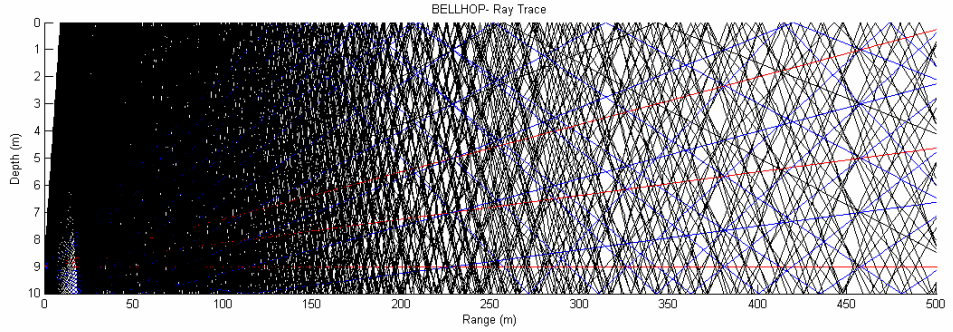

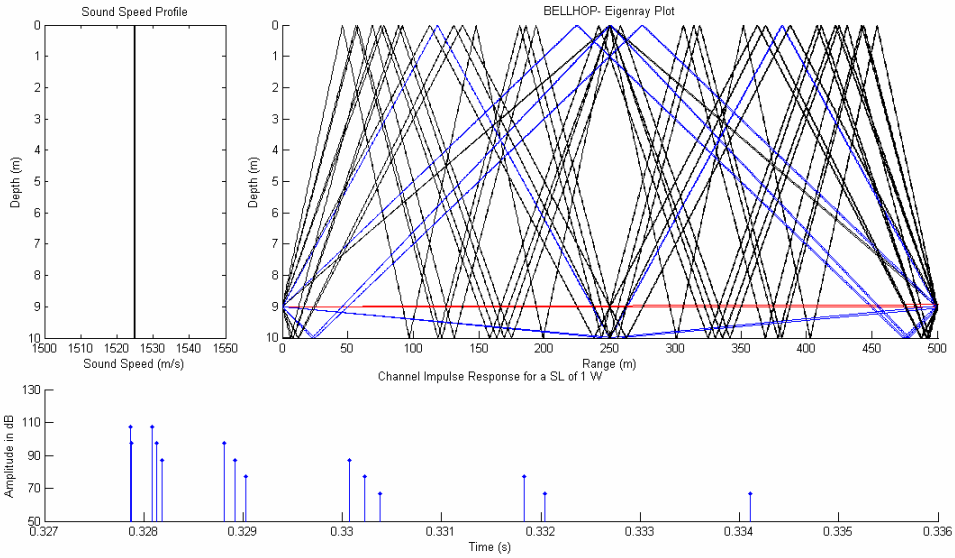

Bellhop Analysis, Case 10.500.1.1.50.Sand.Temp

Parameter	Magnitude
Channel Depth (m)	10
Transmission Range (m)	500
Transmitter Height (m)	1
Receiver Height (m)	1
Frequency (kHz)	50
Bottom Sediment Material	Sand
SSP Gradient	Temperature-Driven

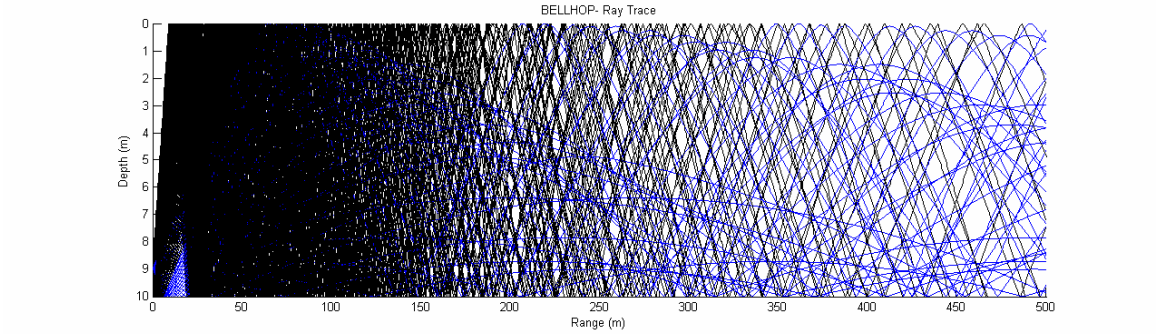

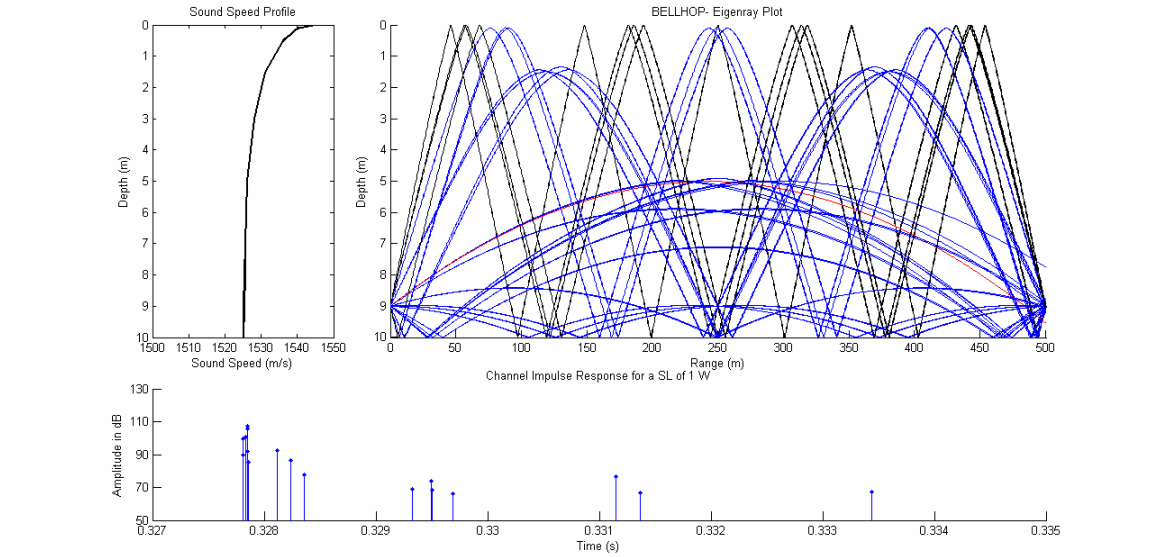

Bellhop Analysis, Case 10.500.1.1.50.Sand.Sal

Parameter	Magnitude
Channel Depth (m)	10
Transmission Range (m)	500
Transmitter Height (m)	1
Receiver Height (m)	1
Frequency (kHz)	50
Bottom Sediment Material	Sand
SSP Gradient	Salinity-Driven

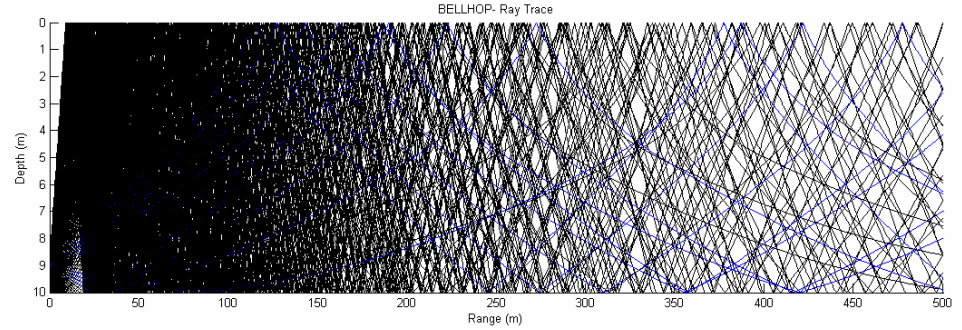

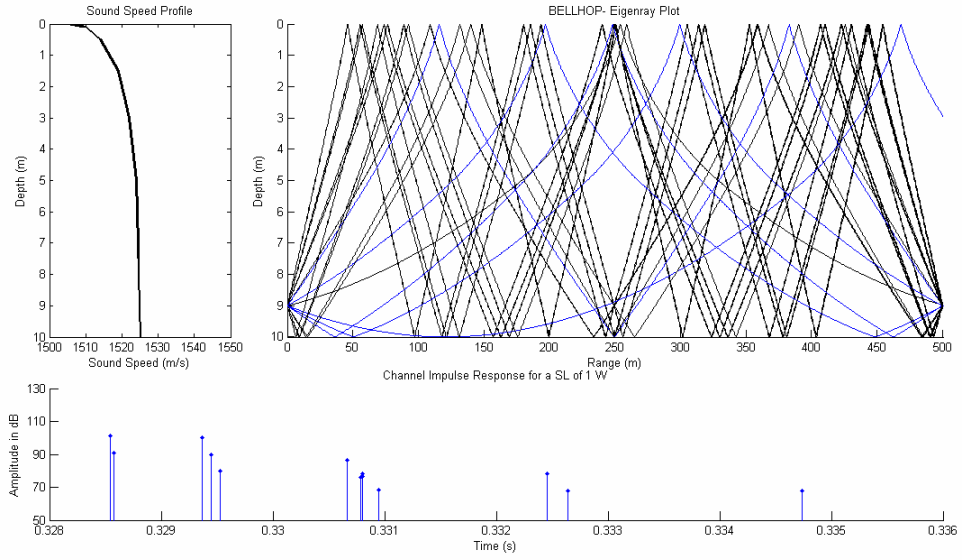

Bellhop Analysis, Case 10.500.1.1.50.Sand.0

Parameter	Magnitude
Channel Depth (m)	10
Transmission Range (m)	500
Transmitter Height (m)	1
Receiver Height (m)	1
Frequency (kHz)	50
Bottom Sediment Material	Sand
SSP Gradient	Isospeed

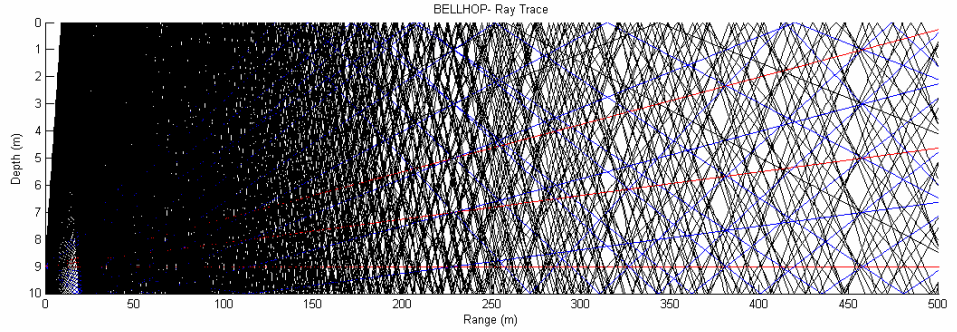

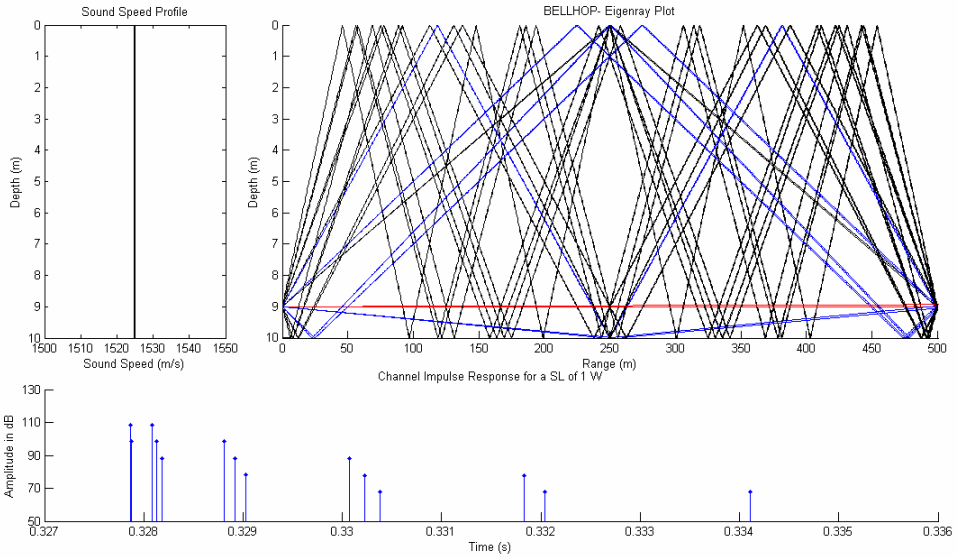

Bellhop Analysis, Case 10.500.1.1.45.Sand.Temp

Parameter	Magnitude
Channel Depth (m)	10
Transmission Range (m)	500
Transmitter Height (m)	1
Receiver Height (m)	1
Frequency (kHz)	45
Bottom Sediment Material	Sand
SSP Gradient	Temperature-Driven

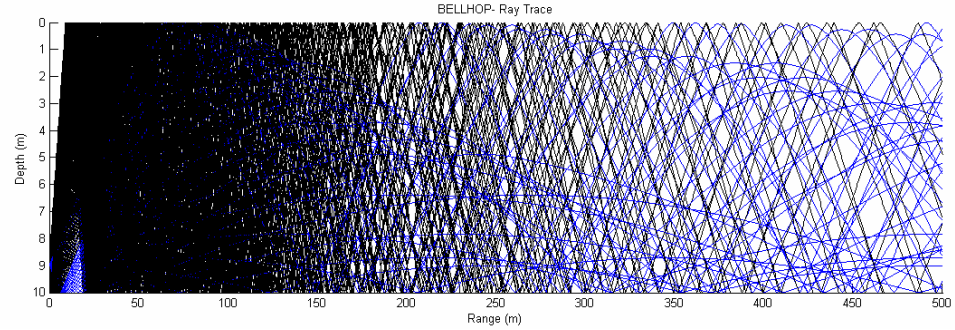

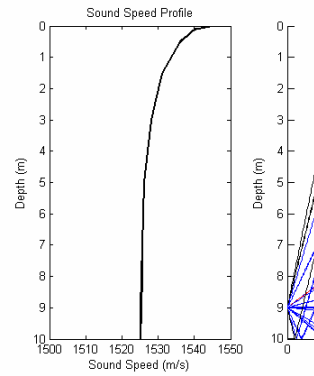

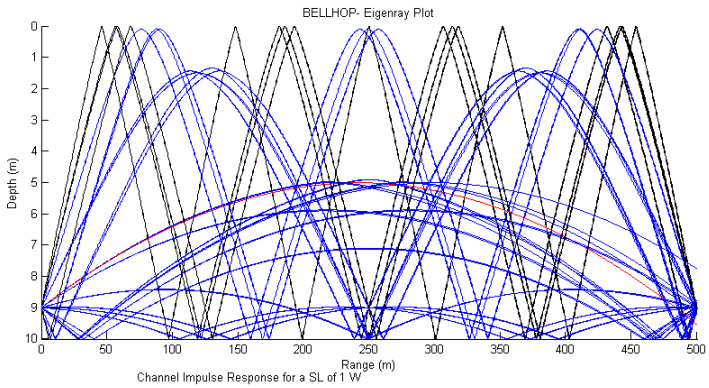

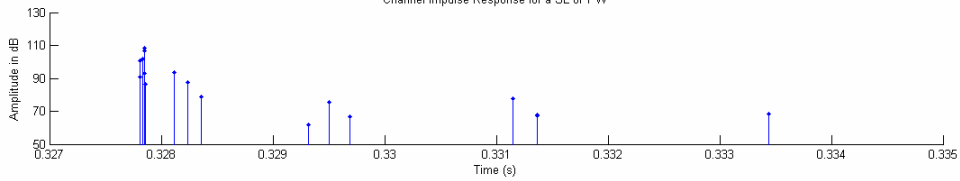

Bellhop Analysis, Case 10.500.1.1.45.Sand.Sal

Parameter	Magnitude
Channel Depth (m)	10
Transmission Range (m)	500
Transmitter Height (m)	1
Receiver Height (m)	1
Frequency (kHz)	45
Bottom Sediment Material	Sand
SSP Gradient	Salinity-Driven

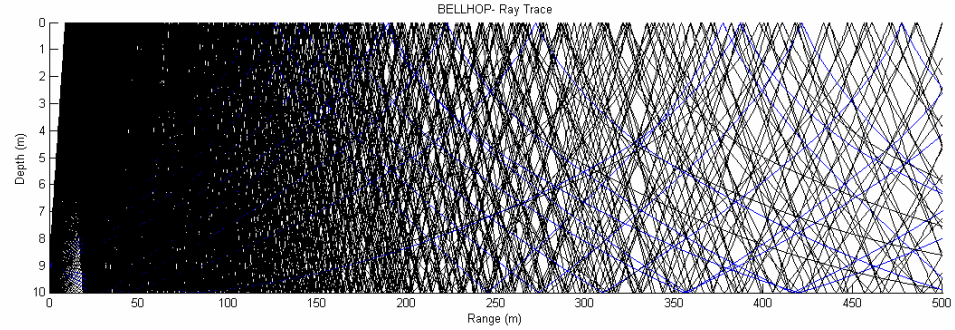

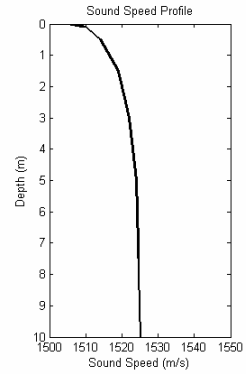

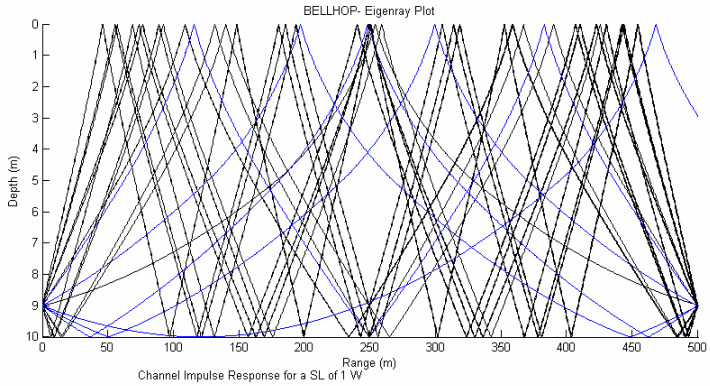

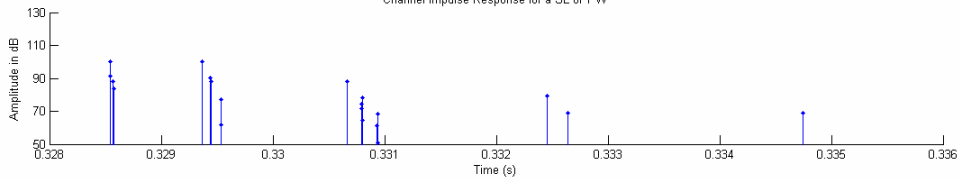

Bellhop Analysis, Case 10.500.1.1.45.Sand.0

Parameter	Magnitude
Channel Depth (m)	10
Transmission Range (m)	500
Transmitter Height (m)	1
Receiver Height (m)	1
Frequency (kHz)	45
Bottom Sediment Material	Sand
SSP Gradient	Isospeed

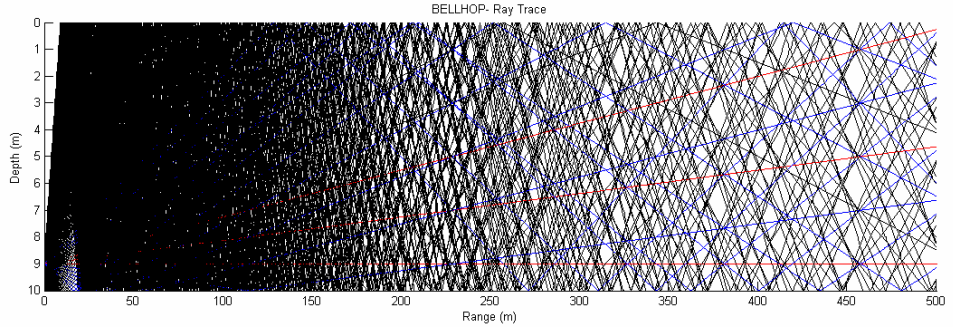

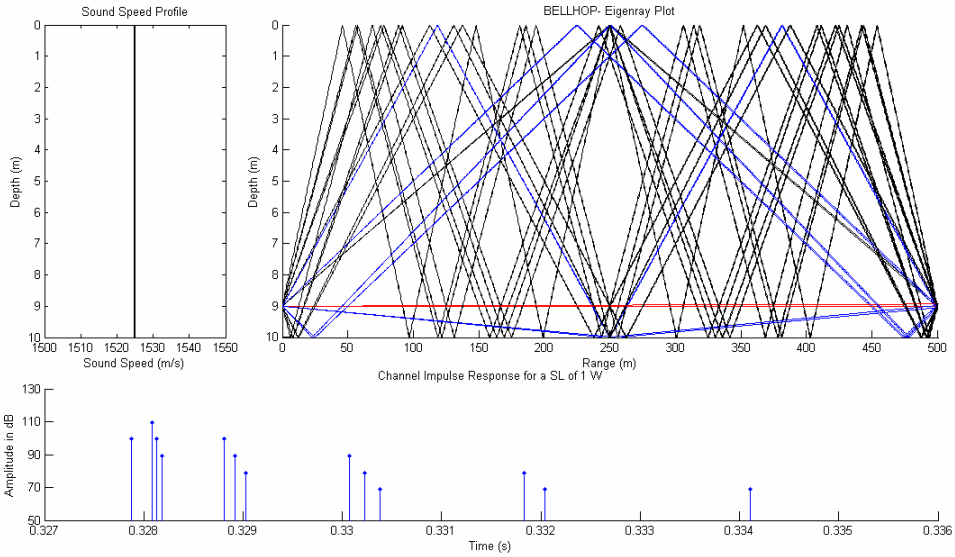

Bellhop Analysis, Case 10.500.1.1.40.Sand.Temp

Parameter	Magnitude
Channel Depth (m)	10
Transmission Range (m)	500
Transmitter Height (m)	1
Receiver Height (m)	1
Frequency (kHz)	40
Bottom Sediment Material	Sand
SSP Gradient	Temperature-Driven

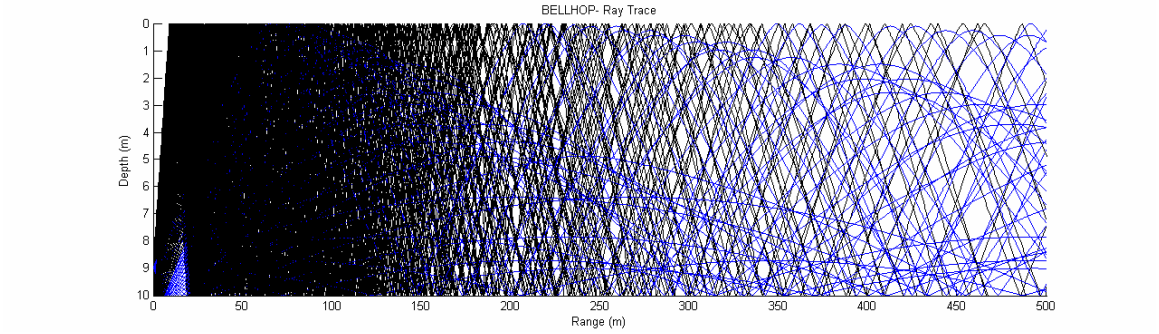

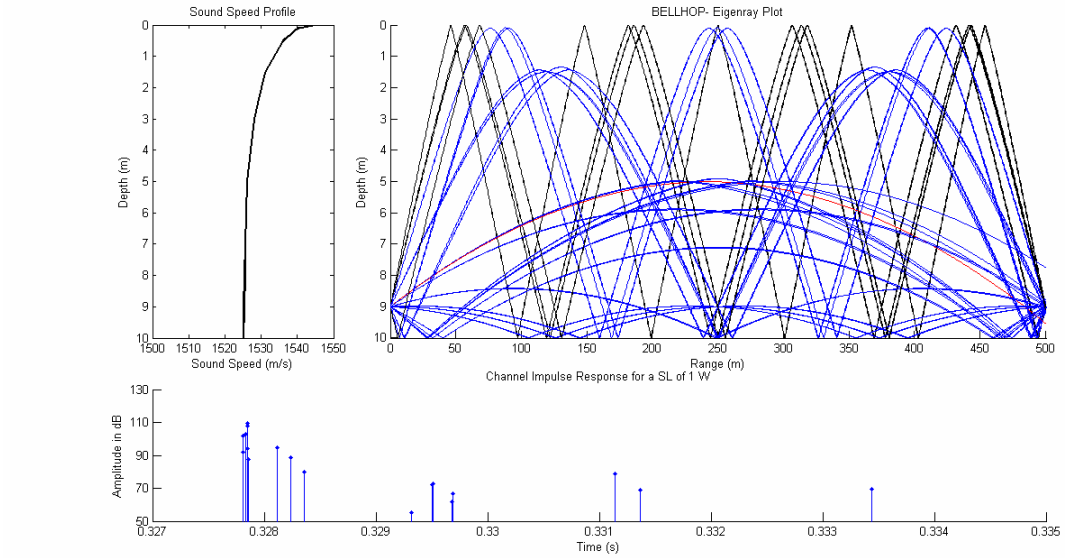

Bellhop Analysis, Case 10.500.1.1.40.Sand.Sal

Parameter	Magnitude
Channel Depth (m)	10
Transmission Range (m)	500
Transmitter Height (m)	1
Receiver Height (m)	1
Frequency (kHz)	40
Bottom Sediment Material	Sand
SSP Gradient	Salinity-Driven

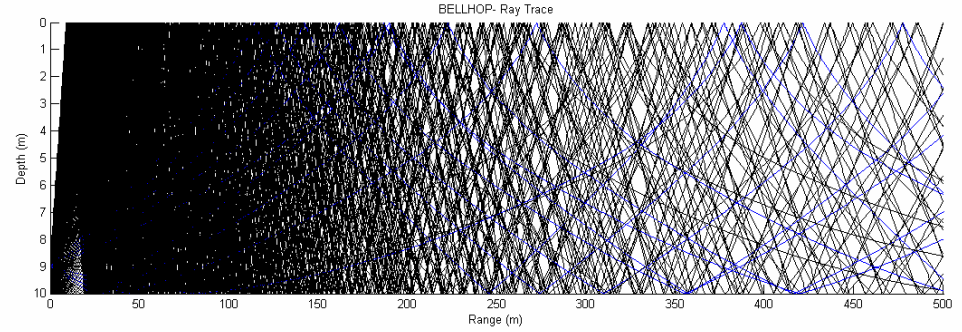

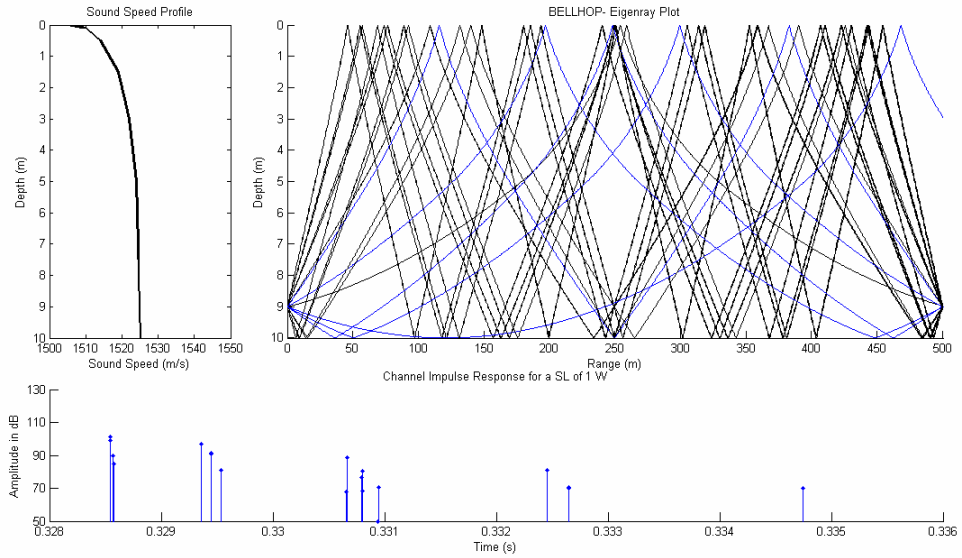

Bellhop Analysis, Case 10.500.1.1.40.Sand.0

Parameter	Magnitude
Channel Depth (m)	10
Transmission Range (m)	500
Transmitter Height (m)	1
Receiver Height (m)	1
Frequency (kHz)	40
Bottom Sediment Material	Sand
SSP Gradient	Isospeed

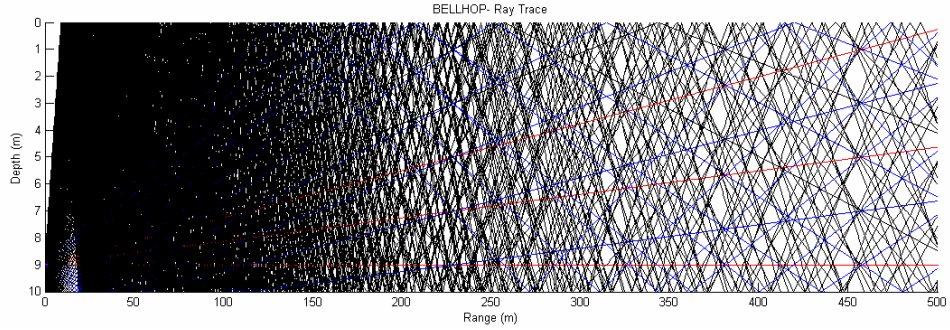

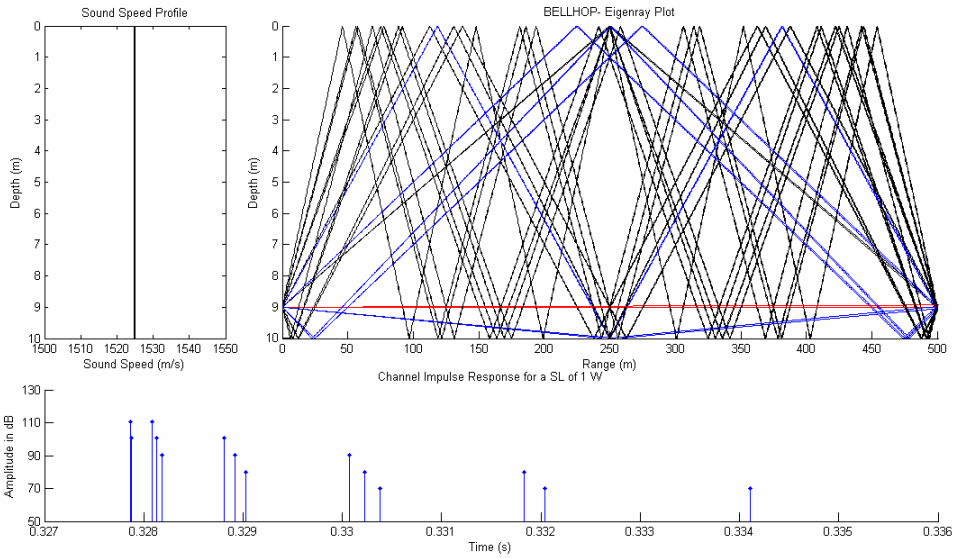

Bellhop Analysis, Case 10.500.1.2.70.Sand.Temp

Parameter	Magnitude
Channel Depth (m)	10
Transmission Range (m)	500
Transmitter Height (m)	1
Receiver Height (m)	2
Frequency (kHz)	70
Bottom Sediment Material	Sand
SSP Gradient	Temperature-Driven

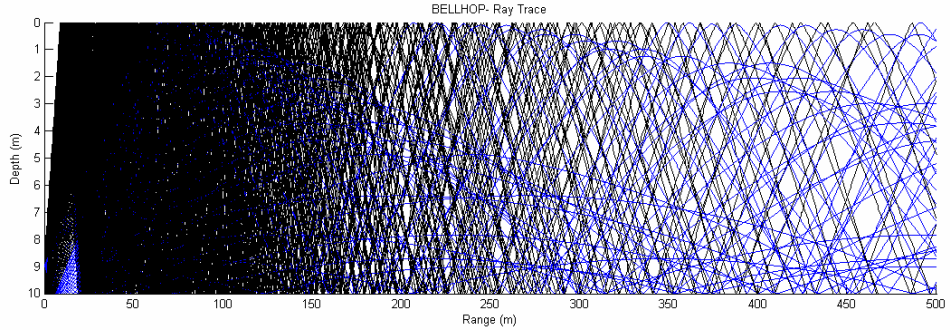

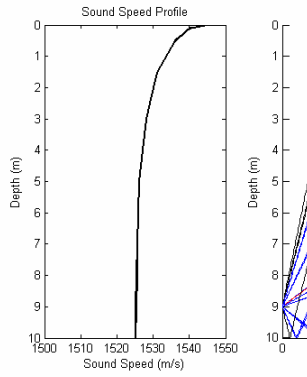

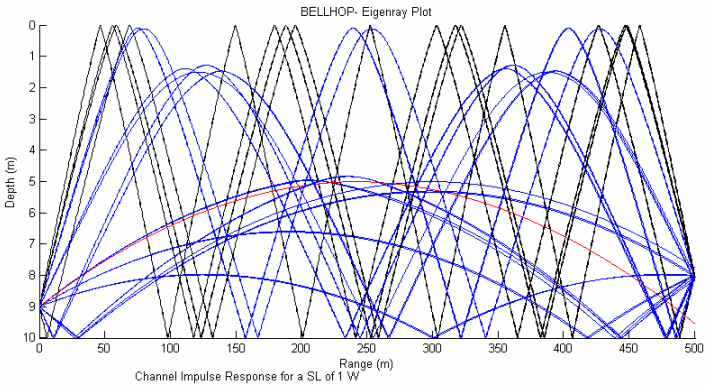

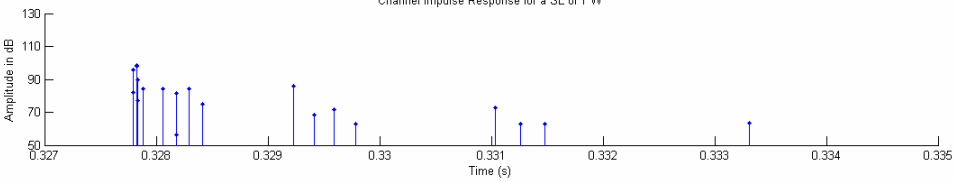

Bellhop Analysis, Case 10.500.1.2.70.Sand.Sal

Parameter	Magnitude
Channel Depth (m)	10
Transmission Range (m)	500
Transmitter Height (m)	1
Receiver Height (m)	2
Frequency (kHz)	70
Bottom Sediment Material	Sand
SSP Gradient	Salinity-Driven

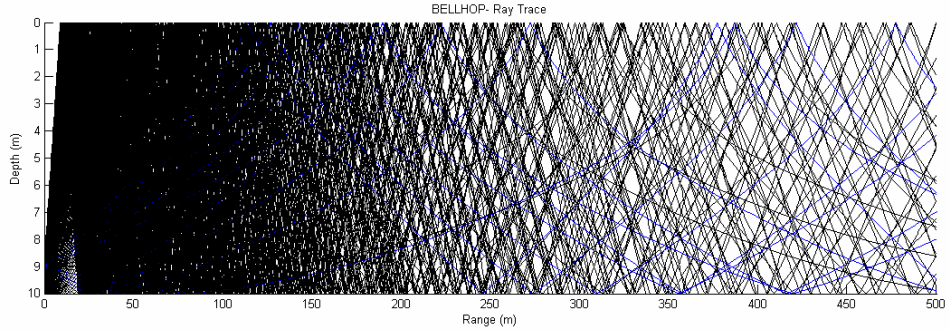

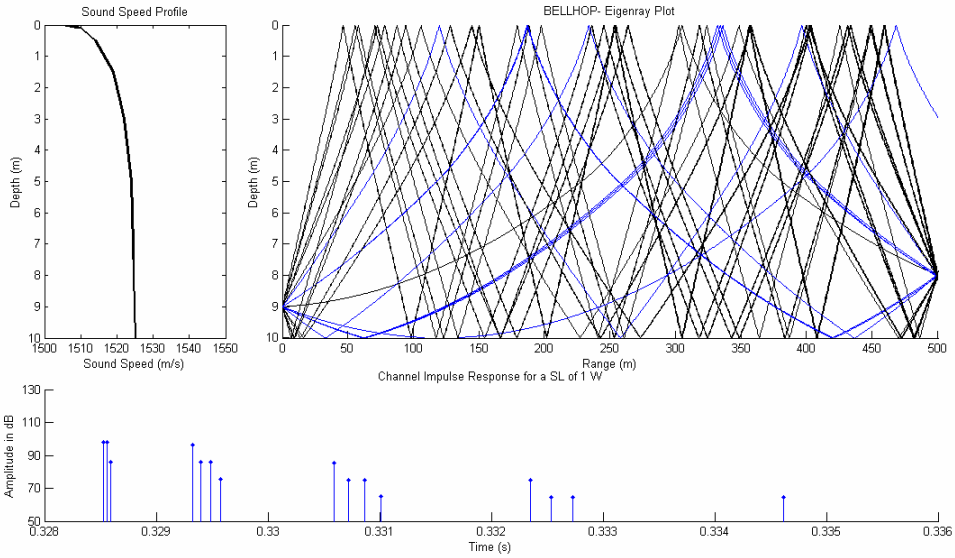

Bellhop Analysis, Case 10.500.1.2.70.Sand.0

Parameter	Magnitude
Channel Depth (m)	10
Transmission Range (m)	500
Transmitter Height (m)	1
Receiver Height (m)	2
Frequency (kHz)	70
Bottom Sediment Material	Sand
SSP Gradient	Isospeed

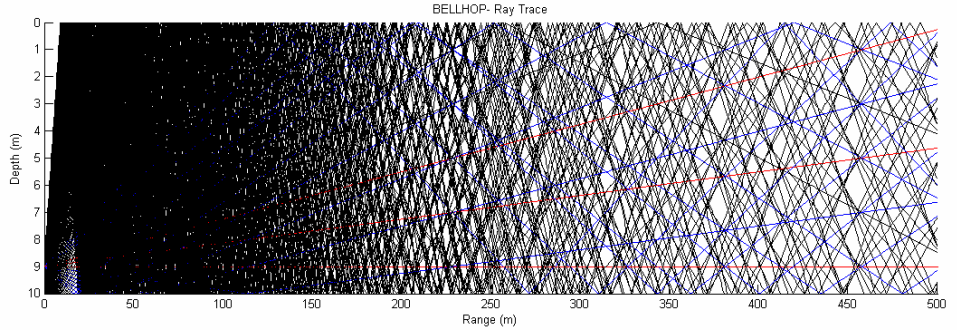

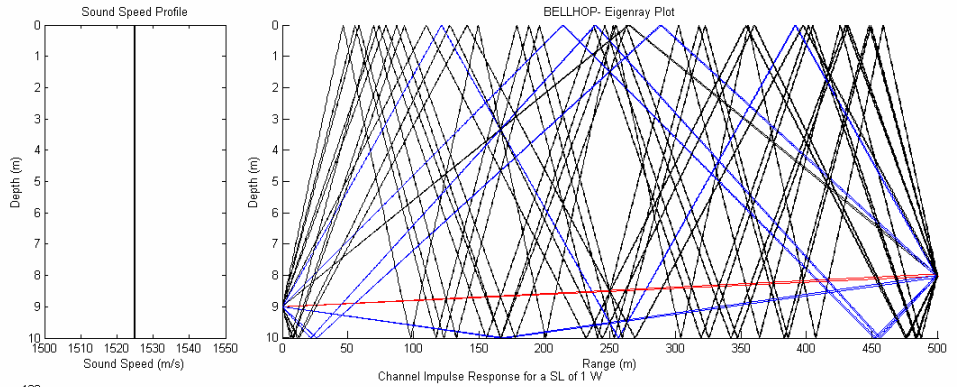

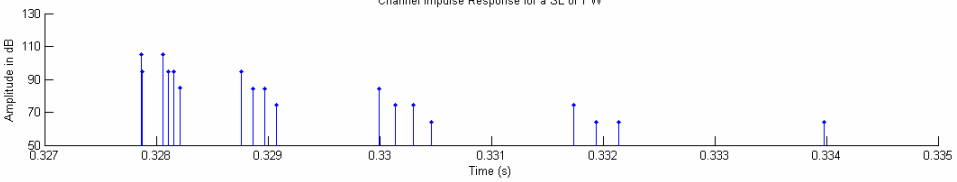

Bellhop Analysis, Case 10.500.1.4.70.Sand.Temp

Parameter	Magnitude
Channel Depth (m)	10
Transmission Range (m)	500
Transmitter Height (m)	1
Receiver Height (m)	4
Frequency (kHz)	70
Bottom Sediment Material	Sand
SSP Gradient	Temperature-Driven

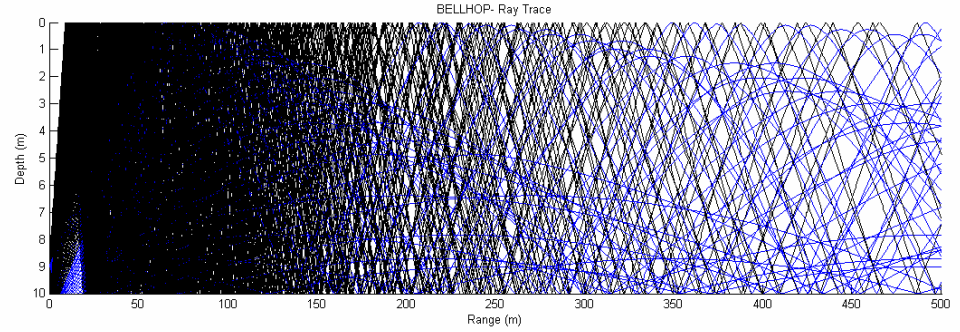

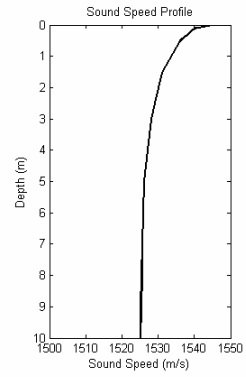

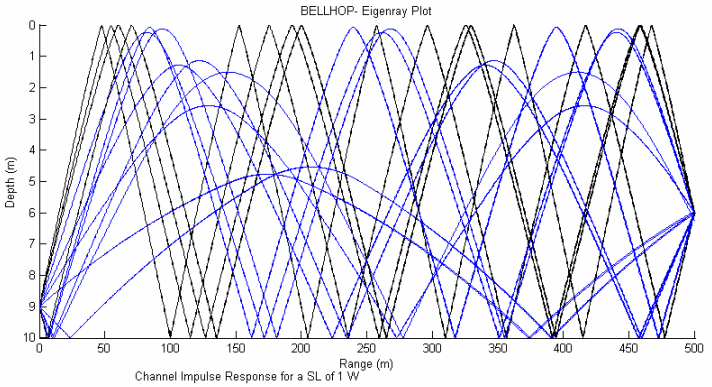

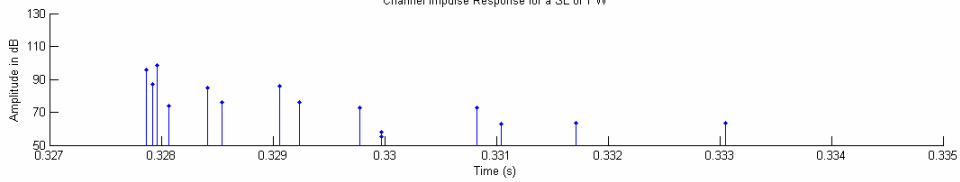

Bellhop Analysis, Case 10.500.1.4.70.Sand.Sal

Parameter	Magnitude
Channel Depth (m)	10
Transmission Range (m)	500
Transmitter Height (m)	1
Receiver Height (m)	4
Frequency (kHz)	70
Bottom Sediment Material	Sand
SSP Gradient	Salinity-Driven

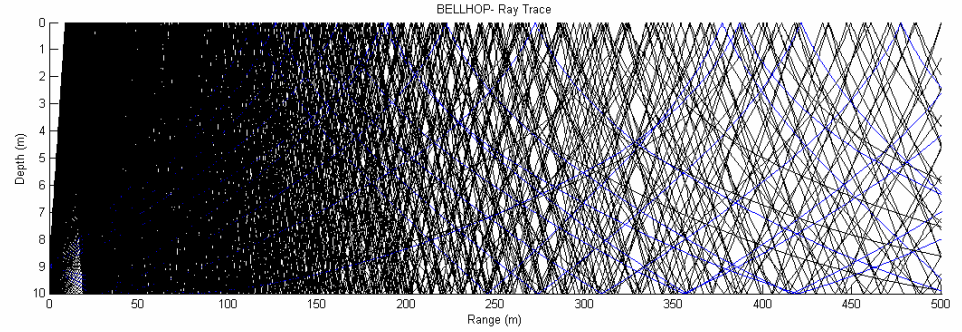

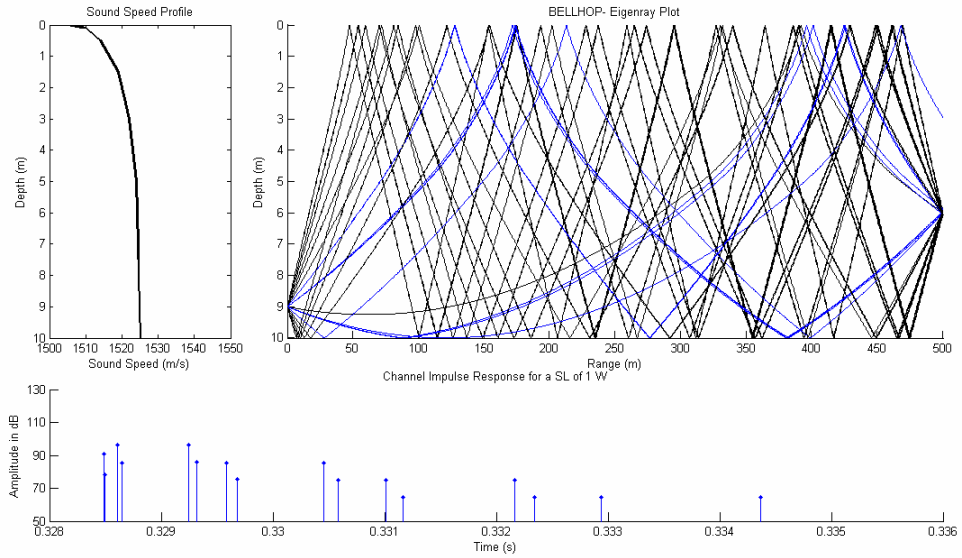

Bellhop Analysis, Case 10.500.1.4.70.Sand.0

Parameter	Magnitude
Channel Depth (m)	10
Transmission Range (m)	500
Transmitter Height (m)	1
Receiver Height (m)	4
Frequency (kHz)	70
Bottom Sediment Material	Sand
SSP Gradient	Isospeed

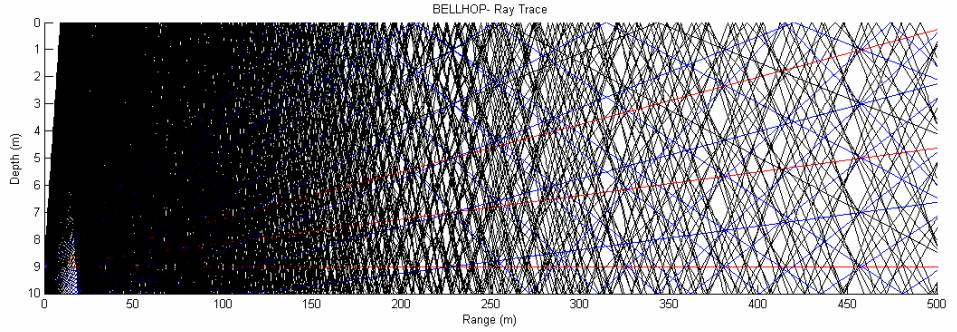

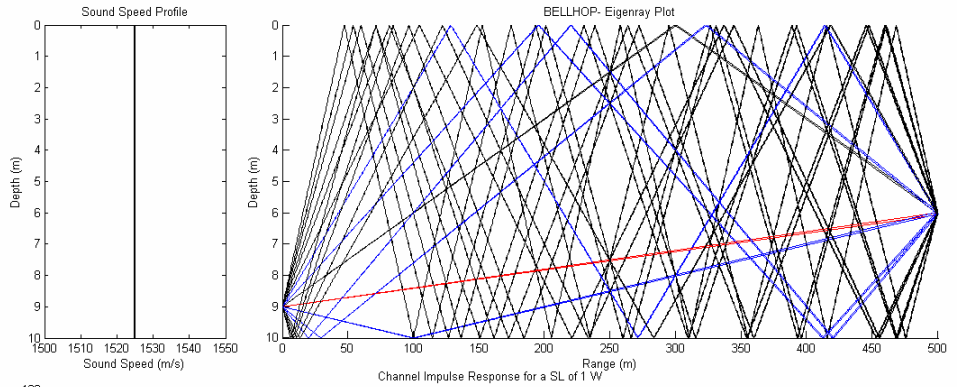

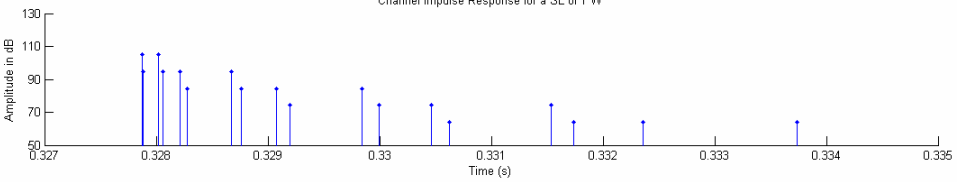

Bellhop Analysis, Case 10.500.2.1.70.Sand.Temp

Parameter	Magnitude
Channel Depth (m)	10
Transmission Range (m)	500
Transmitter Height (m)	2
Receiver Height (m)	1
Frequency (kHz)	70
Bottom Sediment Material	Sand
SSP Gradient	Temperature-Driven

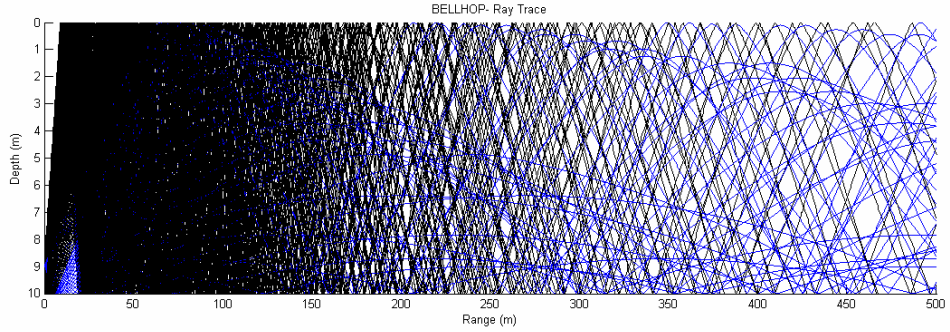

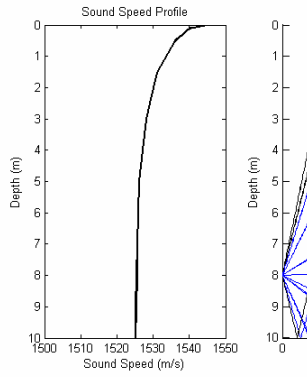

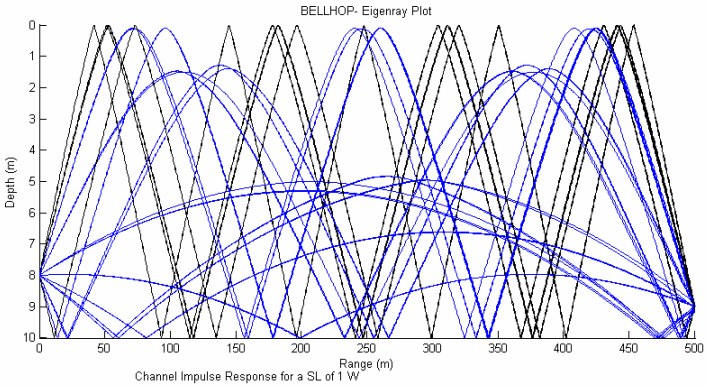

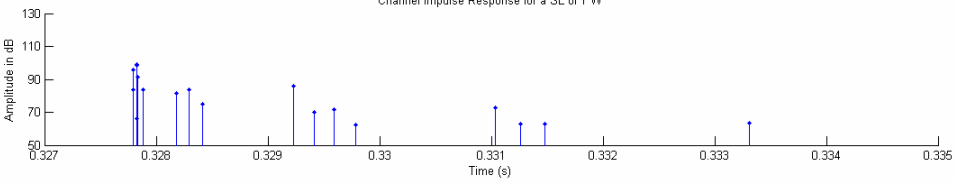

Bellhop Analysis, Case 10.500.2.1.70.Sand.Sal

Parameter	Magnitude
Channel Depth (m)	10
Transmission Range (m)	500
Transmitter Height (m)	2
Receiver Height (m)	1
Frequency (kHz)	70
Bottom Sediment Material	Sand
SSP Gradient	Salinity-Driven

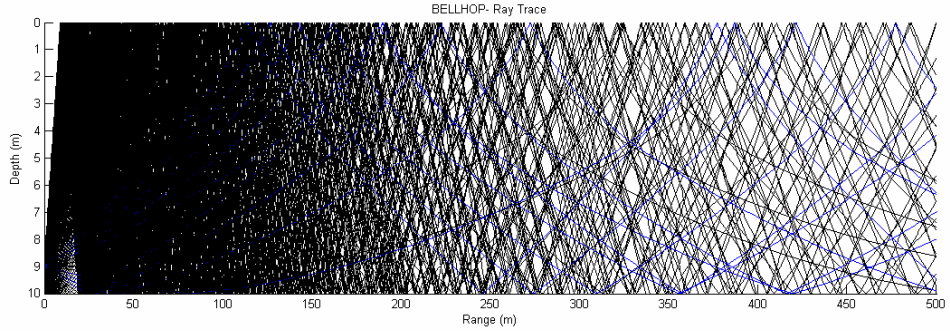

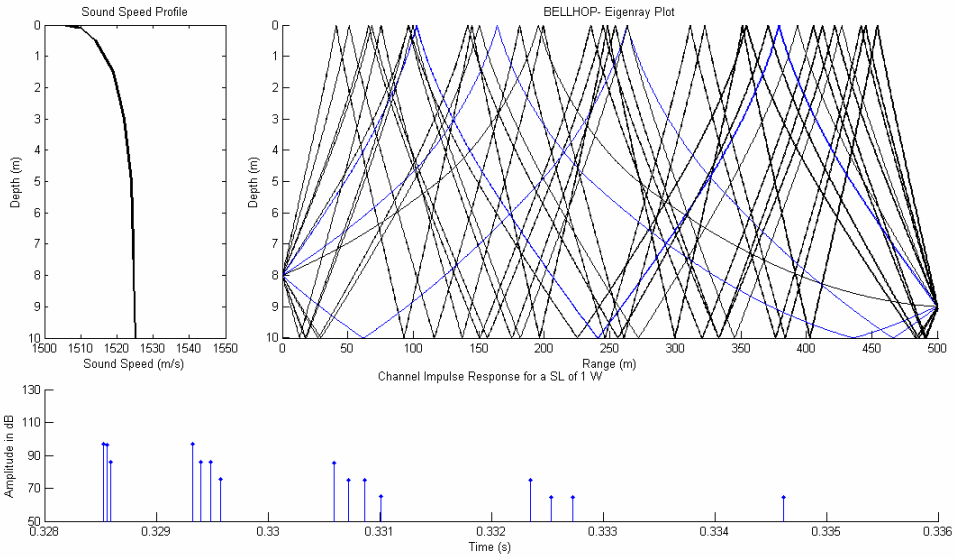

Bellhop Analysis, Case 10.500.2.1.70.Sand.0

Parameter	Magnitude
Channel Depth (m)	10
Transmission Range (m)	500
Transmitter Height (m)	2
Receiver Height (m)	1
Frequency (kHz)	70
Bottom Sediment Material	Sand
SSP Gradient	Isospeed

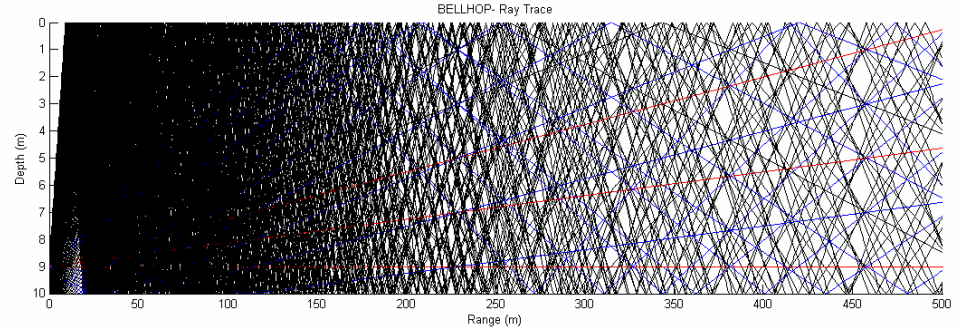

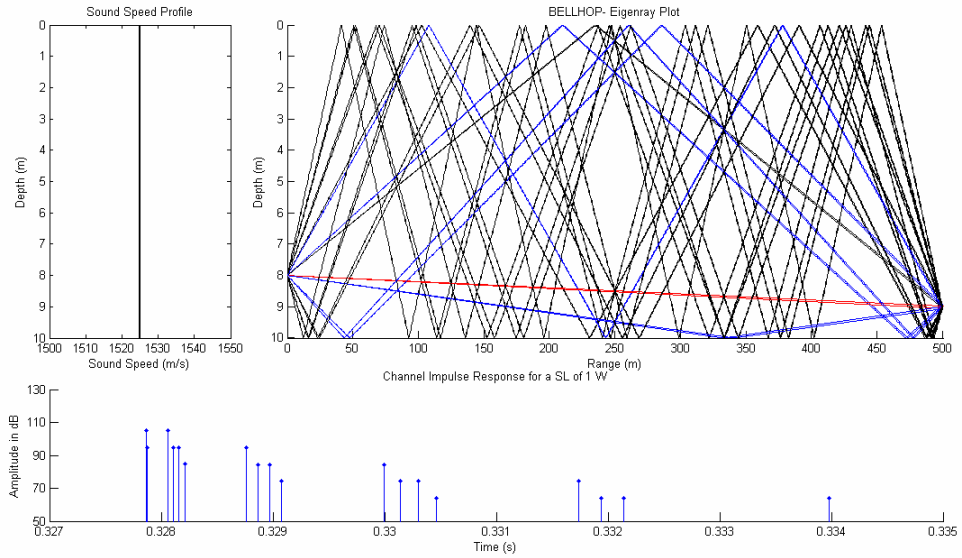

Bellhop Analysis, Case 10.500.2.2.70.Sand.Temp

Parameter	Magnitude
Channel Depth (m)	10
Transmission Range (m)	500
Transmitter Height (m)	2
Receiver Height (m)	2
Frequency (kHz)	70
Bottom Sediment Material	Sand
SSP Gradient	Temperature-Driven

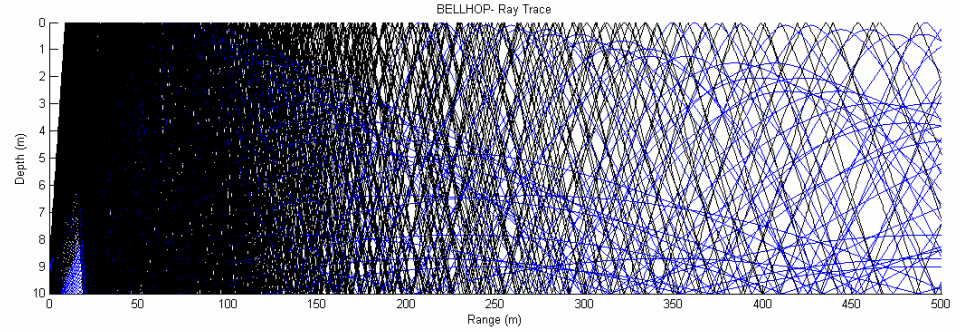

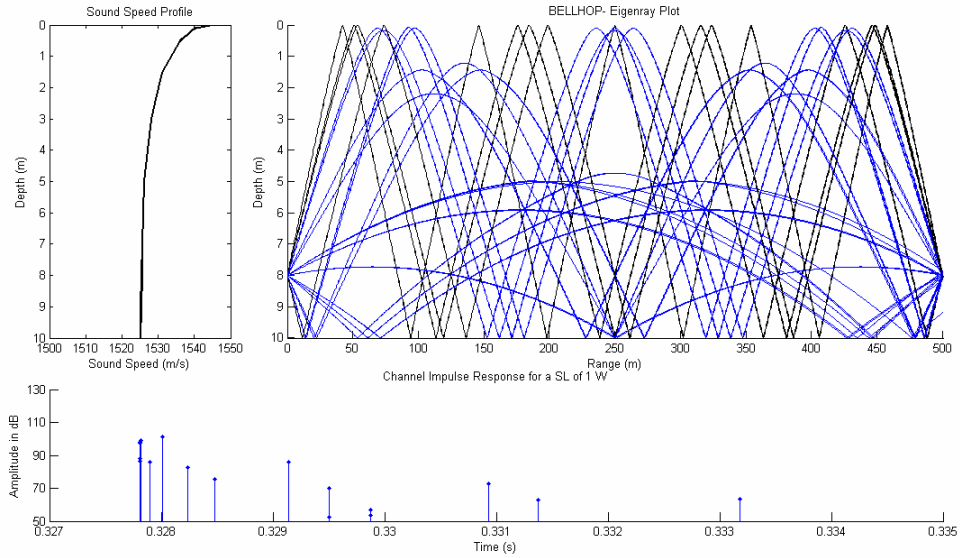

Bellhop Analysis, Case 10.500.2.2.70.Sand.Sal

Parameter	Magnitude
Channel Depth (m)	10
Transmission Range (m)	500
Transmitter Height (m)	2
Receiver Height (m)	2
Frequency (kHz)	70
Bottom Sediment Material	Sand
SSP Gradient	Salinity-Driven

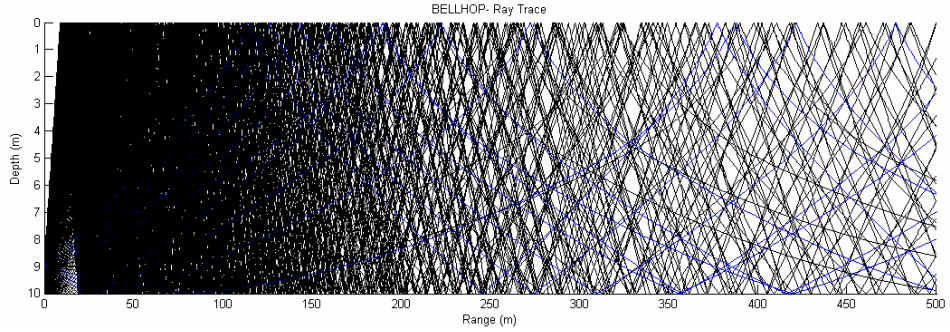

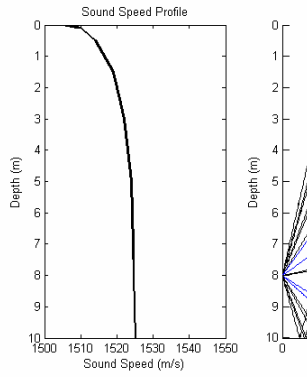

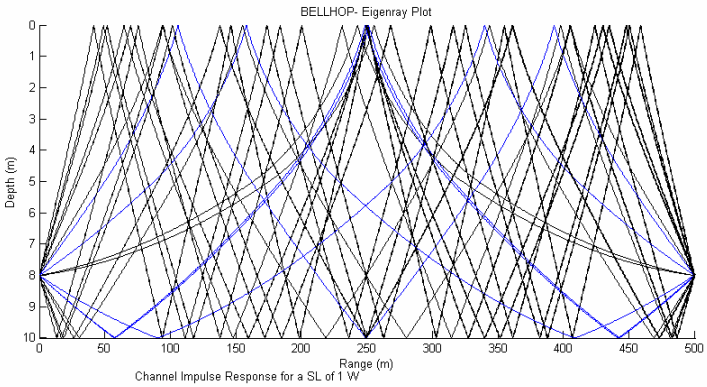

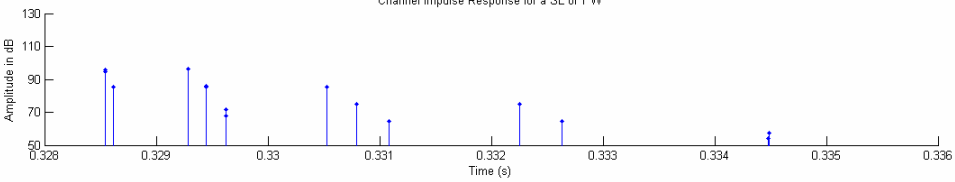

Bellhop Analysis, Case 10.500.2.2.70.Sand.0

Parameter	Magnitude
Channel Depth (m)	10
Transmission Range (m)	500
Transmitter Height (m)	2
Receiver Height (m)	2
Frequency (kHz)	70
Bottom Sediment Material	Sand
SSP Gradient	Isospeed

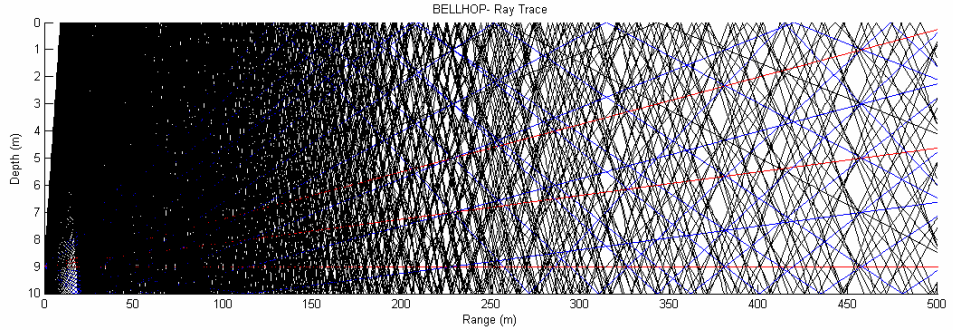

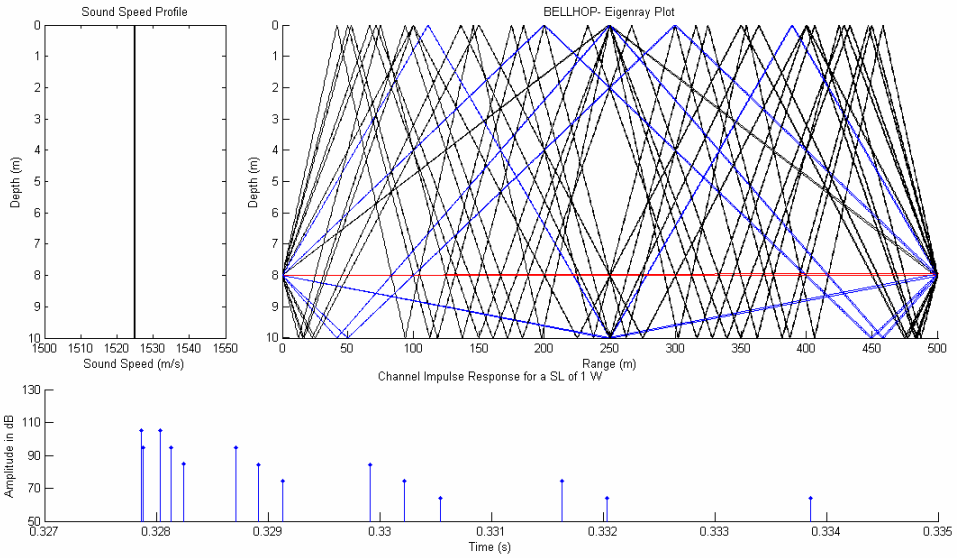

Bellhop Analysis, Case 10.500.2.4.70.Sand.Temp

Parameter	Magnitude
Channel Depth (m)	10
Transmission Range (m)	500
Transmitter Height (m)	2
Receiver Height (m)	4
Frequency (kHz)	70
Bottom Sediment Material	Sand
SSP Gradient	Temperature-Driven

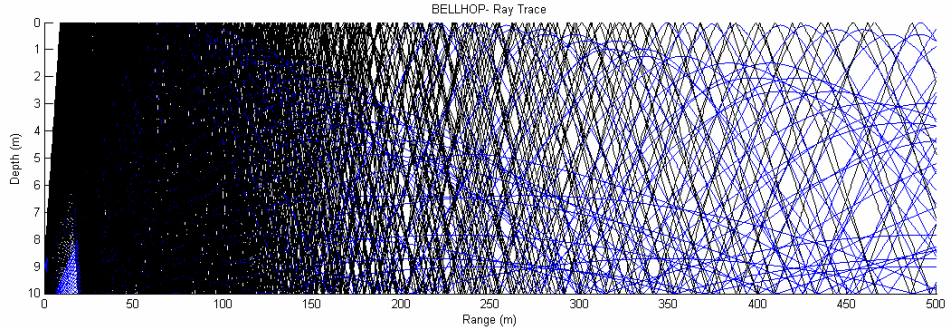

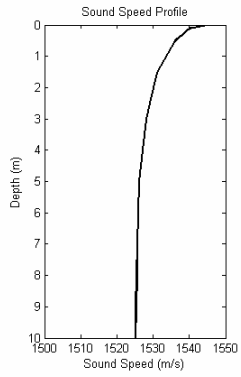

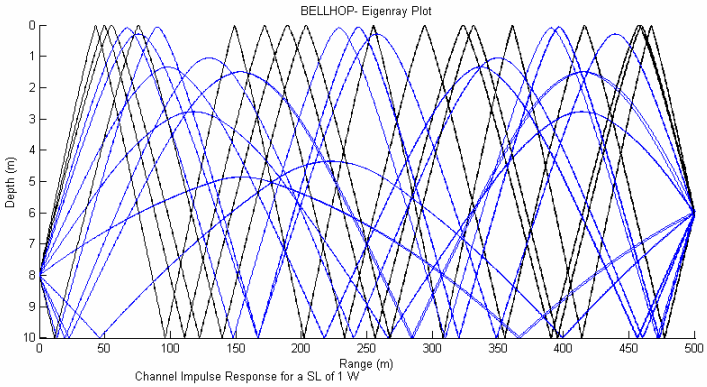

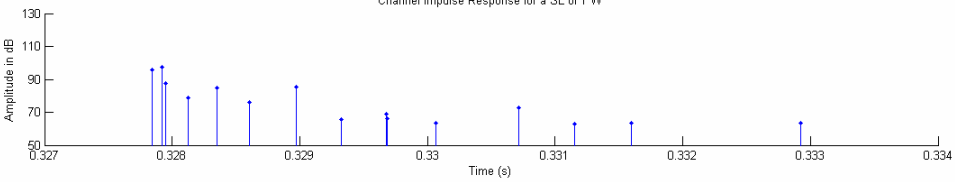

Bellhop Analysis, Case 10.500.2.4.70.Sand.Sal

Parameter	Magnitude
Channel Depth (m)	10
Transmission Range (m)	500
Transmitter Height (m)	2
Receiver Height (m)	4
Frequency (kHz)	70
Bottom Sediment Material	Sand
SSP Gradient	Salinity-Driven

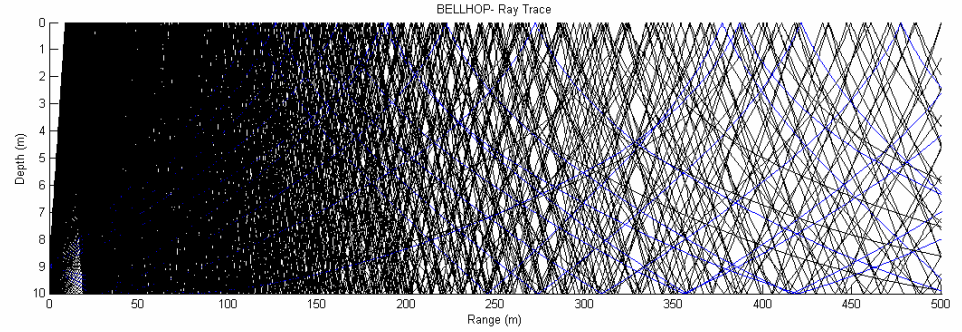

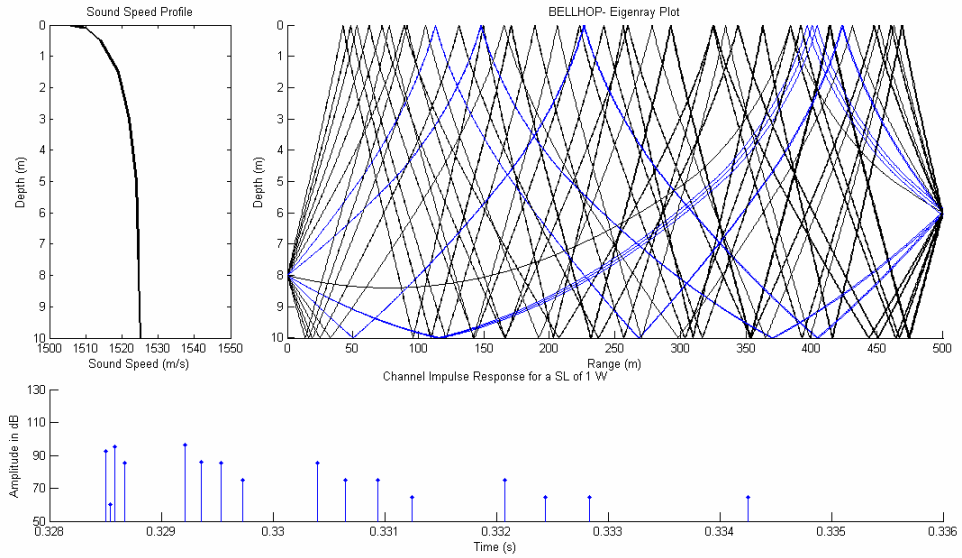

Bellhop Analysis, Case 10.500.2.4.70.Sand.0

Parameter	Magnitude
Channel Depth (m)	10
Transmission Range (m)	500
Transmitter Height (m)	2
Receiver Height (m)	4
Frequency (kHz)	70
Bottom Sediment Material	Sand
SSP Gradient	Isospeed

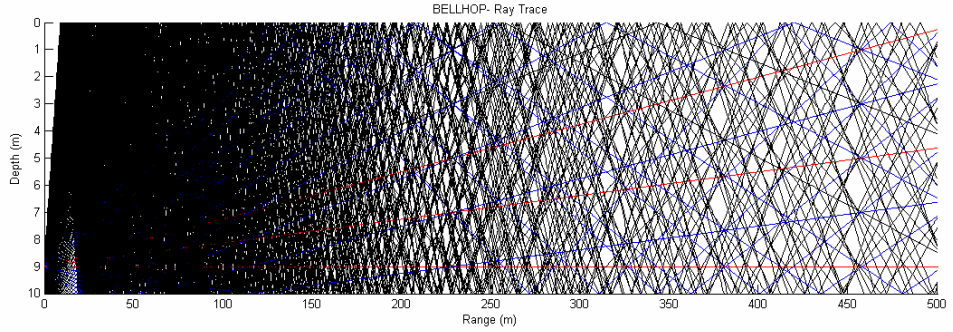

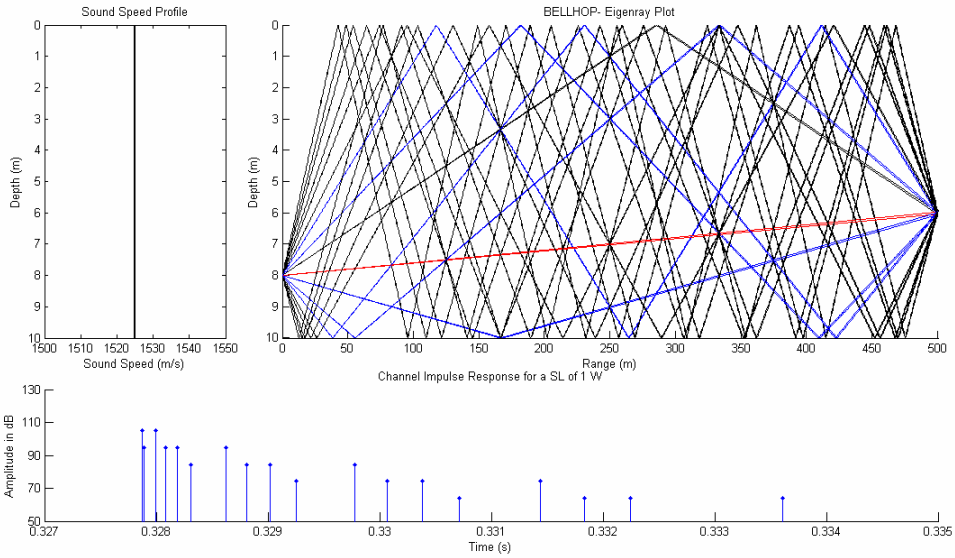

Bellhop Analysis, Case 10.500.4.1.70.Sand.Temp

Parameter	Magnitude
Channel Depth (m)	10
Transmission Range (m)	500
Transmitter Height (m)	4
Receiver Height (m)	1
Frequency (kHz)	70
Bottom Sediment Material	Sand
SSP Gradient	Temperature-Driven

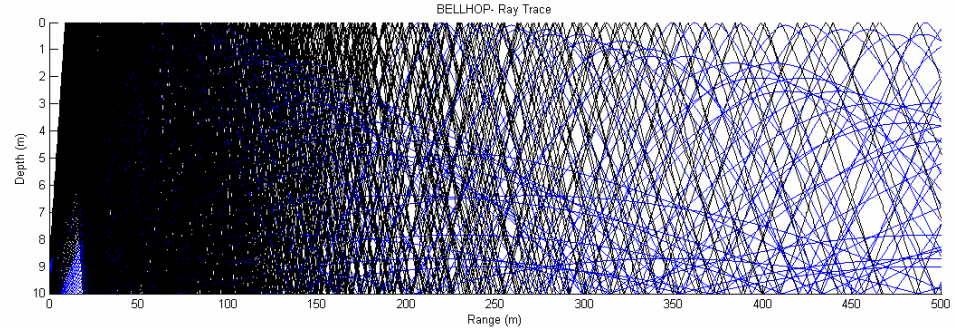

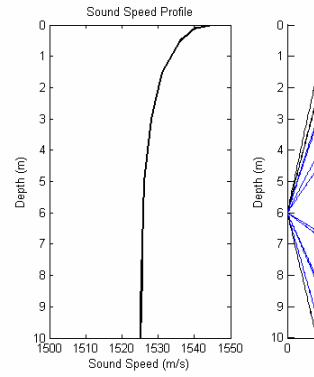

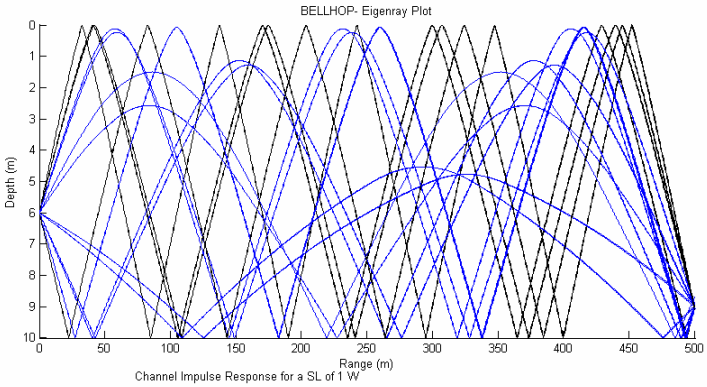

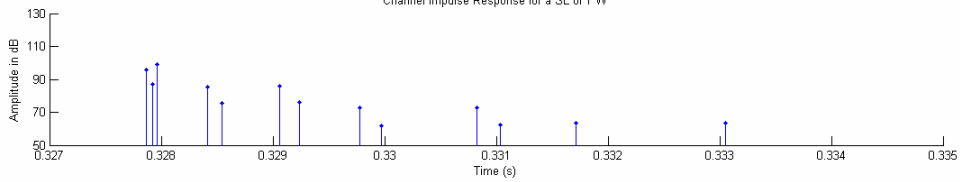

Bellhop Analysis, Case 10.500.4.1.70.Sand.Sal

Parameter	Magnitude
Channel Depth (m)	10
Transmission Range (m)	500
Transmitter Height (m)	4
Receiver Height (m)	1
Frequency (kHz)	70
Bottom Sediment Material	Sand
SSP Gradient	Salinity-Driven

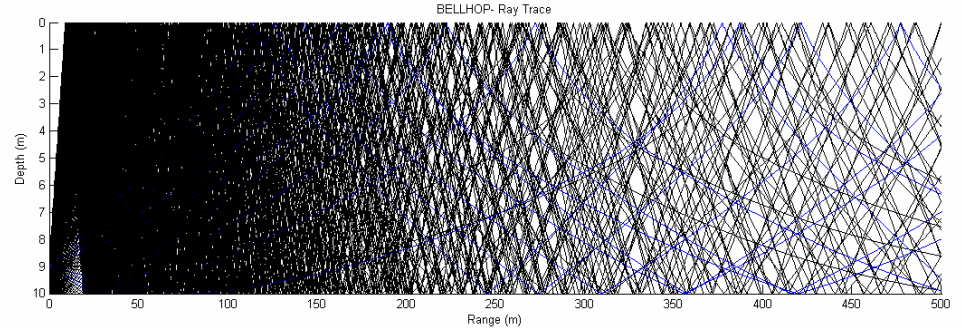

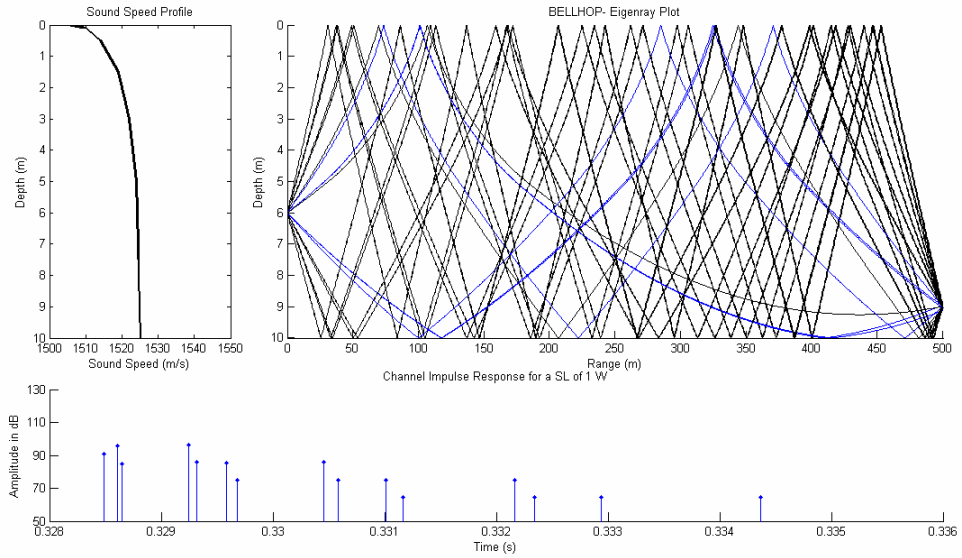

Bellhop Analysis, Case 10.500.4.1.70.Sand.0

Parameter	Magnitude
Channel Depth (m)	10
Transmission Range (m)	500
Transmitter Height (m)	4
Receiver Height (m)	1
Frequency (kHz)	70
Bottom Sediment Material	Sand
SSP Gradient	Isospeed

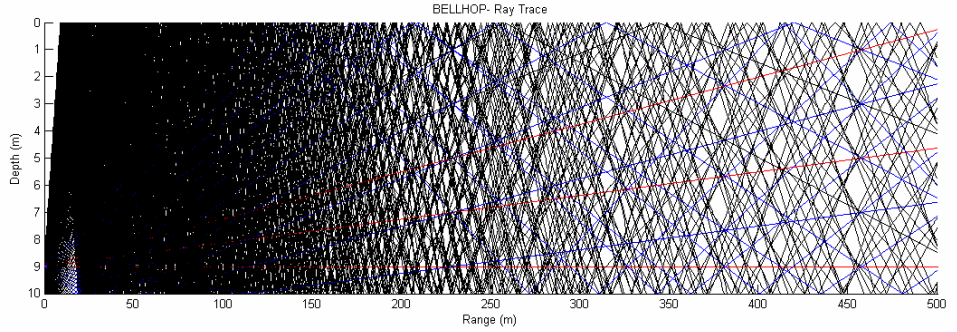

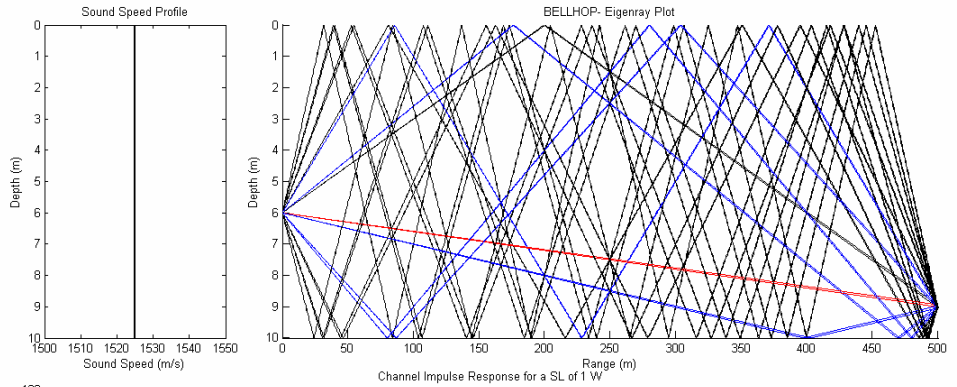

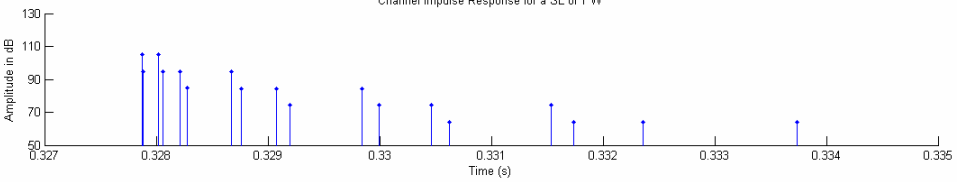

Bellhop Analysis, Case 10.500.4.2.70.Sand.Temp

Parameter	Magnitude
Channel Depth (m)	10
Transmission Range (m)	500
Transmitter Height (m)	4
Receiver Height (m)	2
Frequency (kHz)	70
Bottom Sediment Material	Sand
SSP Gradient	Temperature-Driven

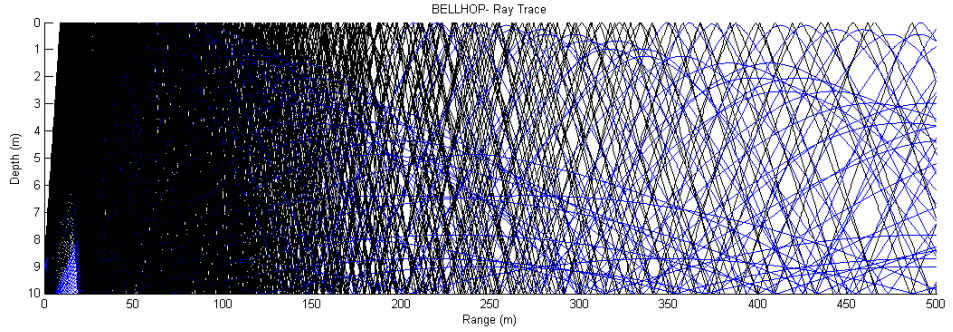

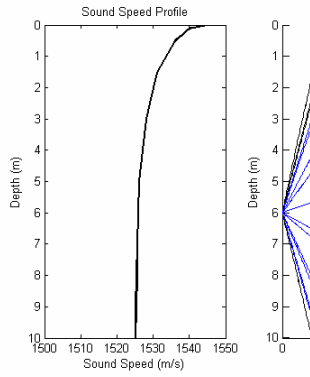

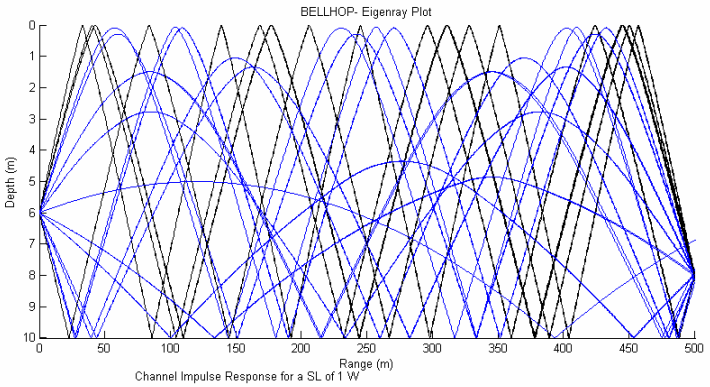

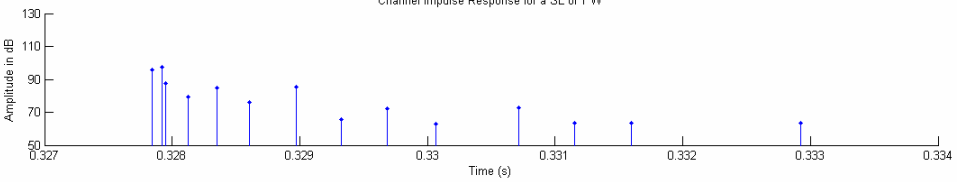

Bellhop Analysis, Case 10.500.4.2.70.Sand.Sal

Parameter	Magnitude
Channel Depth (m)	10
Transmission Range (m)	500
Transmitter Height (m)	4
Receiver Height (m)	2
Frequency (kHz)	70
Bottom Sediment Material	Sand
SSP Gradient	Salinity-Driven

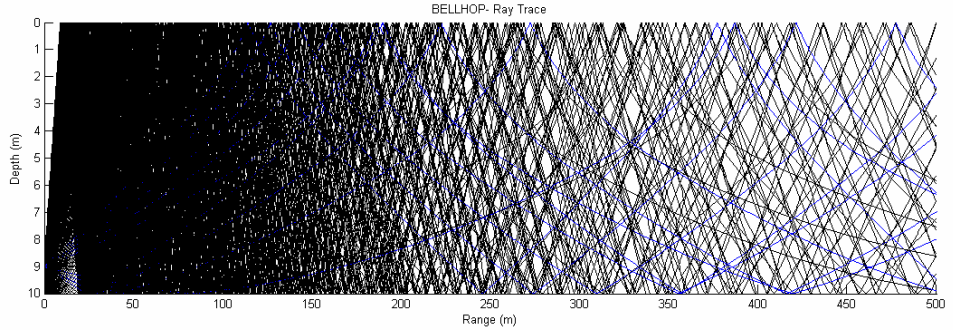

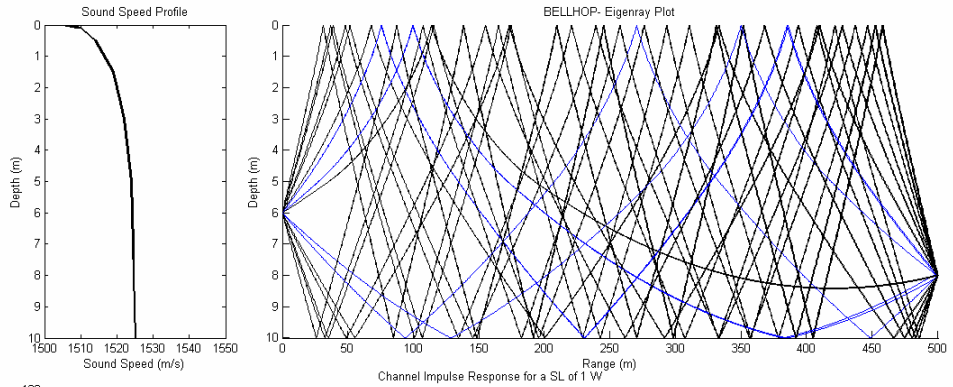

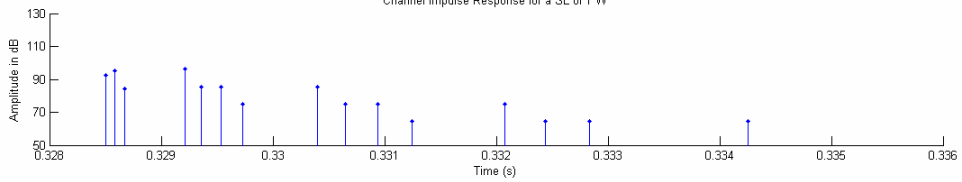

Bellhop Analysis, Case 10.500.4.2.70.Sand.0

Parameter	Magnitude
Channel Depth (m)	10
Transmission Range (m)	500
Transmitter Height (m)	4
Receiver Height (m)	2
Frequency (kHz)	70
Bottom Sediment Material	Sand
SSP Gradient	Isospeed

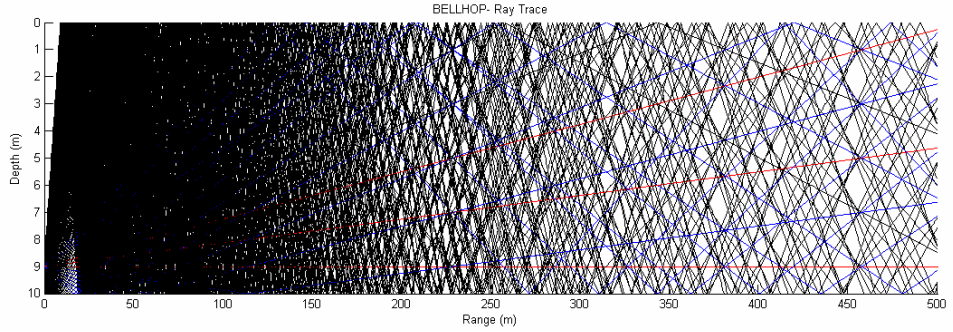

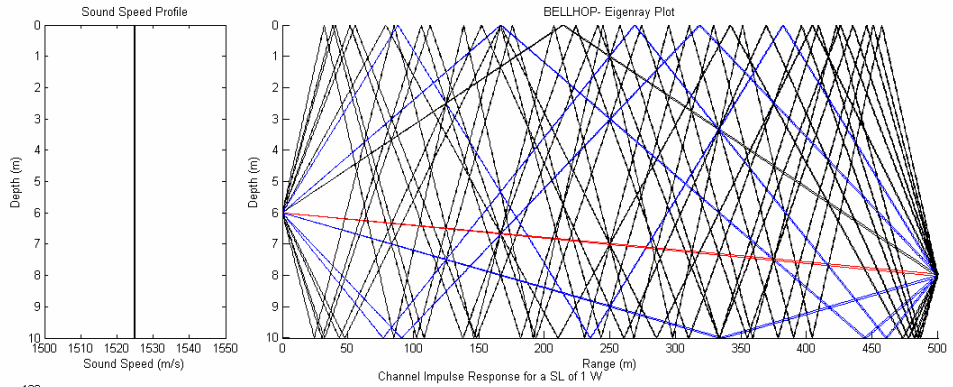

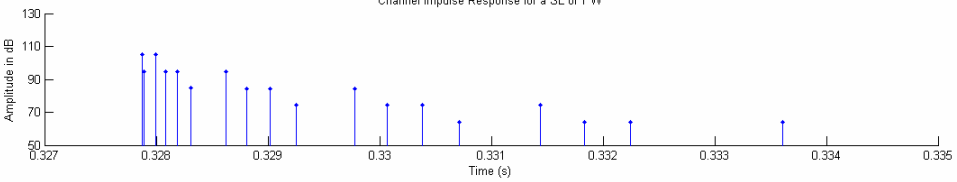

Bellhop Analysis, Case 10.500.4.4.70.Sand.Temp

Parameter	Magnitude
Channel Depth (m)	10
Transmission Range (m)	500
Transmitter Height (m)	4
Receiver Height (m)	4
Frequency (kHz)	70
Bottom Sediment Material	Sand
SSP Gradient	Temperature-Driven

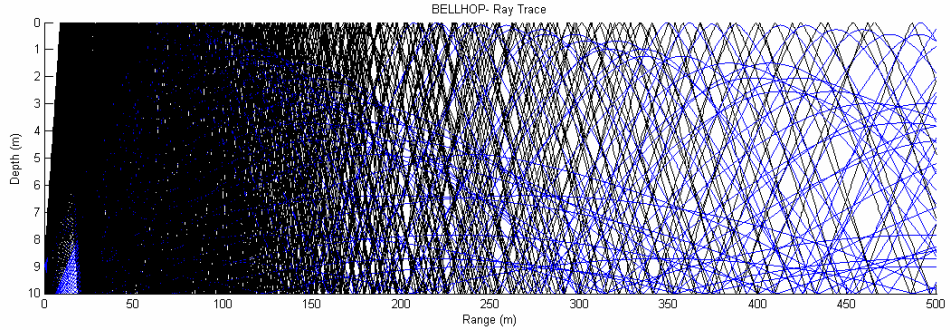

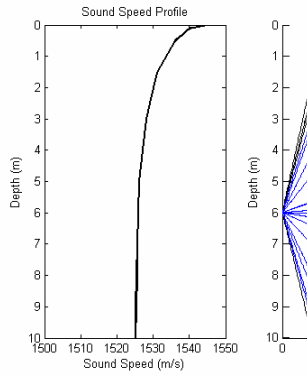

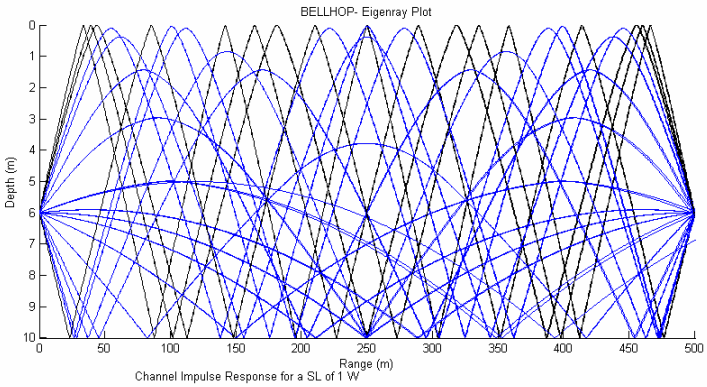

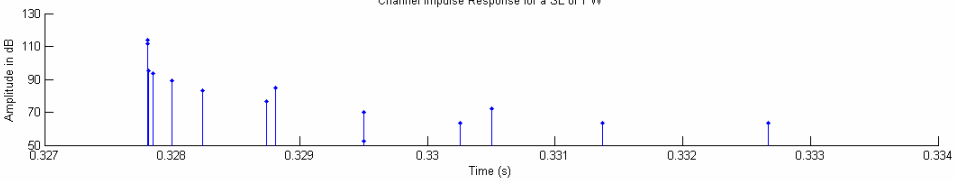

Bellhop Analysis, Case 10.500.4.4.70.Sand.Sal

Parameter	Magnitude
Channel Depth (m)	10
Transmission Range (m)	500
Transmitter Height (m)	4
Receiver Height (m)	4
Frequency (kHz)	70
Bottom Sediment Material	Sand
SSP Gradient	Salinity-Driven

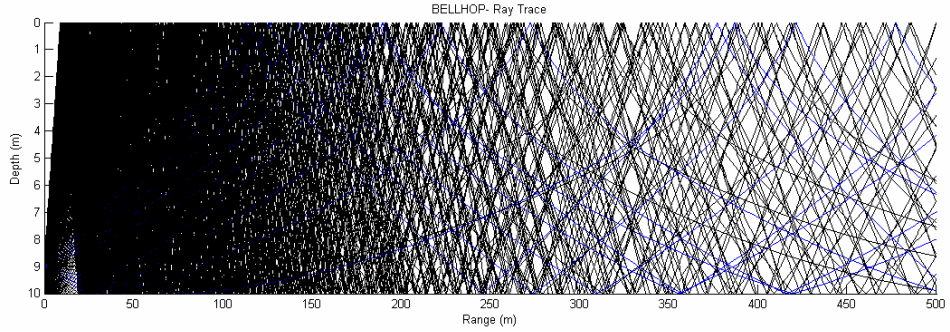

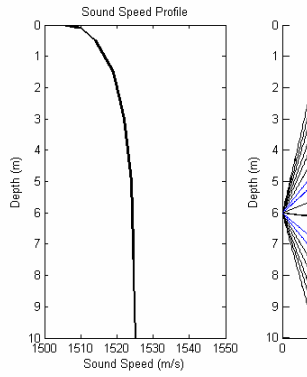

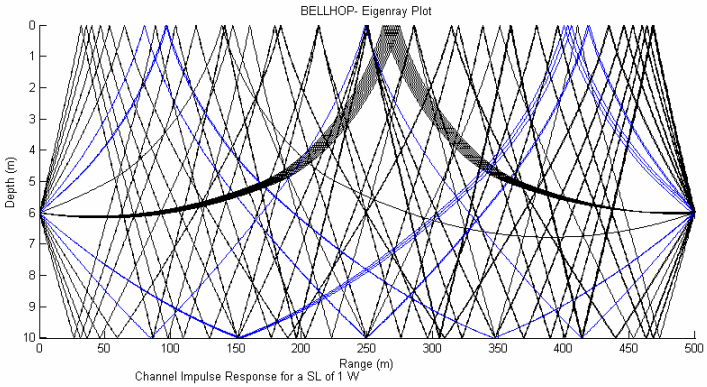

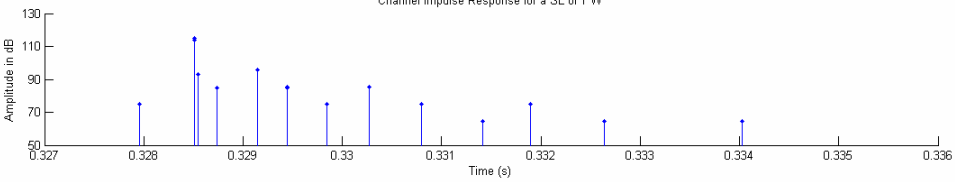

Bellhop Analysis, Case 10.500.4.4.70.Sand.0

Parameter	Magnitude
Channel Depth (m)	10
Transmission Range (m)	500
Transmitter Height (m)	4
Receiver Height (m)	4
Frequency (kHz)	70
Bottom Sediment Material	Sand
SSP Gradient	Isospeed

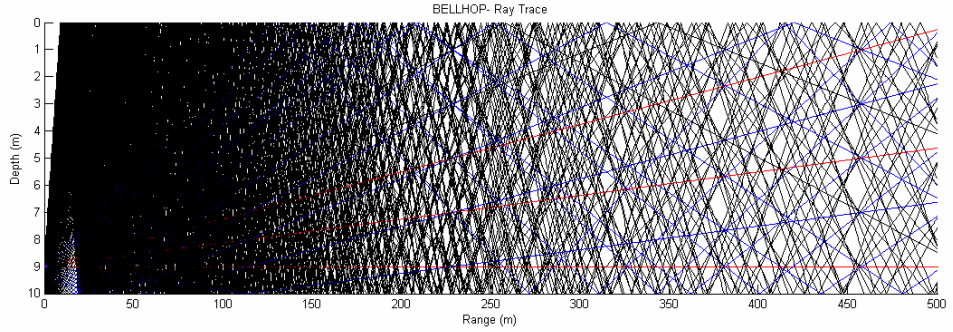

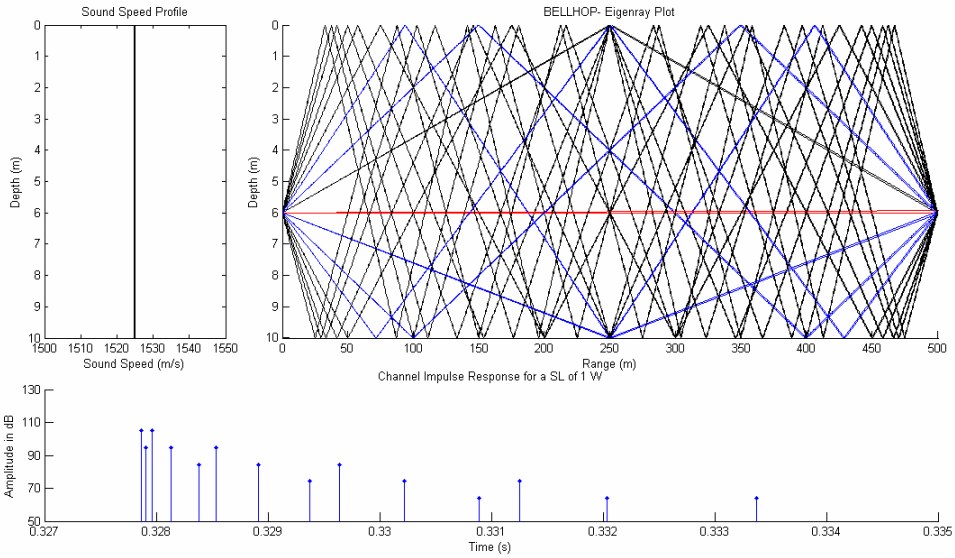

Bellhop Analysis, Case 10.250.1.1.70.Sand.Temp

Parameter	Magnitude
Channel Depth (m)	10
Transmission Range (m)	250
Transmitter Height (m)	1
Receiver Height (m)	1
Frequency (kHz)	70
Bottom Sediment Material	Sand
SSP Gradient	Temperature-Driven

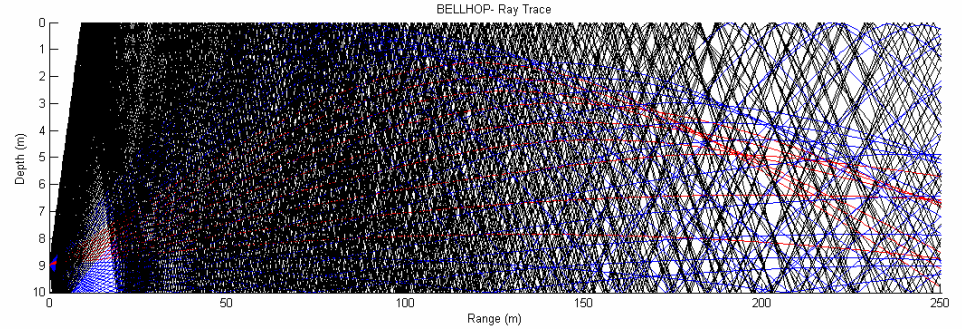

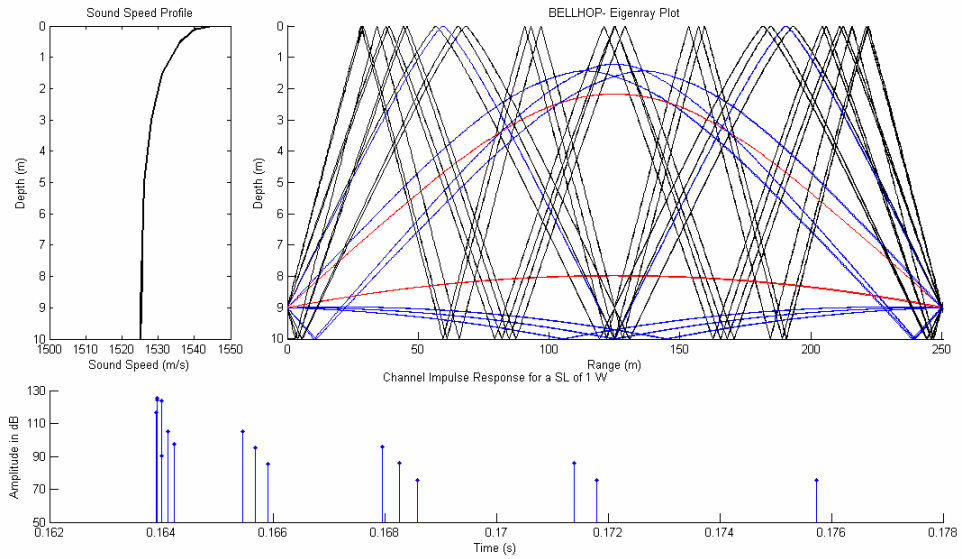

Bellhop Analysis, Case 10.250.1.1.70.Sand.Sal

Parameter	Magnitude
Channel Depth (m)	10
Transmission Range (m)	250
Transmitter Height (m)	1
Receiver Height (m)	1
Frequency (kHz)	70
Bottom Sediment Material	Sand
SSP Gradient	Salinity-Driven

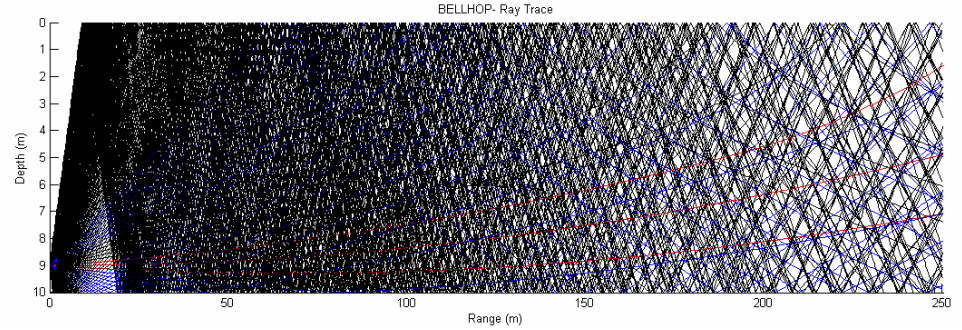

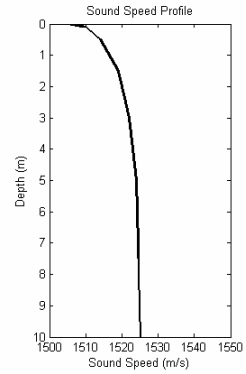

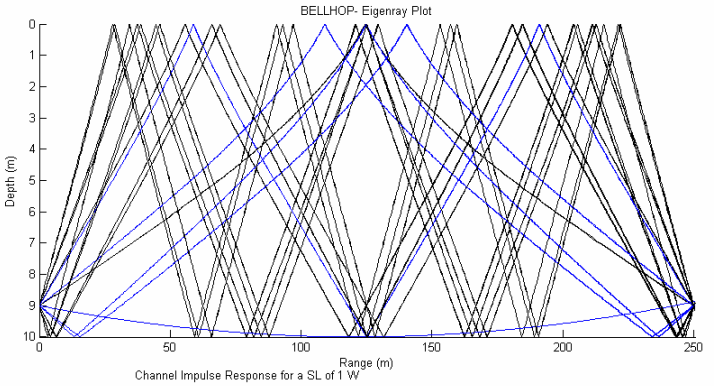

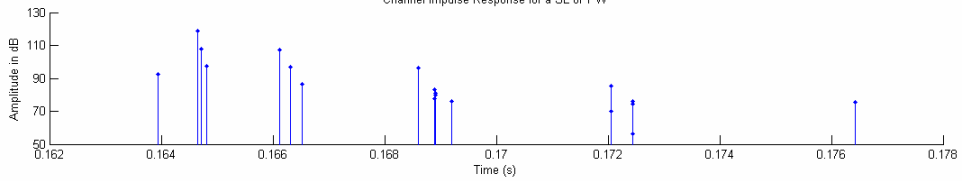

Bellhop Analysis, Case 10.250.1.1.70.Sand.0

Parameter	Magnitude
Channel Depth (m)	10
Transmission Range (m)	250
Transmitter Height (m)	1
Receiver Height (m)	1
Frequency (kHz)	70
Bottom Sediment Material	Sand
SSP Gradient	Isospeed

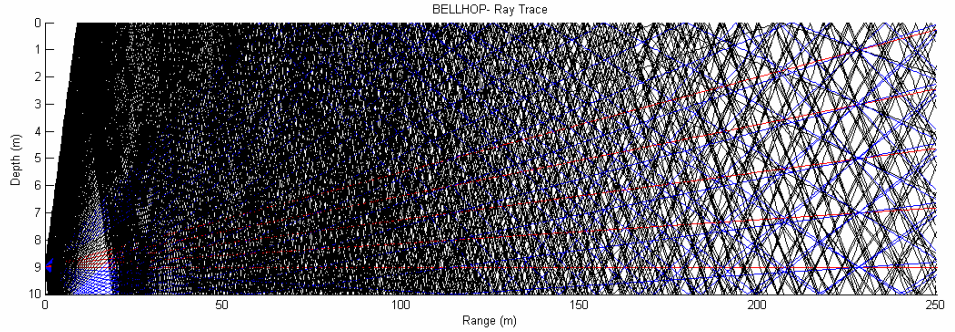

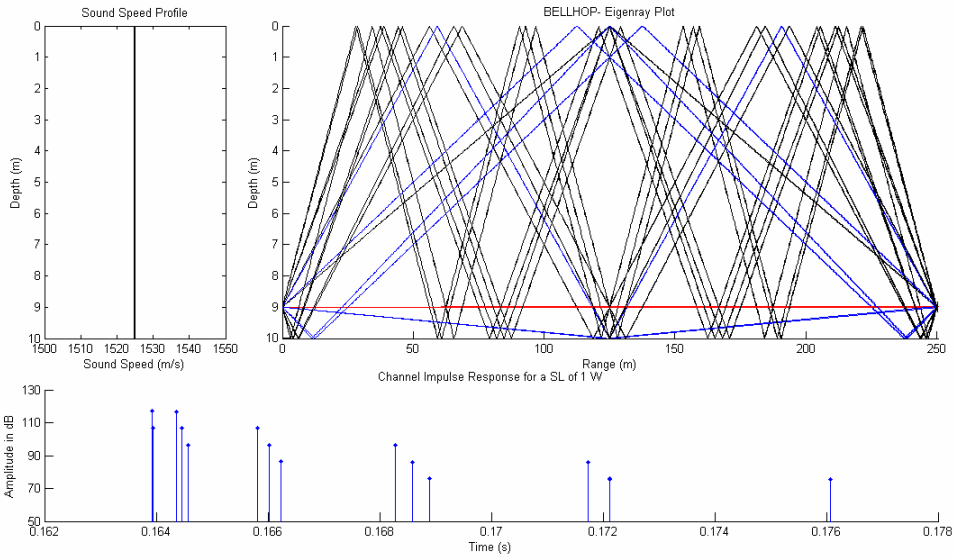

Bellhop Analysis, Case 10.1000.1.1.70.Sand.Temp

Parameter	Magnitude
Channel Depth (m)	10
Transmission Range (m)	1000
Transmitter Height (m)	1
Receiver Height (m)	1
Frequency (kHz)	70
Bottom Sediment Material	Sand
SSP Gradient	Temperature-Driven

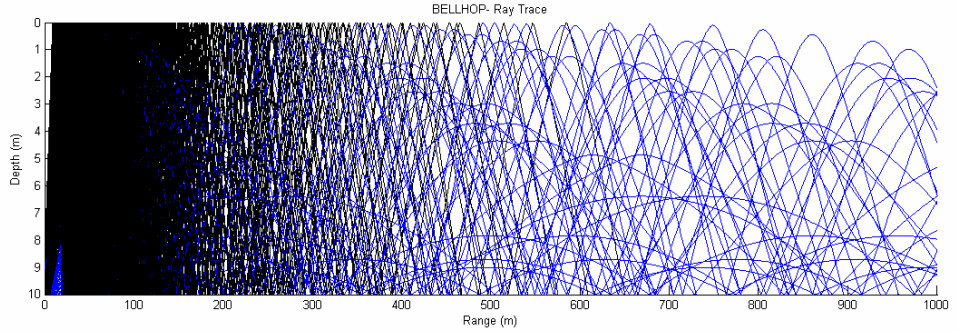

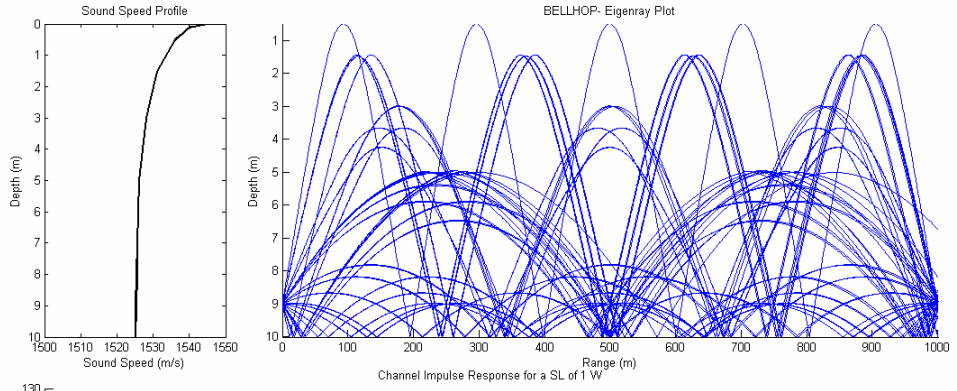

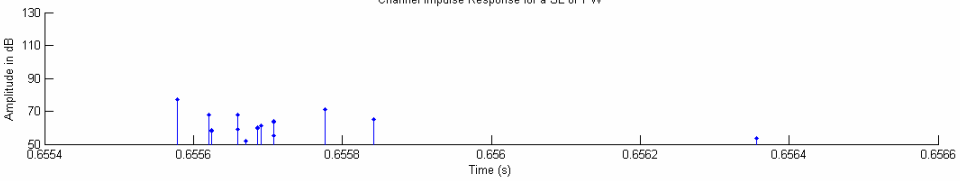

Bellhop Analysis, Case 10.1000.1.1.70.Sand.Sal

Parameter	Magnitude
Channel Depth (m)	10
Transmission Range (m)	1000
Transmitter Height (m)	1
Receiver Height (m)	1
Frequency (kHz)	70
Bottom Sediment Material	Sand
SSP Gradient	Salinity-Driven

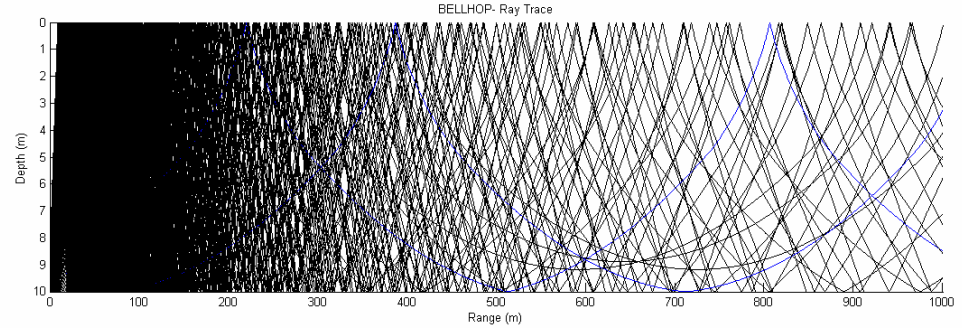

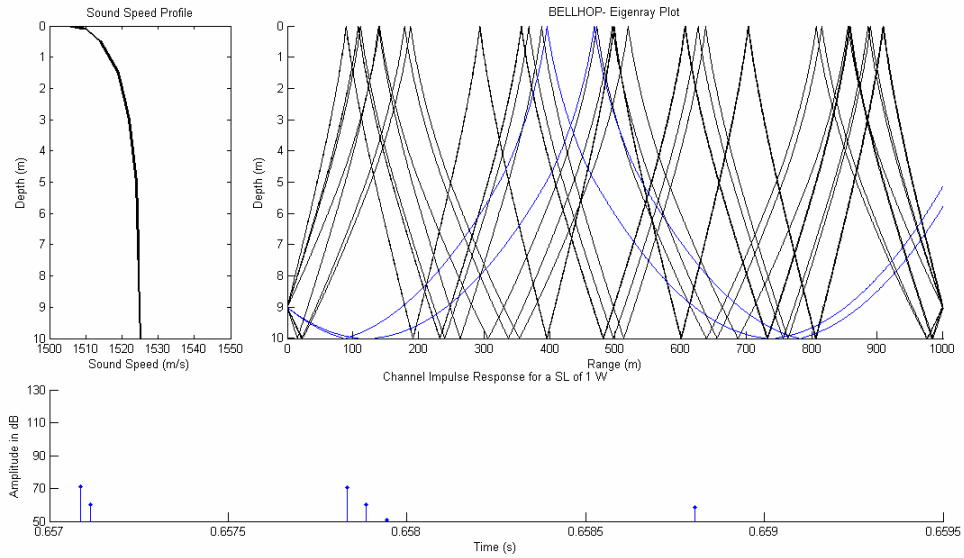

Bellhop Analysis, Case 10.1000.1.1.70.Sand.0

Parameter	Magnitude
Channel Depth (m)	10
Transmission Range (m)	1000
Transmitter Height (m)	1
Receiver Height (m)	1
Frequency (kHz)	70
Bottom Sediment Material	Sand
SSP Gradient	Isospeed

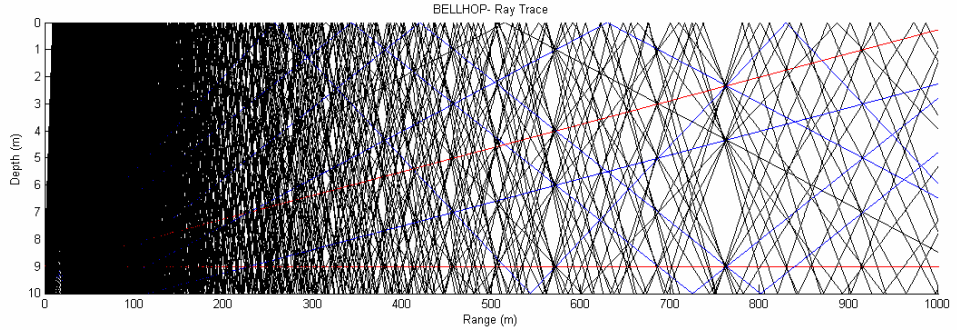

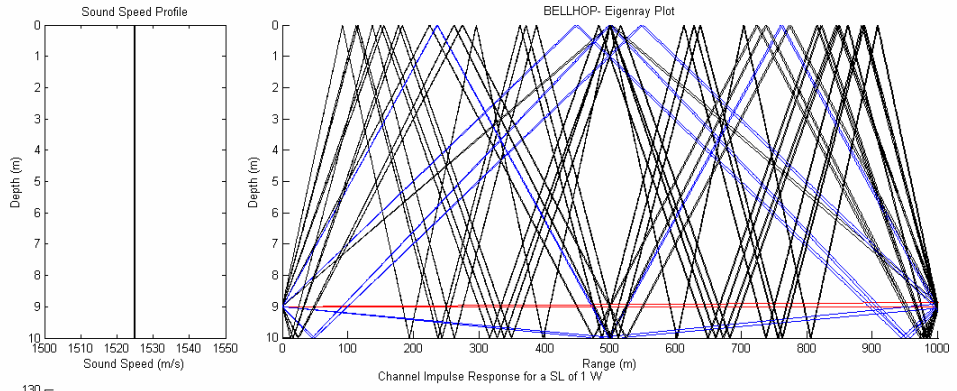

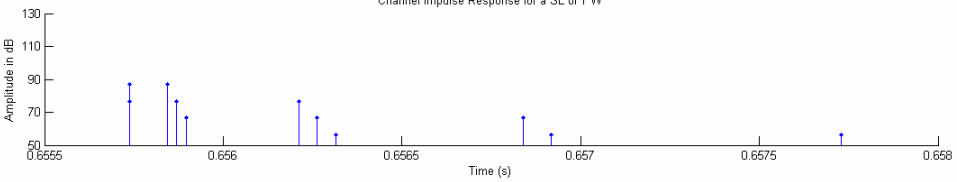

Bellhop Analysis, Case 5.500.1.1.70.Sand.Temp

Parameter	Magnitude
Channel Depth (m)	5
Transmission Range (m)	500
Transmitter Height (m)	1
Receiver Height (m)	1
Frequency (kHz)	70
Bottom Sediment Material	Sand
SSP Gradient	Temperature-Driven

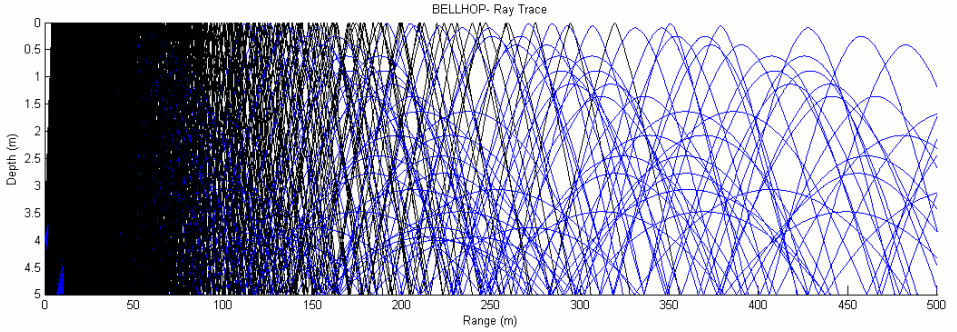

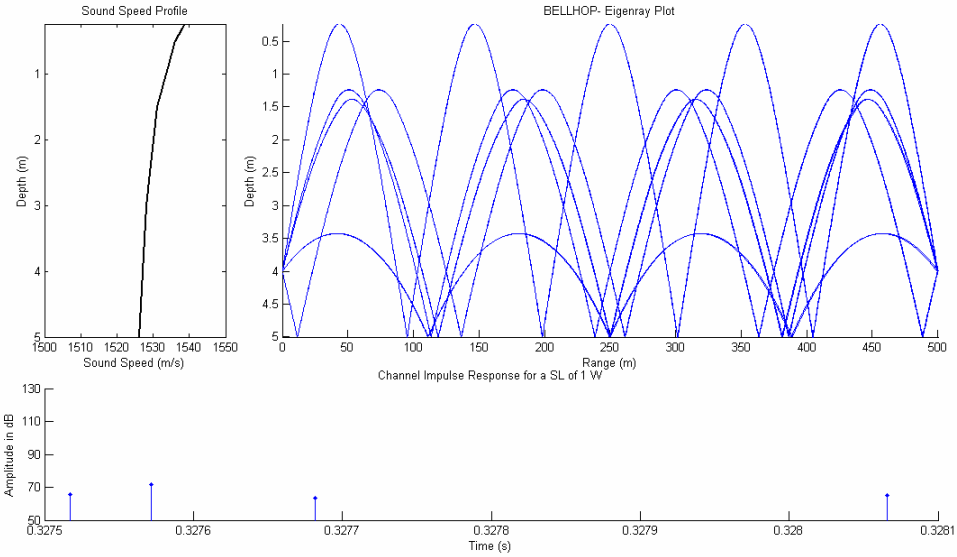

Bellhop Analysis, Case 5.500.1.1.70.Sand.Sal

Parameter	Magnitude
Channel Depth (m)	5
Transmission Range (m)	500
Transmitter Height (m)	1
Receiver Height (m)	1
Frequency (kHz)	70
Bottom Sediment Material	Sand
SSP Gradient	Salinity-Driven

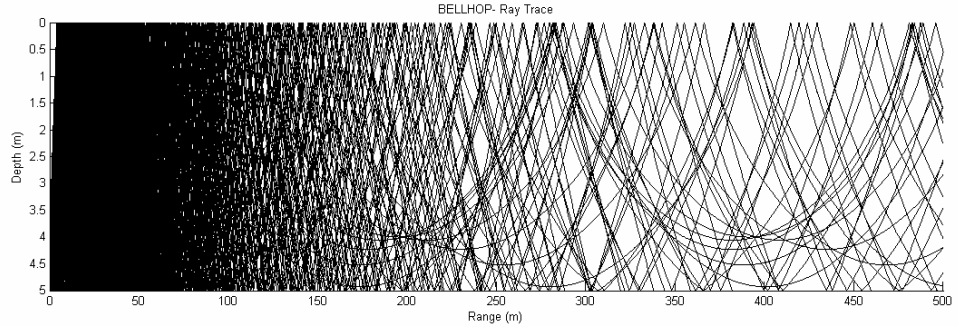

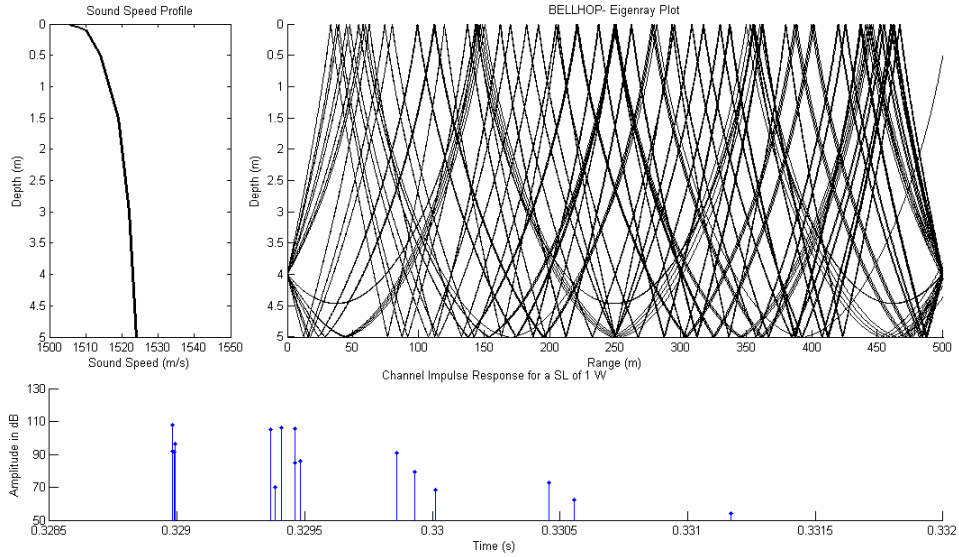

Bellhop Analysis, Case 5.500.1.1.70.Sand.0

Parameter	Magnitude
Channel Depth (m)	5
Transmission Range (m)	500
Transmitter Height (m)	1
Receiver Height (m)	1
Frequency (kHz)	70
Bottom Sediment Material	Sand
SSP Gradient	Isospeed

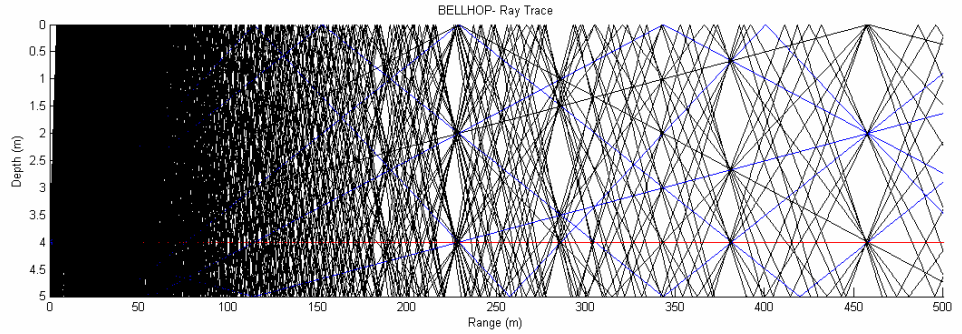

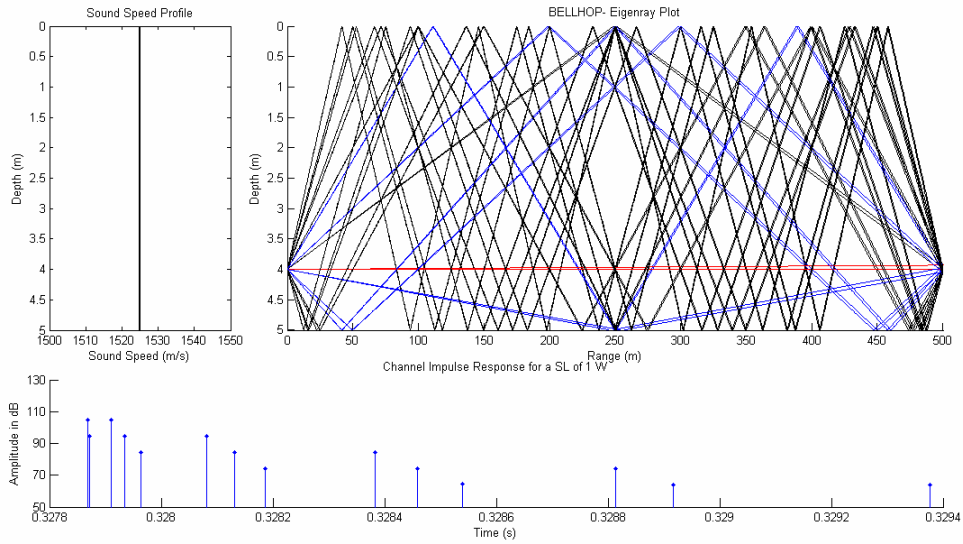

Bellhop Analysis, Case 20.500.1.1.70.Sand.Temp

Parameter	Magnitude
Channel Depth (m)	20
Transmission Range (m)	500
Transmitter Height (m)	1
Receiver Height (m)	1
Frequency (kHz)	70
Bottom Sediment Material	Sand
SSP Gradient	Temperature-Driven

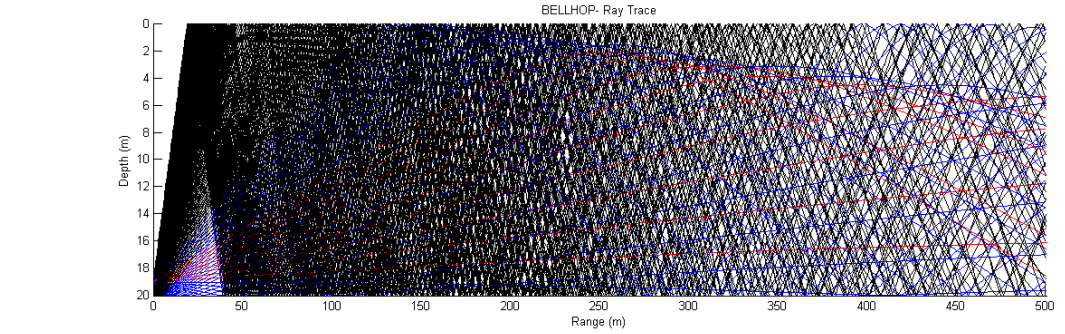

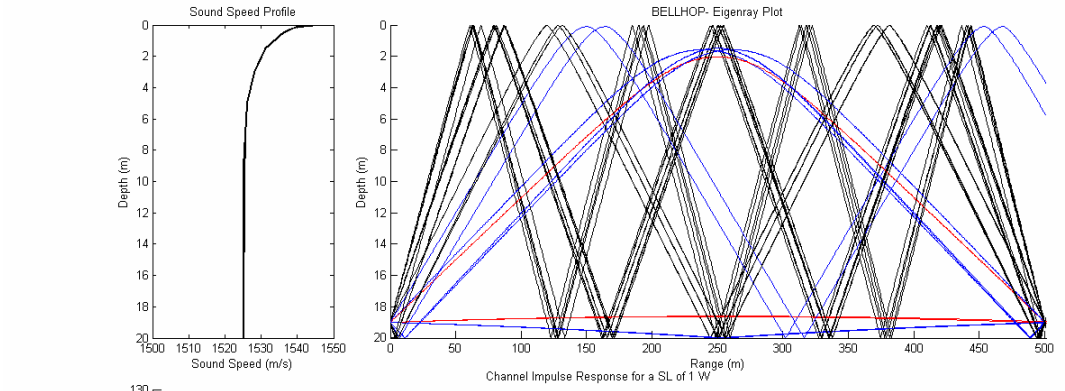

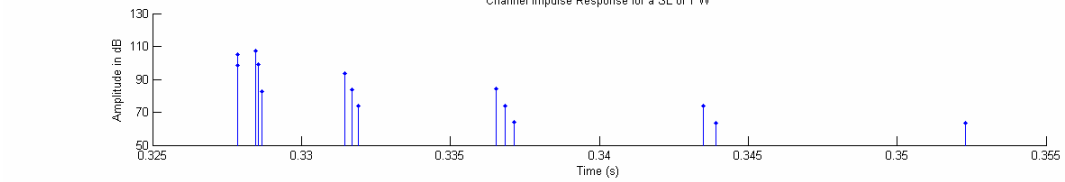

Bellhop Analysis, Case 20.500.1.1.70.Sand.Sal

Parameter	Magnitude
Channel Depth (m)	20
Transmission Range (m)	500
Transmitter Height (m)	1
Receiver Height (m)	1
Frequency (kHz)	70
Bottom Sediment Material	Sand
SSP Gradient	Salinity-Driven

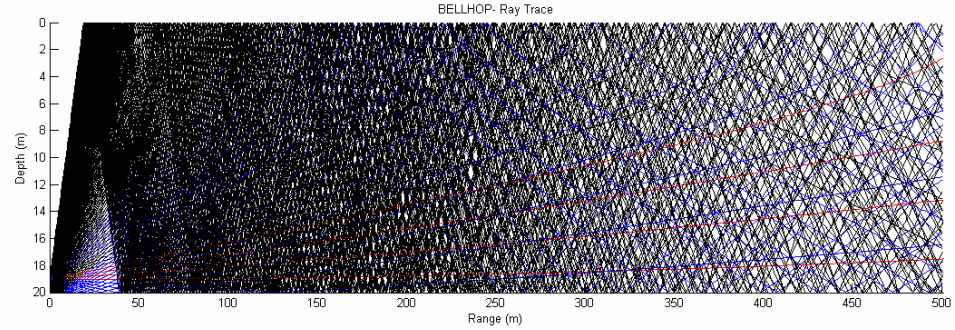

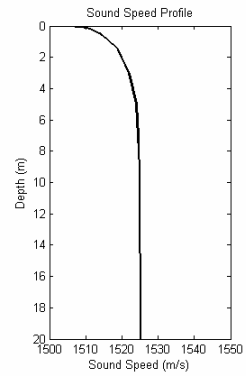

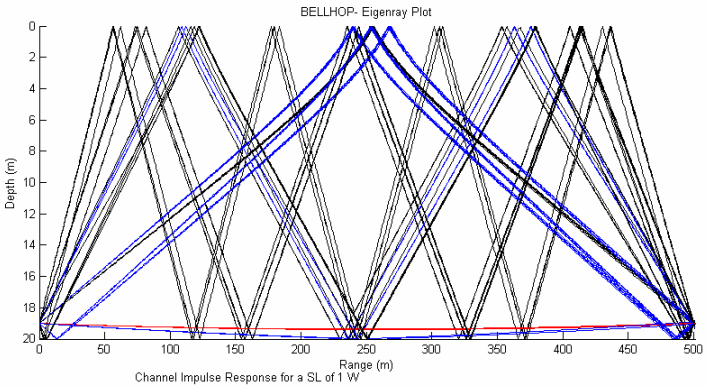

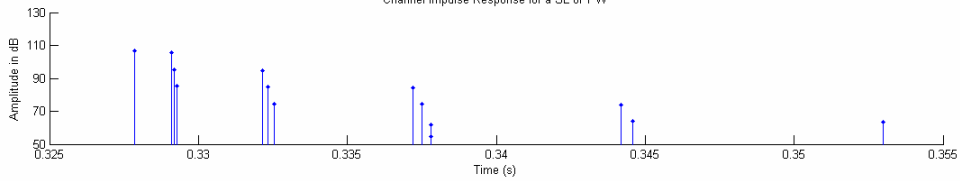

Bellhop Analysis, Case 20.500.1.1.70.Sand.0

Parameter	Magnitude
Channel Depth (m)	20
Transmission Range (m)	500
Transmitter Height (m)	1
Receiver Height (m)	1
Frequency (kHz)	70
Bottom Sediment Material	Sand
SSP Gradient	Isospeed

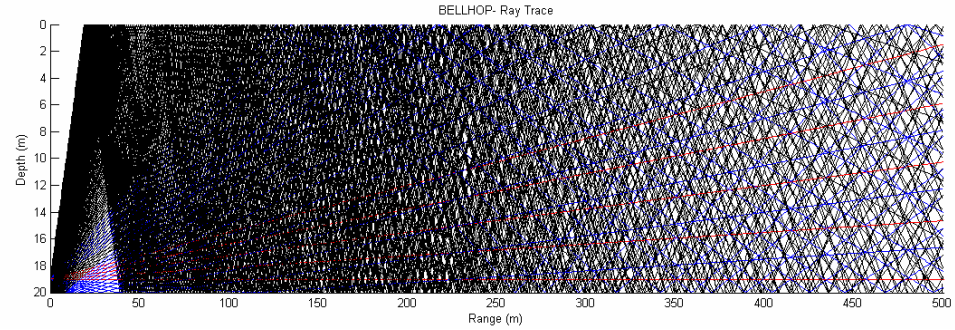

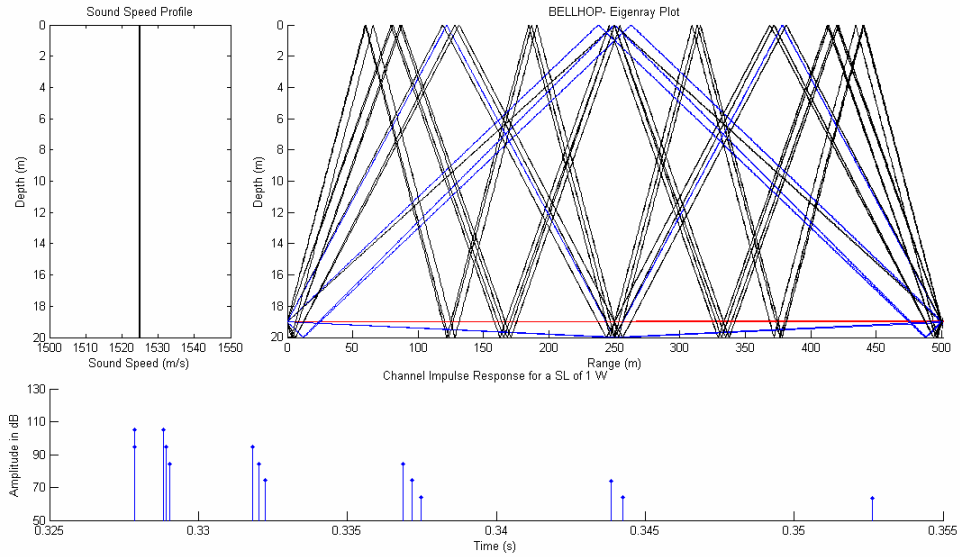

Bellhop Analysis, Case 40.500.1.1.70.Sand.Temp

Parameter	Magnitude
Channel Depth (m)	40
Transmission Range (m)	500
Transmitter Height (m)	1
Receiver Height (m)	1
Frequency (kHz)	70
Bottom Sediment Material	Sand
SSP Gradient	Temperature-Driven

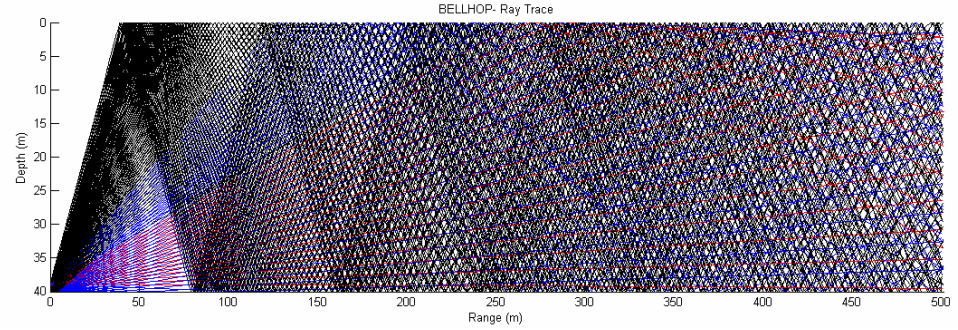

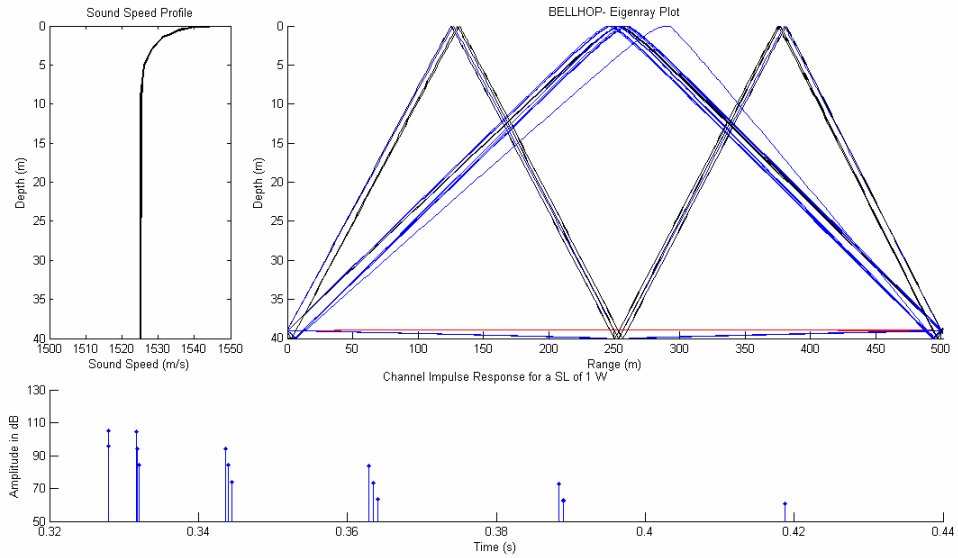

Bellhop Analysis, Case 40.500.1.1.70.Sand.Sal

Parameter	Magnitude
Channel Depth (m)	40
Transmission Range (m)	500
Transmitter Height (m)	1
Receiver Height (m)	1
Frequency (kHz)	70
Bottom Sediment Material	Sand
SSP Gradient	Salinity-Driven

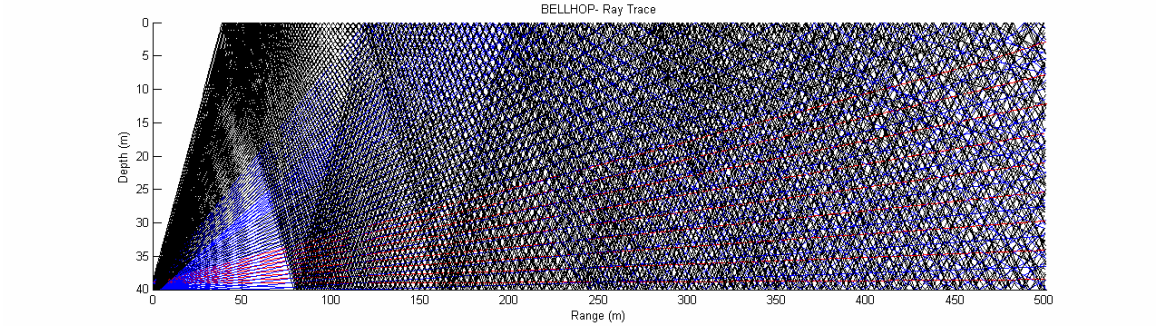

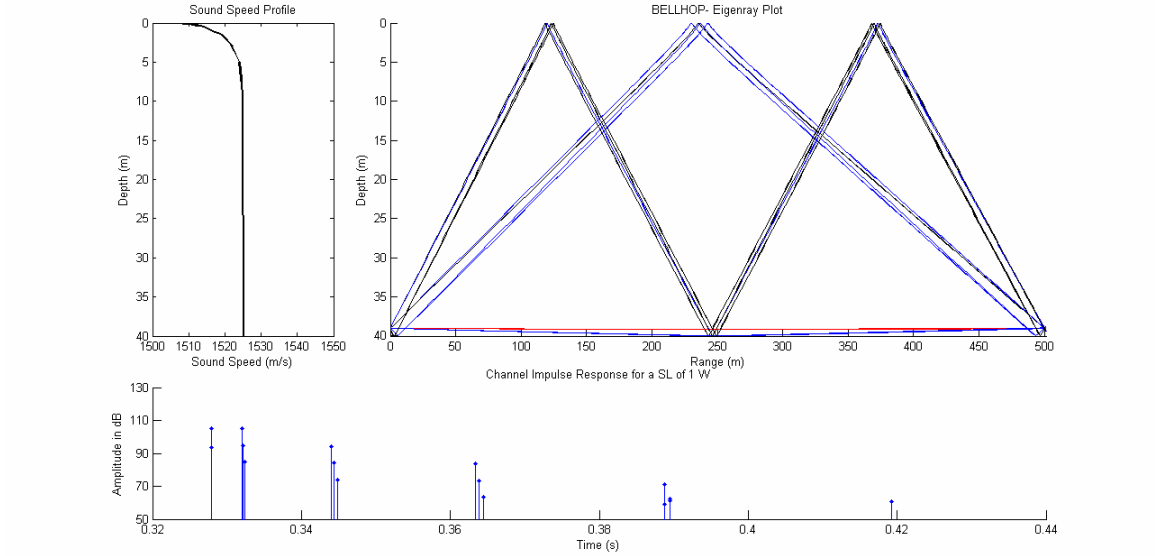

Bellhop Analysis, Case 40.500.1.1.70.Sand.Temp

Parameter	Magnitude
Channel Depth (m)	40
Transmission Range (m)	500
Transmitter Height (m)	1
Receiver Height (m)	1
Frequency (kHz)	70
Bottom Sediment Material	Sand
SSP Gradient	Isospeed

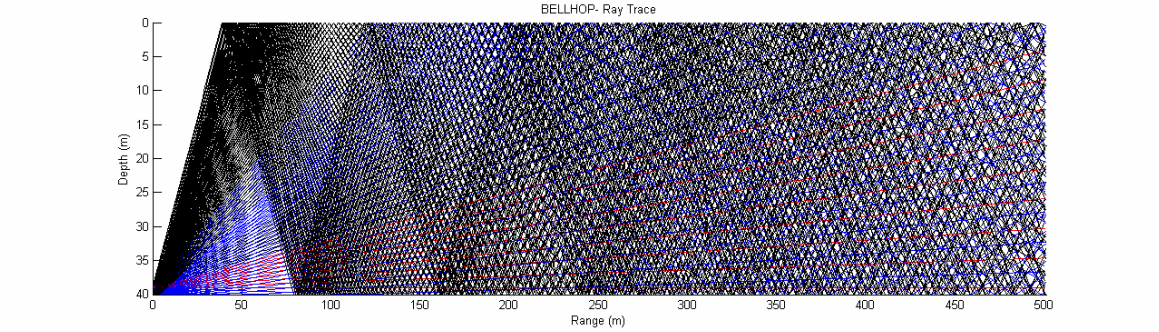

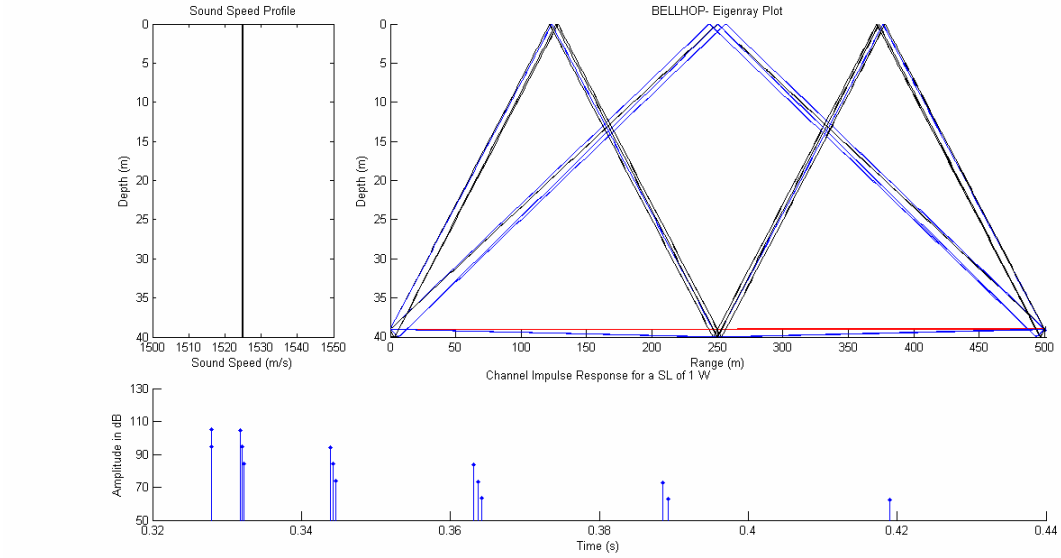

B. ST ANDREW BAY, PANAMA CITY, FL

Bellhop Analysis, Case SAB.10.500.1.1.14.Silt.0725

Parameter	Magnitude
Location	St. Andrew Bay
Channel Depth (m)	10
Transmission Range (m)	500
Transmitter Height (m)	1
Receiver Height (m)	1
Frequency (kHz)	14
Bottom Sediment Material	Silt
SSP Gradient	25 July 2003

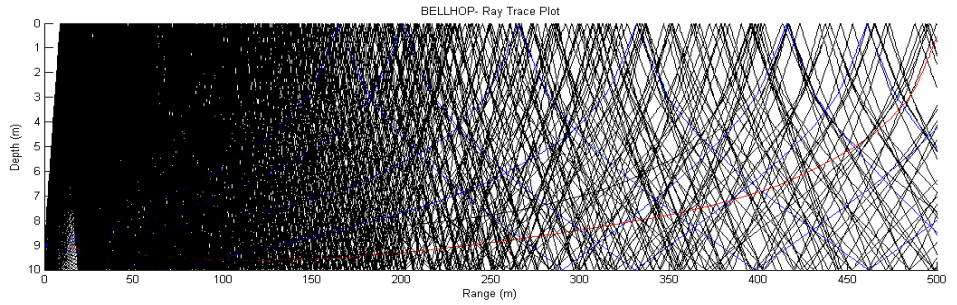

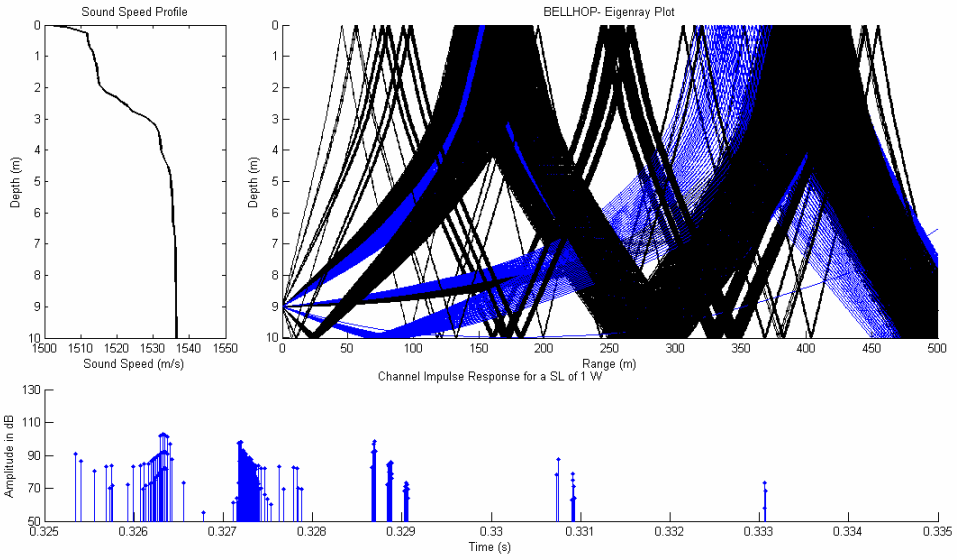

Bellhop Analysis, Case SAB.10.500.1.1.14.Silt.0730

Parameter	Magnitude
Location	St. Andrew Bay
Channel Depth (m)	10
Transmission Range (m)	500
Transmitter Height (m)	1
Receiver Height (m)	1
Frequency (kHz)	14
Bottom Sediment Material	Silt
SSP Gradient	30 July 2003

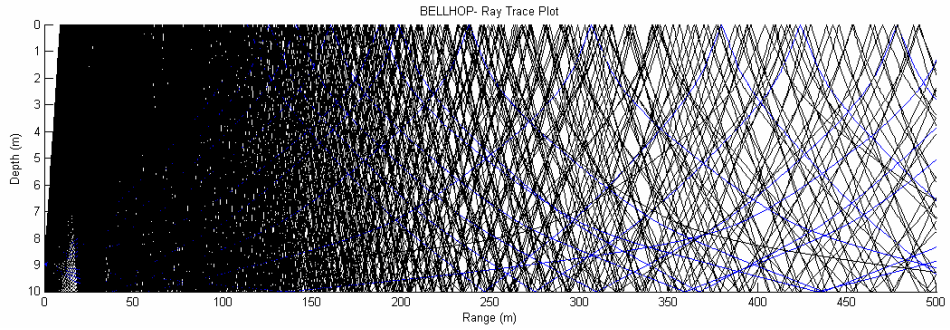

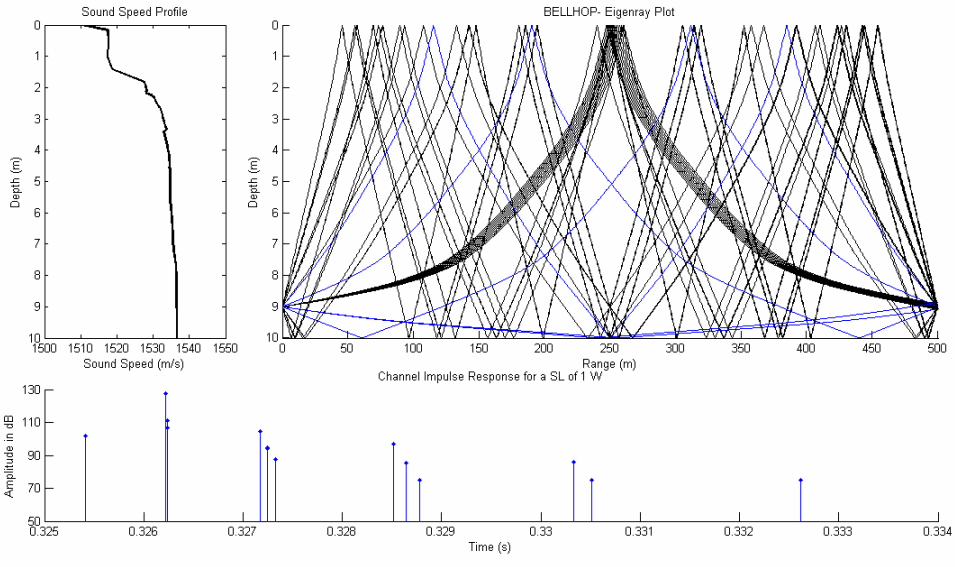

Bellhop Analysis, Case SAB.10.1000.1.1.14.Silt.0731

Parameter	Magnitude
Location	St. Andrew Bay
Channel Depth (m)	10
Transmission Range (m)	1000
Transmitter Height (m)	1
Receiver Height (m)	1
Frequency (kHz)	14
Bottom Sediment Material	Silt
SSP Gradient	31 July 2003

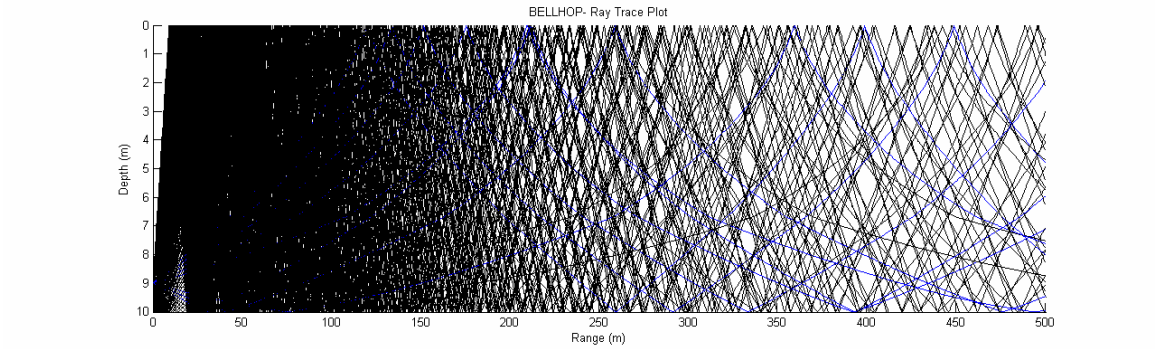

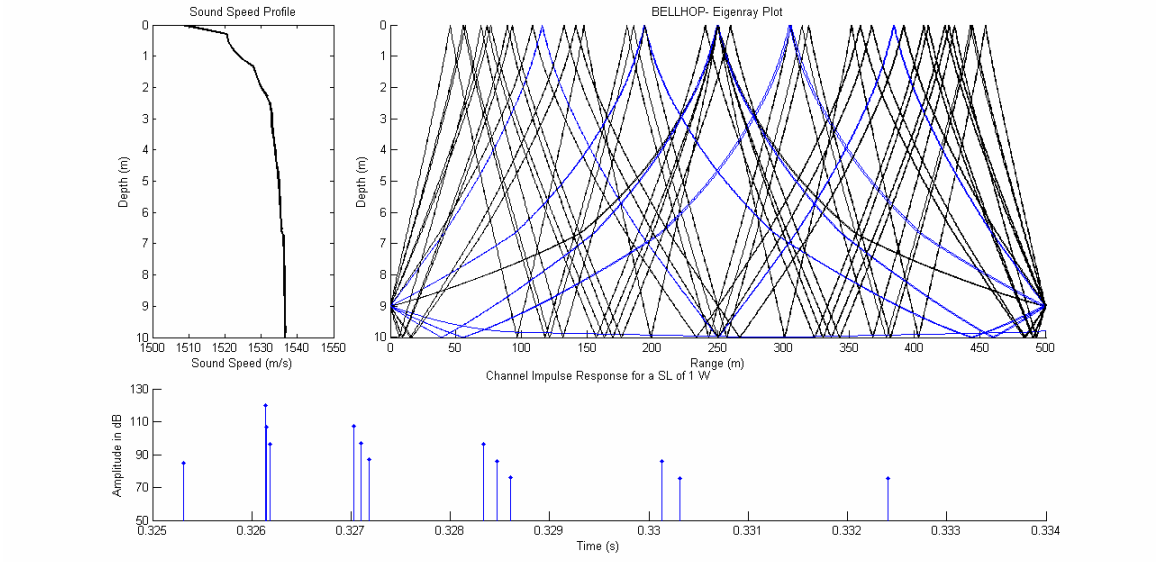

C. CHESAPEAKE BAY, LITTLE CREEK, VA

Bellhop Analysis, Case CB.5.1000.1.1.14.Sand.SM

Parameter	Magnitude
Location	Chesapeake Bay
Channel Depth (m)	5
Transmission Range (m)	1000
Transmitter Height (m)	1
Receiver Height (m)	1
Frequency (kHz)	14
Bottom Sediment Material	Sand
SSP	Slowest Measured

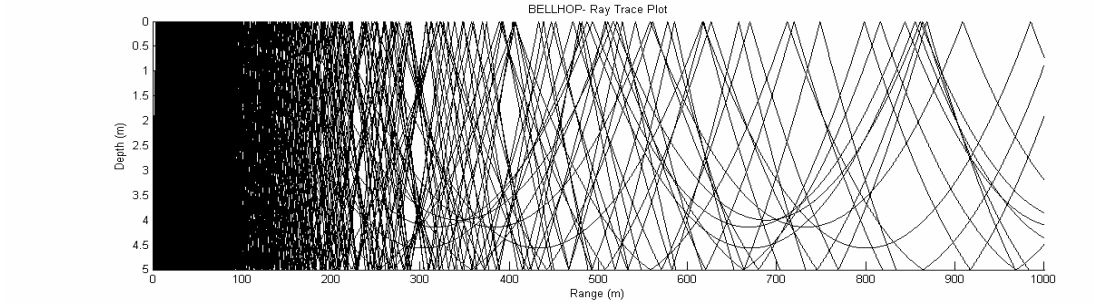

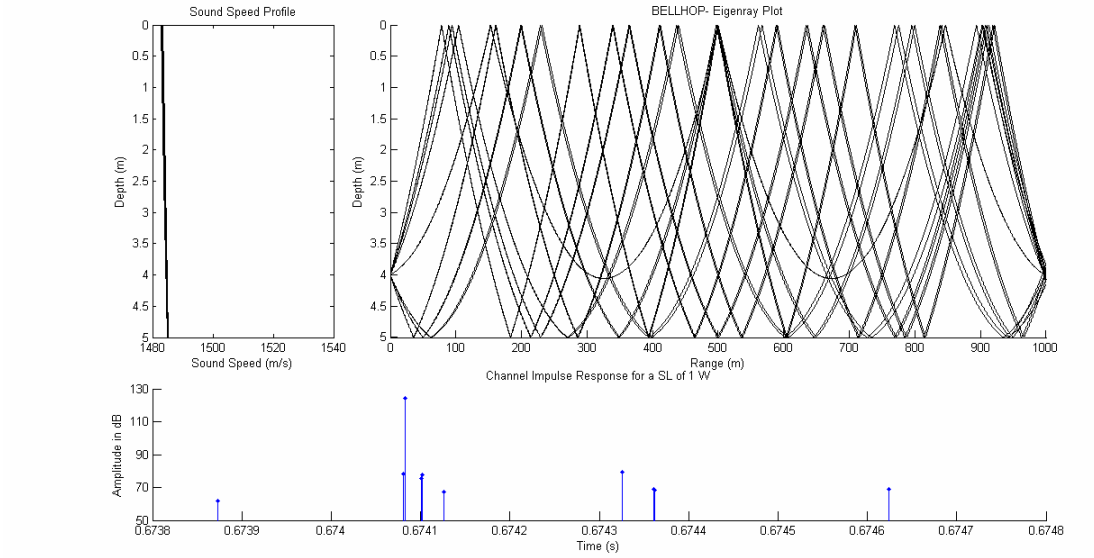

Bellhop Analysis, Case CB.5.1000.1.1.14.Sand.FM

Parameter	Magnitude
Location	Chesapeake Bay
Channel Depth (m)	5
Transmission Range (m)	1000
Transmitter Height (m)	1
Receiver Height (m)	1
Frequency (kHz)	14
Bottom Sediment Material	Sand
SSP	Fastest Measured

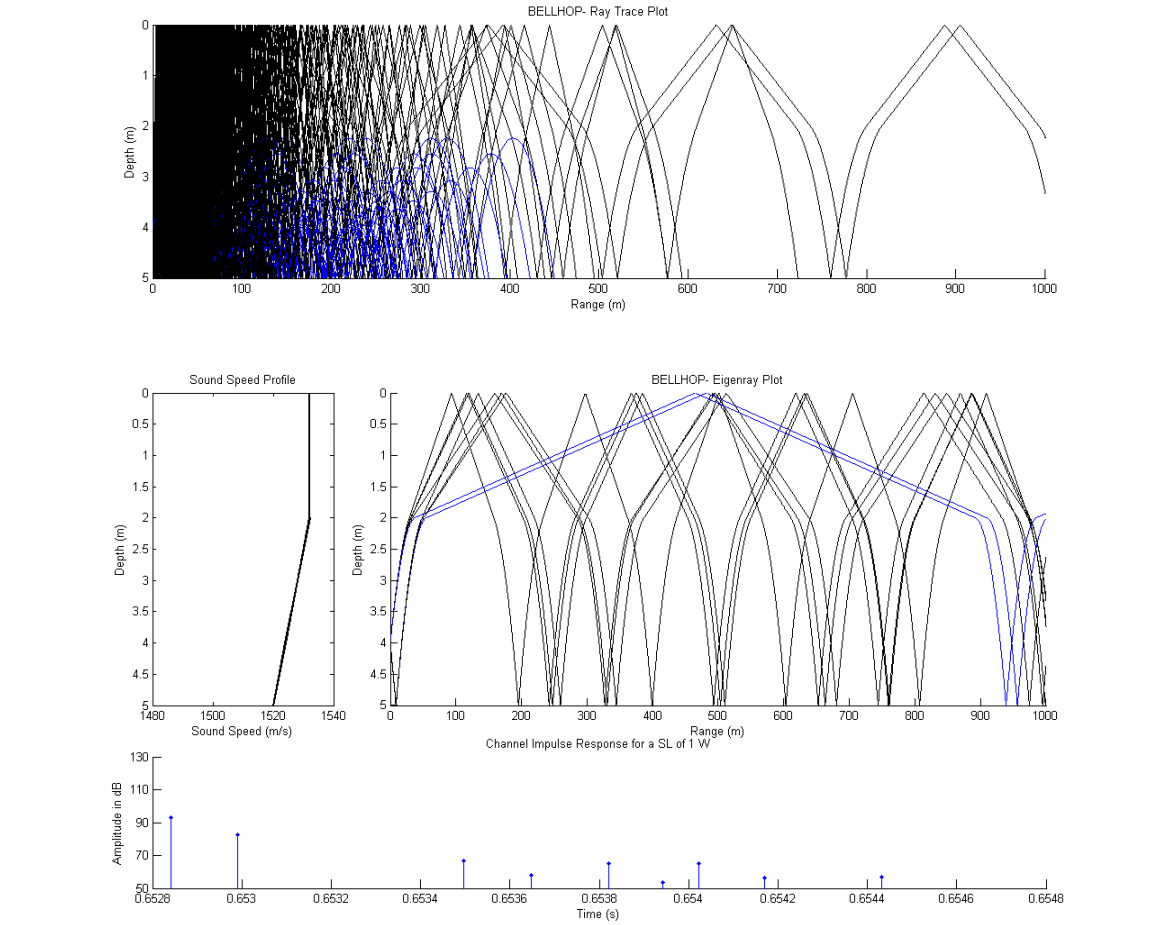

Bellhop Analysis, Case CB.5.1000.1.1.14.Sand.AVG

Parameter	Magnitude
Location	Chesapeake Bay
Channel Depth (m)	5
Transmission Range (m)	1000
Transmitter Height (m)	1
Receiver Height (m)	1
Frequency (kHz)	14
Bottom Sediment Material	Sand
SSP	Average

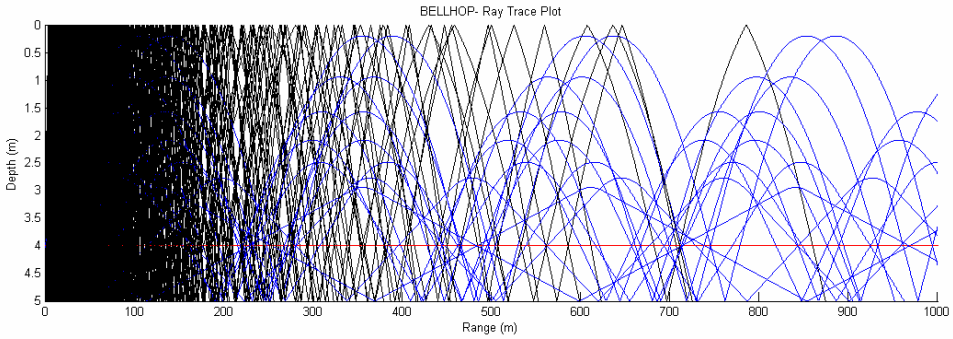

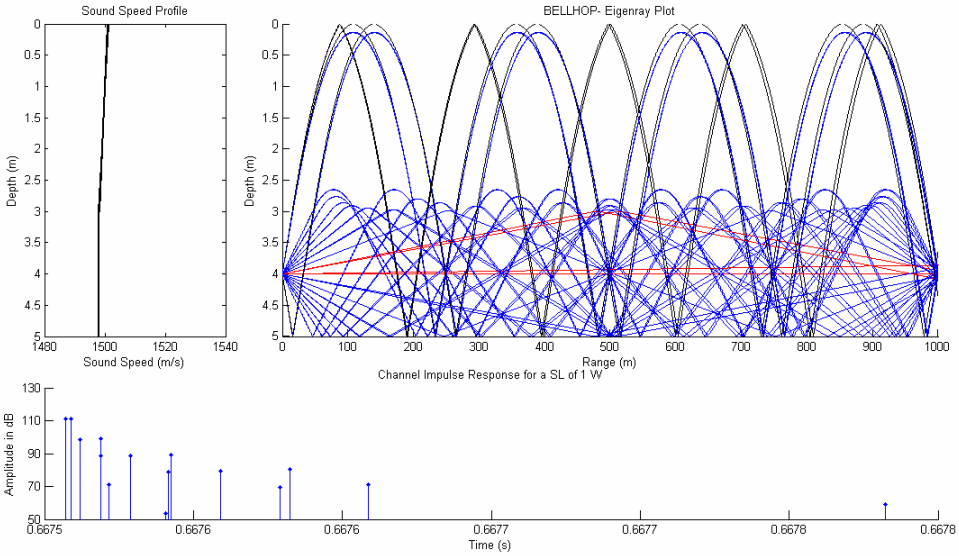

THIS PAGE INTENTIONALLY LEFT BLANK

APPENDIX C. SUMMARY TABLES

A. SSP

SSP	$\|p(r, z)\|/\|p_0\|$	***Amplitude*** (dB)	***Baseline Environment Deviation*** (%)
Temperature-Driven	4.38×10^{-4}	103.6	-1.1
Salinity-Driven	2.13×10^{-4}	97.4	-7.1
Linear with a -2 Slope	1.91×10^{-3}	116.4	11.1
Linear with a -1 Slope	2.10×10^{-4}	97.2	-7.2
Isospeed	5.04×10^{-4}	104.8	--
Linear with a +1 Slope	1.63×10^{-4}	95.0	-9.3
Linear with a +2 Slope	5.21×10^{-5}	85.1	-18.8

Table 4. Amplitude response for different sound-speed profiles (SSP)

B. TRANSMITTER FREQUENCY

1. Salinity-Driven Environment

Frequency (kHz)	$\|p(r, z)\|/\|p_0\|$	***Amplitude*** (dB)	***Baseline Environment Deviation*** (%)
40	3.29×10^{-4}	101.1	3.8
45	2.97×10^{-4}	100.3	2.9
50	3.23×10^{-4}	101.0	3.7
55	2.88×10^{-4}	100.0	2.7
60	2.59×10^{-4}	99.1	1.7
65	2.34×10^{-4}	98.2	0.8
70	2.13×10^{-4}	97.4	--

Table 5. Amplitude response in a salinity-driven environment for different transmission frequencies

2. Temperature-Driven Environment

Frequency (kHz)	$\|p(r, z)\|/\|p_0\|$	***Amplitude*** (dB)	***Baseline Environment Deviation*** (%)
40	8.51×10^{-4}	109.4	5.6
45	7.51×10^{-4}	108.3	4.5
50	6.65×10^{-4}	107.3	3.5
55	5.92×10^{-4}	106.2	2.6
60	5.32×10^{-4}	105.3	1.7
65	4.81×10^{-4}	104.4	0.8
70	4.38×10^{-4}	103.6	--

Table 6. Amplitude response in a temperature-driven environment for different transmission frequencies

3. Isospeed Environment

Frequency (kHz)	$\|p(r, z)\|/\|p_0\|$	***Amplitude*** (dB)	***Baseline Environment Deviation*** (%)
40	9.80×10^{-4}	110.6	5.6
45	8.64×10^{-4}	109.5	4.5
50	7.66×10^{-4}	108.5	3.5
55	6.82×10^{-4}	107.5	2.6
60	6.12×10^{-4}	106.5	1.7
65	5.54×10^{-4}	105.7	0.8
70	5.04×10^{-4}	104.8	--

Table 7. Amplitude response in an isospeed environment for different transmission frequencies

C. TRANSMISSION RANGE

1. Salinity-Driven Environment

Transmission Range (m)	$\|p(r, z)\|/\|p_0\|$	***Amplitude*** (dB)	***Baseline Environment Deviation*** (%)
250	2.50×10^{-3}	118.8	21.9
500	2.13×10^{-4}	97.4	--
1000	1.03×10^{-5}	71.1	-27.0

Table 8. Amplitude response in a salinity-driven environment for different transmission ranges

2. Temperature-Driven Environment

Transmission Range (m)	$\|p(r, z)\|/\|p_0\|$	***Amplitude*** (dB)	***Baseline Environment Deviation*** (%)
250	5.46×10^{-3}	125.5	21.2
500	4.38×10^{-4}	103.6	--
1000	2.06×10^{-5}	77.1	-25.6

Table 9. Amplitude response in a temperature-driven environment for different transmission ranges

3. Isospeed Environment

Transmission Range (m)	$\|p(r, z)\|/\|p_0\|$	***Amplitude*** (dB)	***Baseline Environment Deviation*** (%)
250	2.01×10^{-3}	116.9	11.5
500	5.04×10^{-4}	104.8	--
1000	6.36×10^{-5}	86.9	-17.1

Table 10. Amplitude response in an isospeed environment for different transmission ranges

D. CHANNEL DEPTH

1. Salinity-Driven Environment

Channel Depth (m)	$\|p(r, z)\|/\|p_0\|$	*Amplitude* (dB)	*Baseline Environment Deviation* (%)
5	7.09×10^{-4}	107.8	10.7
10	2.13×10^{-4}	97.4	--
20	6.22×10^{-4}	106.7	9.5
40	5.09×10^{-4}	104.9	7.7

Table 11. Amplitude response in a salinity-driven environment with different channel depths

2. Temperature-Driven Environment

Channel Depth (m)	$\|p(r, z)\|/\|p_0\|$	*Amplitude* (dB)	*Baseline Environment Deviation* (%)
5	1.07×10^{-5}	71.4	-31.1
10	4.38×10^{-4}	103.6	--
20	6.52×10^{-4}	107.1	3.4
40	5.04×10^{-4}	104.8	1.2

Table 12. Amplitude response in a temperature-driven environment with different channel depths

3. Isospeed Environment

Channel Depth (m)	$\|p(r, z)\|/\|p_0\|$	*Amplitude* (dB)	*Baseline Environment Deviation* (%)
5	5.04×10^{-4}	104.8	0.0
10	5.04×10^{-4}	104.8	--
20	5.04×10^{-4}	104.8	0.0
40	5.04×10^{-4}	104.8	0.0

Table 13. Amplitude response in an isospeed environment with different channel depths

E. BOTTOM SEDIMENT MATERIAL

1. Salinity-Driven Environment

Bottom Type	$\|p(r, z)\|/\|p_0\|$	***Amplitude*** (dB)	***Baseline Environment Deviation*** (%)
Sand	2.13×10^{-4}	97.4	--
Clay	1.37×10^{-4}	93.5	-4.0
Silt	1.78×10^{-4}	95.8	-1.6
Gravel	2.29×10^{-4}	98.0	0.6

Table 14. Amplitude response in a salinity-driven environment with different bottom sediment materials

2. Temperature-Driven Environment

Bottom Type	$\|p(r, z)\|/\|p_0\|$	***Amplitude*** (dB)	***Baseline Environment Deviation*** (%)
Sand	4.38×10^{-4}	103.6	--
Clay	1.82×10^{-4}	96.0	-7.3
Silt	3.06×10^{-4}	100.5	-3.0
Gravel	5.05×10^{-4}	104.9	1.2

Table 15. Amplitude response in a temperature-driven environment with different bottom sediment materials

3. Isospeed Environment

Bottom Type	$\|p(r, z)\|/\|p_0\|$	***Amplitude*** (dB)	***Baseline Environment Deviation*** (%)
Sand	5.04×10^{-4}	104.8	--
Clay	5.04×10^{-4}	104.8	0.0
Silt	5.04×10^{-4}	104.8	0.0
Gravel	5.04×10^{-4}	104.8	0.0

Table 16. Amplitude response in an isospeed environment with different bottom sediment materials

F. TRANSMITTER AND RECEIVER HEIGHT

1. Salinity-Driven Environment

Transmitter Height (m)	***Receiver Height*** (m)	$\|p(r, z)\|/\|p_0\|$	***Amplitude*** (dB)	***Baseline Environment Deviation*** (%)
1	1	$2.13\text{x}10^{-4}$	97.4	--
1	2	$2.26\text{x}10^{-4}$	97.9	0.5
1	4	$1.88\text{x}10^{-4}$	96.3	-1.1
2	1	$2.05\text{x}10^{-5}$	97.0	-0.4
2	2	$1.89\text{x}10^{-4}$	96.3	-1.1
2	4	$1.90\text{x}10^{-4}$	96.4	-1.1
4	1	$1.87\text{x}10^{-4}$	96.2	-1.2
4	2	$1.85\text{x}10^{-4}$	96.1	-1.3
4	4	$1.56\text{x}10^{-3}$	114.7	17.7

Table 17. Amplitude response for different transmitter and receiver depth combinations in a salinity-driven environment

2. Temperature-Driven Environment

Transmitter Height (m)	***Receiver Height*** (m)	$\|p(r, z)\|/\|p_0\|$	***Amplitude*** (dB)	***Baseline Environment Deviation*** (%)
1	1	$4.38\text{x}10^{-4}$	103.6	--
1	2	$2.50\text{x}10^{-4}$	98.8	-4.7
1	4	$2.43\text{x}10^{-4}$	98.5	-4.9
2	1	$2.60\text{x}10^{-4}$	99.1	-4.3
2	2	$3.30\text{x}10^{-4}$	101.2	-2.3
2	4	$2.10\text{x}10^{-4}$	97.2	-6.1
4	1	$2.50\text{x}10^{-4}$	98.8	-4.7
4	2	$2.12\text{x}10^{-3}$	97.3	-6.1
4	4	$1.42\text{x}10^{-3}$	113.8	9.9

Table 18. Amplitude response for different transmitter and receiver depth combinations in a temperature-driven environment

3. Isospeed Environment

Transmitter Height (m)	***Receiver Height*** (m)	$\|p(r, z)\|/\|p_0\|$	***Amplitude*** (dB)	***Baseline Environment Deviation*** (%)
1	1	5.04×10^{-4}	104.8	--
1	2	5.04×10^{-4}	104.8	0.0
1	4	5.04×10^{-4}	104.8	0.0
2	1	5.04×10^{-4}	104.8	0.0
2	2	5.04×10^{-4}	104.8	0.0
2	4	5.04×10^{-4}	104.8	0.0
4	1	5.04×10^{-4}	104.8	0.0
4	2	5.04×10^{-4}	104.8	0.0
4	4	5.04×10^{-4}	104.8	0.0

Table 19. Amplitude response for different transmitter and receiver depth combinations in an isospeed environment

THIS PAGE INTENTIONALLY LEFT BLANK

LIST OF REFERENCES

Dessalermos, Spyridon. "Undersea Acoustic Propagation Channel Estimation." MS thesis, Naval Postgraduate School, 2005.

Greig, James. "Development of a Fully Range-Dependent Underwater Acoustic Ray Tracing Program". MS thesis, Curtin University, 2006.

Hansen, Joseph T. "Link Budget Analysis for Undersea Acoustic Signaling." MS Thesis, Naval Postgraduate School, 2002.

Jensen, Finn B., William A. Kuperman, Michael B. Porter, Henrik Schmidt. *Computational Ocean Acoustics.* New York: Springer-Verlag New York Inc, 2000.

Johnson, Johnny R. *Introduction to Digital Signal Processing.* Englewood Cliffs: Prentice Hall, 1989.

Kinsler, Lawrence E., Austin R. Frey, Alan B. Coppens, James V. Sanders. *Fundamentals of Acoustics 4th Edition*. New York: John Wiley & Sons Ltd., 2000.

Marsh, H.W. and M. Schulkin, "Shallow Water Transmission." *The Journal of the Acoustical Society of America* 34 (1962): 863-864.

Officer, Charles B. *Introduction to the Theory of Sound Transmission*. New York: McGraw-Hill, 1958.

Porter, Michael B. and Yong-Chun Liu, "Finite-Element Ray Tracing." In *Proceedings of the International Conference on Theoretical and Computational Acoustics*, edited by D. Lee and M. H. Schultz, 947-956. New York: World Scientific, 1994.

Porter, Michael B. and Homer P. Bucker. "Gaussian beam tracing for computing ocean acoustic fields." *The Journal of the Acoustical Society of America* 82 (1987): 1349-1359.

Riley, Kenneth F., Michael P. Hobson, Stephen J. Bence. *Mathematical Methods for Physics and Engineering.* Cambridge: Cambridge University Press, 1998.

Urick, Robert. *Principles of Underwater Sound for Engineers 3rd Edition*. Los Altos: Peninsula Publishing, 1996.

Waite, Ashley D. *SONAR for Practising Engineers*. West Sussex: John Wiley & Sons Ltd., 2002.

THIS PAGE INTENTIONALLY LEFT BLANK

INITIAL DISTRIBUTION LIST

1. Defense Technical Information Center
   Ft. Belvoir, Virginia

2. Dudley Knox Library
   Naval Postgraduate School
   Monterey, California

3. Joseph A. Rice
   Department of Physics
   Naval Postgraduate School
   Monterey, California

4. RADM (Ret.) Raymond Jones, USN
   Chair, Undersea Warfare
   Naval Postgraduate School
   Monterey, California

5. LCDR Bjorn Kerstens, NE
   Department of Physics
   Naval Postgraduate School
   Monterey, California

6. Paul Baxley
   SPAWAR Systems Center
   San Diego, California

7. Bill Marn
   SPAWAR Systems Center
   San Diego, California

8. Bob Creber
   SPAWAR Systems Center
   San Diego, California

9. Chris Fletcher
   SPAWAR Systems Center
   San Diego, California

10. Warren Paez
    SPAWAR Systems Center
    San Diego, California

11. Michael B. Porter
HLS Research
San Diego, California

12. Dana Hesse
ONR 312 MS
Arlington, Virginia

13. Tom Swean
ONR 312 OE
Arlington, Virginia

14. CAPT Rick Ruehlin
NAVSEA PMS NSW
Washington, District of Columbia

15. LCDR Patrick Lafontant
NAVSEA PMS NSW
Washington, District of Columbia

16. Dean Wakeham
Naval Special Warfare Group 3
Coronado, California

17. Joel Peak
Naval Surface Warfare Center
Panama City, Florida

18. Juan C. Torres
United States Navy
El Paso, Texas